Développement d'interfaces cerveau machine visant à compenser les déficits moteurs chez des patients tétraplégiques. Etudes expérimentales précliniques

Thomas Costecalde

UNIVERSITÉ DE GRENOBLE

THÈSE

Pour obtenir le grade de

DOCTEUR DE L'UNIVERSITÉ DE GRENOBLE

Spécialité : **Biotechnologie, instrumentation, signal et imagerie pour la biologie, la médecine et l'environnement**

Arrêté ministériel : 7 août 2006

Présentée par

Thomas COSTECALDE

Thèse dirigée par **Stéphan Chabardès**

préparée au sein du **Laboratoire CEA-Leti-Clinatec**
dans **l'École Doctorale « Ingénierie pour la Santé, la Cognition et l'Environnement »**

Développement d'interfaces cerveau machine visant à compenser les déficits moteurs chez des patients tétraplégiques. Etudes expérimentales précliniques.

Thèse soutenue publiquement le **« 12 Décembre 2012 »**,
devant le jury composé de :

Pr Stéphan, CHABARDES
Directeur
Dr Blaise, YVERT
Rapporteur
Dr SGAMBATO-FAURE
Rapporteur
Dr Cécile, MORO
Membre
Pr Alim-Louis, BENABID
Président
Dr Karim JERBI
Membre

Université Joseph Fourier / Université Pierre Mendès France / Université Stendhal / Université de Savoie / Grenoble INP

UNIVERSITÉ DE GRENOBLE

Brain computer interface with chronic cortical electrode arrays for motor deficit compensation in motor disabled patients.
Experimental study in rodents.

COSTECALDE Thomas

PhD Report

Scientific adviser: MORO Cécile

Director: CHABARDES Stephan

January 2010- December 2012

University Joseph Fourier, Grenoble

CEA-LETI-Clinatec
MINATEC Campus, 17 rue des Martyrs
38054 GRENOBLE Cedex 9

Ecole Doctorale: EDISCE

AKNOWLEDGEMENTS

This thesis is the result of three years of research, I would like to express my sincere gratitude to all those who have supported me during this work. First, I would like to thank my research supervisors Dr Moro Cecile, Pr Benabid Alim-Louis and Pr Torres Napoleon for the opportunity to have worked in their research team, in addition to their support for the guidance and encouragement along my thesis. I would like to give thanks for my committee members: Pr Alim Louis Benabid, Pr Stéphan Chabardès, Dr Cécile Moro, Dr Véronique Sgambato-Faure, Dr Blaise Yvert and Dr Karim Jerbi, especially for the time invested to read and review my thesis.

Next, I extend my thanks to all the researchers, engineers and technicians of the different disciplines presents in the Clinatec Institut.

I would like to express my deepest gratitude to my parents, brothers and all my friends for the love, help and decompression time required to complete this project.

This work was supported by the “Fondation Motrice”, the “Fondation pour l’Avenir”, Floralis and Synthelis without them this work would not have been possible.

I. GENERAL INTRODUCTION

A brain-computer interface (BCI) is currently defined as a hardware and software communication system that permits cerebral activity alone to control external devices. The immediate goal of BCI research is to provide communication capabilities to severely disabled people who are totally paralyzed or 'locked in' by neuromuscular disorders, such as amyotrophic lateral sclerosis, brain stem stroke, or spinal cord injury. The burden for the patient, the family, the society of paralytic consequences of motor disabled patients is becoming a dramatic, huge, and, costly problem. The current treatments provide survival after the traumatism, and the re-adaptation to a new lifestyle, mostly bedridden, that keeps the patient in an almost total dependency. Any kind of therapeutic approach able to decrease this dependency by compensating the lack of motricity has a huge impact on the psychological, familial, and even social conditions of the patient, and must be taken as a priority.

Two studies provided the prevalence, and incidence of Spinal Cord Injury (SCI). The published data on prevalence of SCI was insufficient to consider the range of 223–755 per million inhabitants to be representative for a worldwide estimate. Reported incidence of SCI lies between 10.4 and 83 per million inhabitants per year. One-third of patients with SCI are reported to be tetraplegic and 50% of patients with SCI to have a complete lesion. The mean age of patients at is reported as 33 years old, and the sex distribution (men/women) as 3.8/1 [1].

Following the growing number of severe motor disabilities as a result of neurological pathologies, research efforts have recently focused on the development of brain guided neuroprosthesis. Of these, the BCI can establish a direct communication link between the brain of a patient and an electronic external device (robot, computer, etc.), in order to be able to drive the device, using on line analysis of brain electrical activity. The BCI integrates the most recent advances in the knowledge of brain function and represent the hope of reintegration to current life of subjects with severely impaired nervous pathways through the restoration of paralyzed limbs or the control of robotic systems.

The BCI aims to provide an alternative non-muscular communication bypass and control system for the individuals with severe motor disability to send the command to the external world using the measures of brain activity. During the last decades, several approaches and methods were developed to face the problem of brain movement related signal decoding. Promising results were obtained in animals and in human studies [2]. Recently, Hochberg's

team implanted microelectrodes array in the cortex of tetraplegic patients. They demonstrated patient's capacity to pilot mouse computer using an acquisition data system connected to a computer by a wired connexion. In 2012, John Donoghue and colleagues have demonstrated that people with tetraplegia can learn to use neural signals from the motor cortex to control a robotic arm in order to reach and grasp a glass [3].

But the clinical use seems difficult due to limitations of these systems: an inflammatory risk around electrodes implanted into the cortex, and an infectious risk at the skin opening. Practical applications of BCI technology are currently impeded by the limitations and requirements of both existing non-invasive and invasive methods [4] (see figure 1).

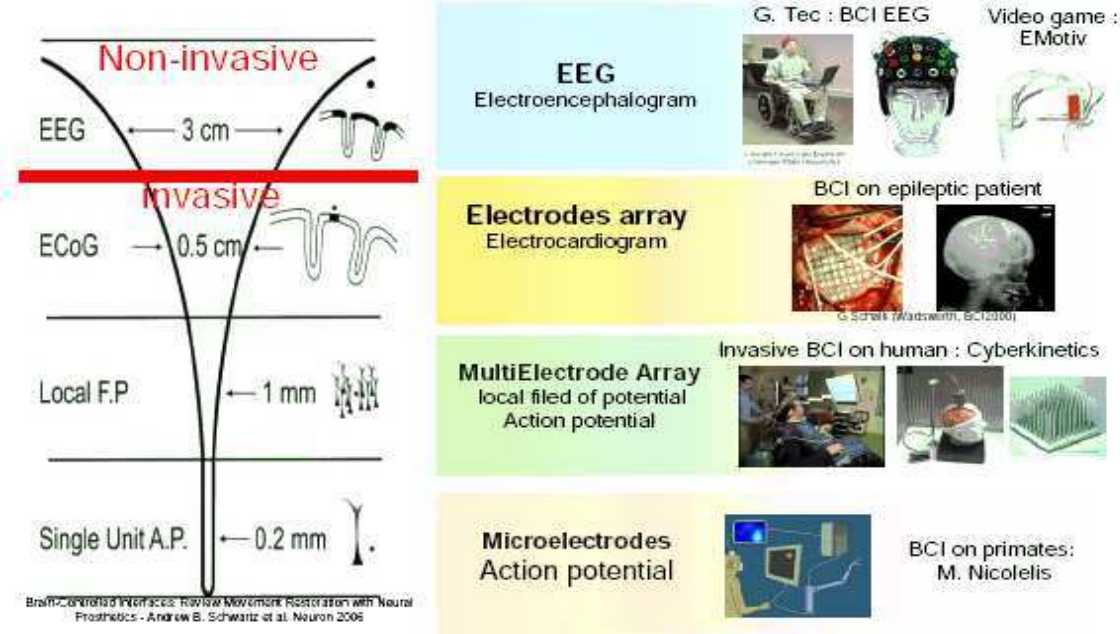

Figure 1: Illustration of the different level to record brain activity [4].

· Invasive BCIs use neural activity from multiple neurons recorded within the brain with electrodes implanted into the cortex. Clinical implementations are impeded mainly by the risks of surgical implantation of array of hundreds of intracortical electrodes and by the substantial stability problem of long term recordings. The inflammatory reaction induces a decreased signal to noise ratio. The electrophysiological signals are sometimes progressively hidden by noise.

· Non-invasive BCIs use mainly electroencephalographic activity (EEG). Despite the great advantage of not exposing the patient to the risks of brain surgery, EEG-based techniques

provide communication channels of limited capacity that is not sufficient to provide control of the movements with multiple degrees of freedom.

The most promising solution for human BCI seems to use electrical activity of the cortex: the electrocorticography (ECoG), which is less invasive than implanted microelectrodes, and provides better signals than EEG [5]. First results (patients piloting a joystick through modulation of their cortical activity) increase the hope of BCI with an array of microelectrodes chronically implanted at the cortex's surface, which doesn't exist yet. Recent experiments demonstrated the capacity for a tetraplegic to control a robotic arm [3 and 6].

A BCI program has been started at Leti-Clinatec in CEA Grenoble: it aims at conceiving, building, testing, a human prototype of an implantable BCI neuroprosthesis allowing a tetraplegic handicapped person to restore some mobility thanks to an external device driven by his/her brain activity. This BCI project is an interdisciplinary research combining disciplines such as micro-nanoelectronics, applied mathematics and informatics, basic and clinical neurosciences (including neurosurgery), and robotics at the same place. The overall goal of the present project is to develop a self-paced preclinical BCI prototype validated on animal in natural environment, based on ECoG signal analysis to prefigure human implant. The project develops an original method of data acquisition and treatment (patents [7 and 8]) in order to drive multiple degrees of freedom.

The main objective of the present PhD program was to design, built and test *in vivo* in rodents a prototype of BCI (implantation of chronic cortical electrodes, recording and analysis of cortical signals in order to produce a motor task from brain commands) capable of compensating motor deficits such as in patients. The applicant has evolved inside a multidisciplinary team in the CLINATEC Institute, which is dedicated to the application of micro and nanotechnologies to neurosciences. Clinatec has capabilities in the area of technology (built-in prototypes), biology and animal research (allowing preclinical evaluation), and additional medical-surgical competences allowing concept-testing in selected human patients. This work was done in close contact with 3 sectors: technology (producing prototypes), experimental (preclinical evaluation) and medical (testing the concept in patients). This 3 year scholarship of a graduate student reinforced the biologist team by participating in the experimental phase and in the development of the biological-technological interface.

The PhD work contributes to preclinical studies, performed in parallel of technical development to provide validation of the human experimental protocol in successive steps. It

contributes to develop ECoG recording device for rats, to implant them in the corresponding animals and record their ECoG activity during freely moving behavioural experiments to control an external effector. The experimental work includes surgery to implant electrodes, validation of their functional localization, behavioural trainings and mathematical treatment of data.

II. INTRODUCTION TO NEUROSCIENCES

1_Anatomical and functional basis of the brain

1_1) Central Nervous System (CNS) and Peripheral Nerve System (PNS)

The central nervous system (CNS) is one of the two major divisions of the nervous system and the other is the peripheral nervous system (PNS) which is outside the brain and spinal cord. The central nervous system is composed by the spinal cord and brain as illustrated in figure 2.

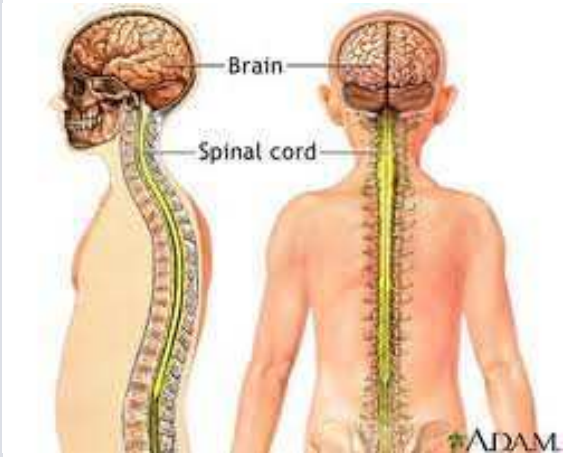

Figure 2: Central Nervous System and its components (http://adam.about.net/encyclopedia/Central-nervous-system_1.htm).

1_1_a) The CNS

1_1_a1) The spinal cord

The spinal cord consists of nerve fibers (in longitudinal, ascending and descending, bundles) and of neuronal cell bodies (grouped in a longitudinal grey matter H-shaped structure, centered by the ependymal canal and presenting horns: motor, anterior, emitting the axons of the motor nerves and sensory, posterior, receiving the axons of the sensory nerve roots). The fiber bundles conduct sensory information from the peripheral nervous system to the brain and motor information from the brain to various effectors (skeletal muscles, cardiac muscle, smooth muscle and glands). The spinal cord also acts as a minor coordinating center, responsible at each metameric level for some simple reflexes like the withdrawal reflex. Thirty-one pairs of spinal nerves originate in the spinal cord: 8 cervical, 12 thoracic, 5 lumbar, 5 sacral, and 1 coccygeal. Like the brain, the spinal cord is covered by three connective-tissue envelopes called the meninges (see figure 3). The subarachnoidal space between the middle (arachnoid) and inner (pia-mater) envelopes is filled with cerebrospinal fluid (CSF) that cushions the spinal cord, also known simply as the cord, against shock.

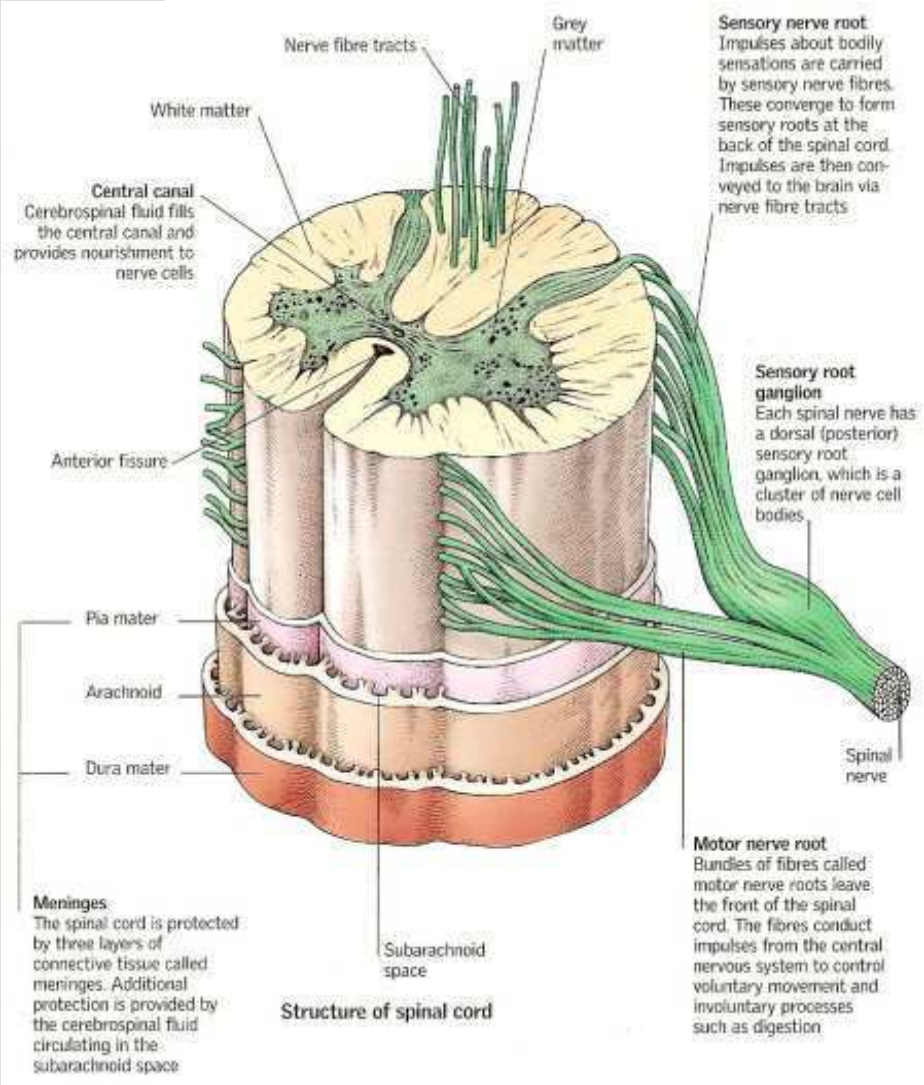

Figure 3: Spinal cord and its organization (http://www.daviddarling.info/encyclopedia/S/spinal_cord.html).

1_1_a2) The brain

The brain receives sensory input from the spinal cord as well as from its own nerves (olfactory and optic nerves) and devotes most of its volume (and computational power) to processing its various sensory inputs and initiating appropriated and coordinated motor outputs. The brain of all vertebrates develops from three swellings at the anterior end of the neural tube of the embryo. From front to back these develop into the forebrain (also known as the prosencephalon), the midbrain (mesencephalon) and the hindbrain (rhombencephalon). The cerebellum is located in the posterior fossa of the skull and is covered by cortex and

consists of two hemispheres, each of which is divided into lobes. Its most clearly-understood function is to coordinate body movements.

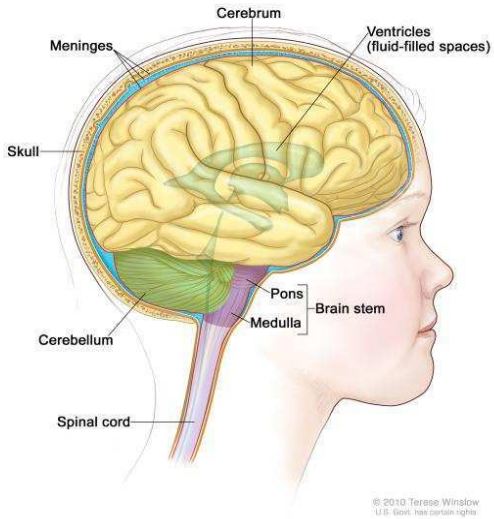

Figure 4: Brain structure and cerebellum (http://www.meb.uni-bonn.de/Cancernet/CDR0000574295.html).

The human brain receives nerve impulses from the spinal cord (previously described) and 12 pairs of cranial nerves. Some of the cranial nerves are "mixed", containing both sensory and motor axons. Others like the optic and olfactory nerves (numbers I and II) contain sensory axons only or in contrary the nerve III controlling eyeball muscles contains motor axons only. As previously explained, there are three different parts of brain: the forebrain, midbrain and hindbrain (see figure 4). The forebrain is made up of the cerebrum, thalamus and hypothalamus. The mid brain consists of the tectum (roof) and tegmentum (floor). The hindbrain is made up of the cerebellum, pons and medulla. The midbrain, pons and medulla form the brain stem.

_ The cerebrum is the largest part of the brain that is located in the forebrain. The cerebrum is divided into two equal halves called the hemispheres and consists of four lobes. Cerebrum is responsible for controlling our thoughts and actions. The cerebrum has four lobes. The parietal lobe area of the brain is responsible for recognition, movement, orientation and perception of stimuli. The frontal lobe is associated with reasoning, planning, parts of speech, movement, emotions and problem solving. The occipital lobe is associated with visual

processing. And the temporal lobe is associated with the perception and recognition of memory, speech and auditory stimuli see figure 5.

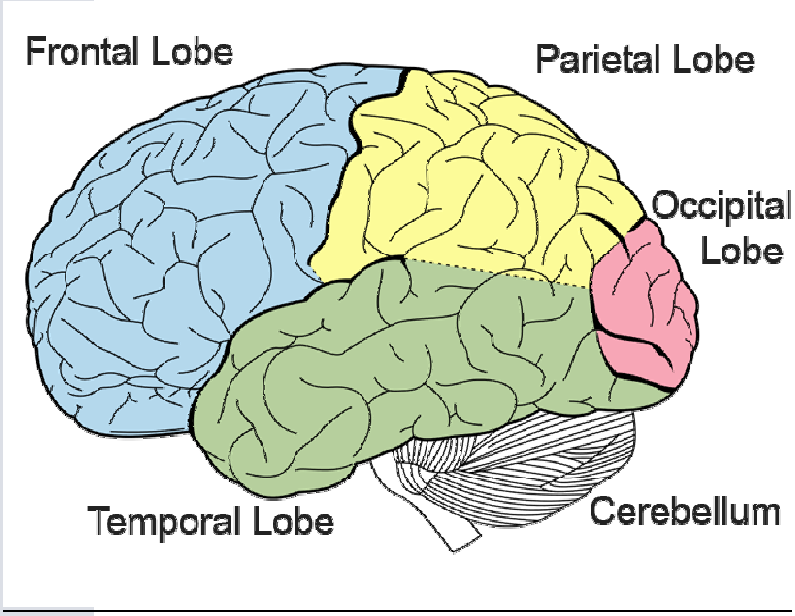

Figure 5: Brain areas and cerebellum (http://en.wikipedia.org/wiki/Frontal_lobe).

The cerebral cortex is highly wrinkled. Essentially this makes the brain more efficient, by increase the surface area of the brain and the amount of neurons within it.

_ The cerebellum ("little brain") is a structure that is located at the back of the brain, underlying the occipital and temporal lobes of the cerebral cortex (see figure 4), although the cerebellum accounts for approximately 10% of the brain's volume. Historically, the cerebellum has been considered a motor structure, because cerebellar damage leads to impairments in motor control and posture and because the majority of the cerebellum's outputs are connected to parts of the motor system. Motor commands are not initiated in the cerebellum; rather, the cerebellum modifies the motor commands of the descending pathways to make movements more adaptive and accurate. The cerebellum is important for making postural adjustments in order to maintain balance.

The description of the CNS and especially of the brain can be approached with some attention on the functional areas identified. Two important areas (motor and sensory cortices, see figure 5) have been identified by stimulation on dog in 1870 by Hitzig and Fritsch [9 and 10].

The somatosensory homunculus represents each area of the body, it is distorted from the body surface areas as it is proportional to the density of sensory receptors on the surface of the body. So it depends on the genome of the species and is modulated by environmental factors. The motor homunculus represents the various muscles depending on the intensity of their activity. It also depends on environmental factors. The importance of the cortical representation of body parts varies greatly from one species to another. It is correlated to the "lifestyle" of the animal. For example, in rodents, the whiskers are largely represented in the somatosensory cortex while the fingers of the legs or tail are only slightly.

The model of the homunculus of Penfield is illustrated in the schematic representation below (see figure 6).

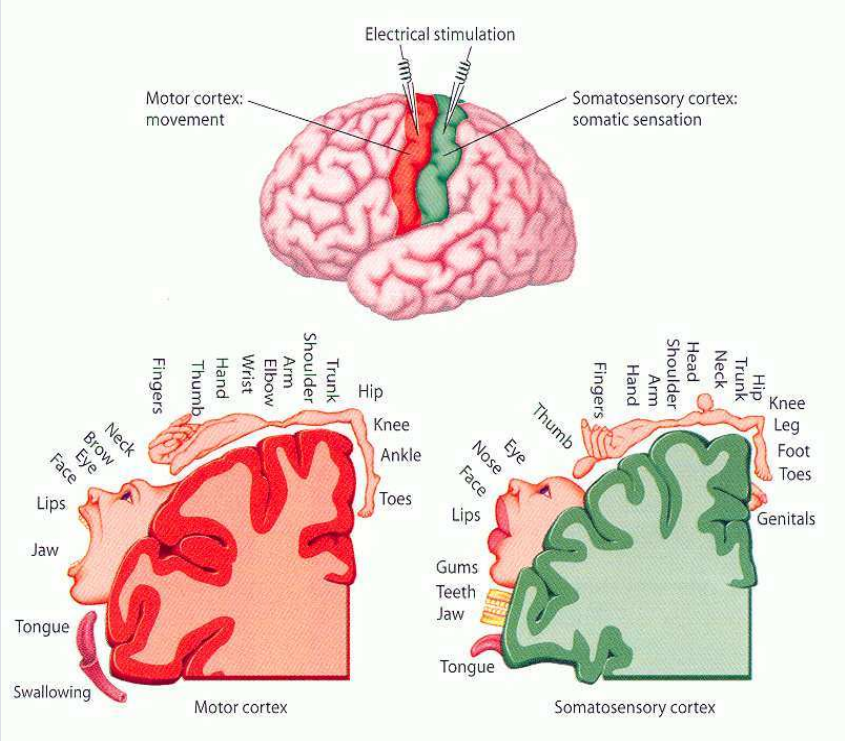

Figure 6: Representation of the Homonculus (http://tecfa-bio-news.blogspot.fr/2009_05_01_archive.html).

1_1_b) The PNS

This second part of the nervous system connects the CNS to sensory organs, other organs of the body, muscles, blood vessels and glands. The PNS consists of sensory neurons running from external and internal receptors that inform the CNS and motor neurons running from the CNS to the muscles and glands (called effectors). The PNS is subdivided into the sensory-somatic nervous system and the autonomic nervous system. The figure 7 described all this organization.

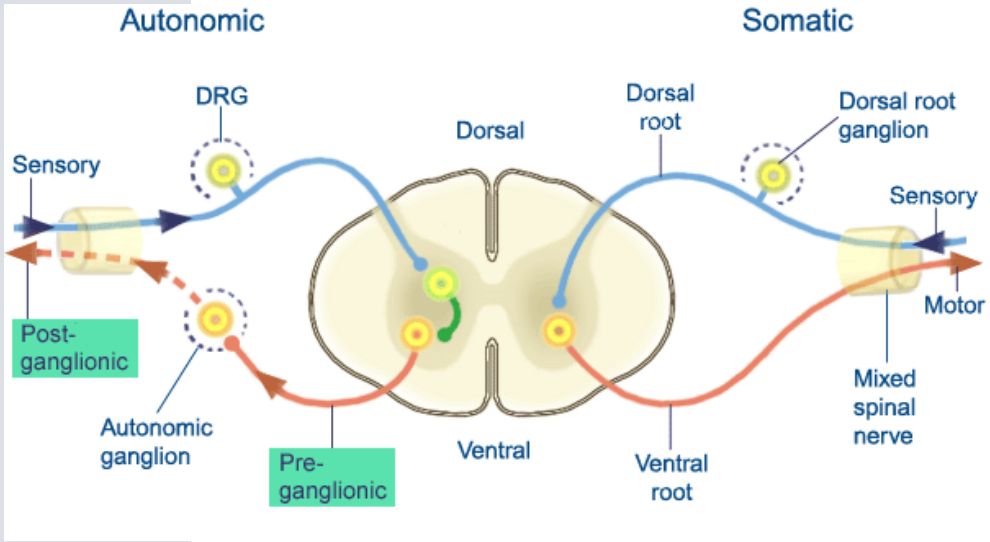

Figure 7: Peripheral Nervous System and its components (http://alexandria.healthlibrary.ca/documents/notes/bom/unit_2/L-03%20the%20Autonomic%20Nervous%20System.xml).

The peripheral nerves include the 12 cranial nerves, the spinal nerves and roots, and what are called the autonomic nerves that are concerned specifically with the regulation of the heart muscle, the muscles in blood vessel walls, and glands.

1_2) The functional brain activity

Electrical activity in brain tissue, compared with other signs of activity (chemical, metabolic, vascular), has unique values. It can be recorded with high temporal resolution and high spatial resolution (down to single channels) in three dimensions. This advantage over other signs of activity is particularly clear when multiple, closely spaced electrodes are used. Other methods for visualizing activity have also been productive of insights: voltage-sensitive dyes, oxygen

consumption, local temperature, blood flow, positron emission tomography, magnetic resonance imaging, and other indicators.

1_2_a) The brain signal

The electrical activity of the brain corresponds to the summation and coordination of the electrical activity of the neurons, which are the single units of the signal generated. To understand how to measure brain neural activity it is necessary to explain briefly the organization and the mechanism of action of a neuron.

This nervous system is composed of billions of cells, the most essential being the nerve cells or neurons. There are estimated to be as many as 100 billion neurons in our nervous system.

A typical neuron possesses a cell body (often called the soma), dendrites, and an axon (see figure 8). Dendrites are filaments that arise from the cell body, often extending for hundreds of micrometers and branching multiple times, giving rise to a complex "dendritic tree". An axon is a special cellular filament that arises from the cell body.

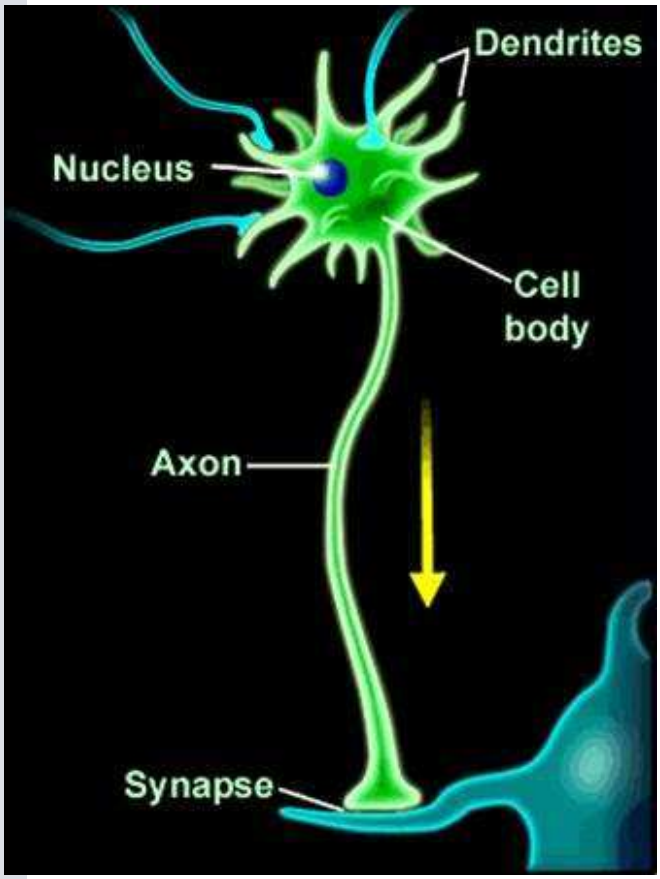

Figure 8: Representation of a neural cell (http://fwjmath.wordpress.com/2010/11/26/miniature-neural-network-in-a-computer/).

1_2_a1) The neuron

Neurons are an electrically excitable cell that processes and transmits information by electrical and chemical signalling. Every neuron maintains electrical potential between the extra- and intracellular spaces by means of generation of ion concentration difference. If this concentration changes significantly enough, electrochemical pulse (action potential) is generated. The pulse travels along the cell's axon and through the dendrites it can activates other cells. In this way, information is transmitted from one neuron to others and a great number of connections create a neural network.

1_2_a2) The Action Potential (AP)

The basal activity of a neuron is to generate AP. The AP is the all-or-none electrical impulse used to communicate information between neurons and from neurons to muscle fibers. The energy used to generate action potentials comes in the form of electrochemical gradients of ions (in particular, sodium and potassium ions) that are established by ion pumps, see figure 9.

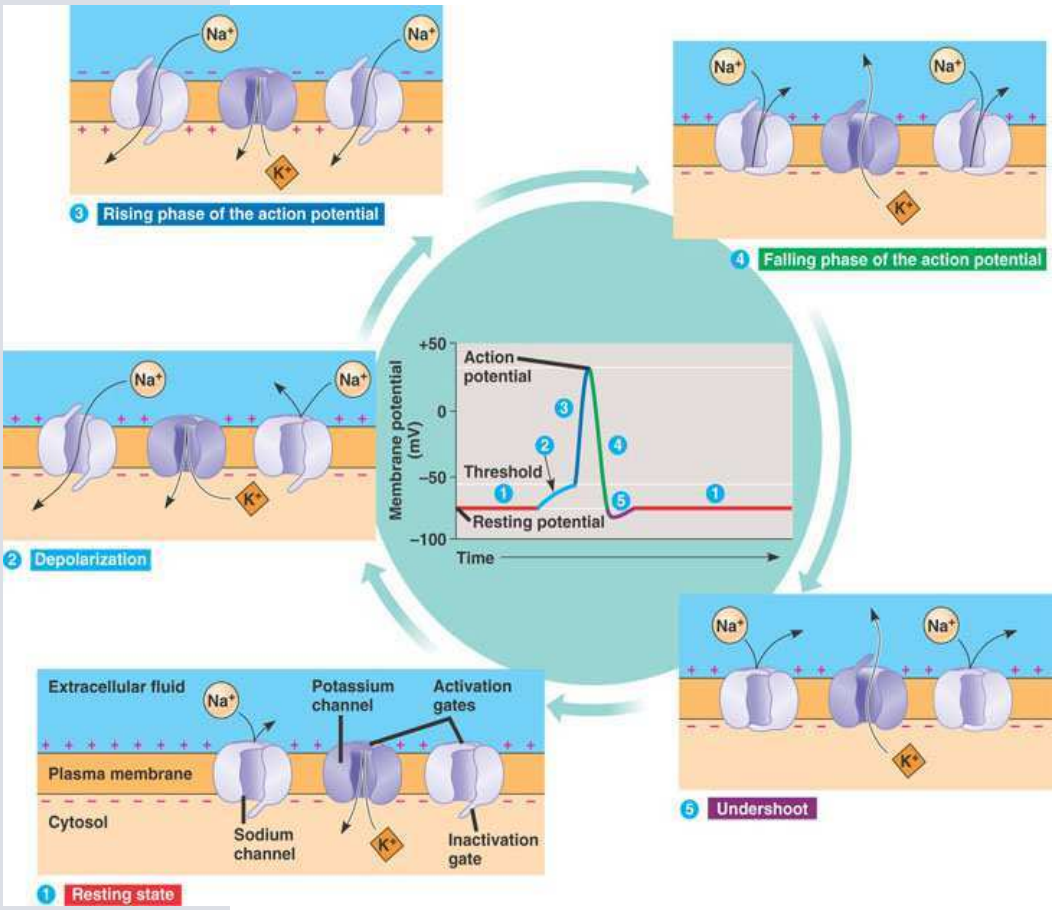

Figure 9: Description of an Action Potential (http://kvhs.nbed.nb.ca/gallant/biology/action_potential_generation.html).

The rising phase of APs is caused by the auto-catalytic opening of a large number of Sodium selective ion channels in response to sufficiently large increases in membrane potential. The falling phase of the AP is caused by two factors which come to dominate the electrical response after a few milliseconds: the tendency of sodium channels to close shortly after they open and the tendency of potassium channels to open in response to depolarization.

The axon can be compared to an electrical cable. The neuronal membrane, formed by a stable insulating layer of phospholipids, has a charge storage capacity, whereas the conductive cytoplasm of the cell can be characterised as a resistance. The membrane can regulate ion movements between extracellular and intracellular spaces (with several types of ion channels, pumps and exchangers) and plays an important role in establishing the resting electrical transmembrane potential. An AP is a transient and reversible change in the resting membrane potential. It can be divided in a resting, a depolarising, a rising, a falling (repolarization) and a

hyperpolarising (undershoot) phase (see figure 9). Each change in transmembrane potential is the result of ions exchange as described in the figure above.

1_2_b) The different levels for recording brain activity

The first step necessary for a BCI is to be able to record brain signals. The signals from the brain are generated by the neurons and can be recorded at this cellular level by implantation of microelectrodes deeply in the cortex. Different levels of implantation between this cellular level of recordings and the recordings, the most external, by non-invasive electrodes along the scalp (EEG) have been used with different benefits or possible disadvantages.

BCI are always faced with the trade-off between invasiveness and robustness of signal. At the one extreme, EEG relies on signals from non-invasive electrodes placed directly on the scalp. While one and two-dimensional control has been demonstrated with EEG [11 and 12], the poorer accuracy and learning rates have limited its efficacy compared to other methods of BCI. In contrast, intracortical electrodes have been demonstrated as an effective source for a BCI [13 and 14]. However, these types of recordings require complicated, highly invasive surgeries. Additionally, the quality of these recordings tends to decay over time as electrodes become encapsulated by the immunologically reactive tissue. An intermediate signal recording modality, known as subdural electrocorticography (ECoG), has also been proposed as a possible signal source for a BCI. Previously, event-related potential changes of the ECoG signal have been used to identify the onset and timing of various motor actions on individual trials [15].

A brief overview of these different levels of brain recordings is detailed below.

1_2_b1) The ElectroEncephaloGraphy (EEG)

On the physical level, signal measured with the EEG is caused by the electrical activity at pyramidal neurons in the cerebral cortex [16]. Changing of the electrical potentials in the extracellular space leads to appearance of currents flowing around the region of a synapse. Summation of the currents from millions of neurons (a typical cortical macro-column has diameter about 3-4 mm) can be detected in the EEG (see figure 10).

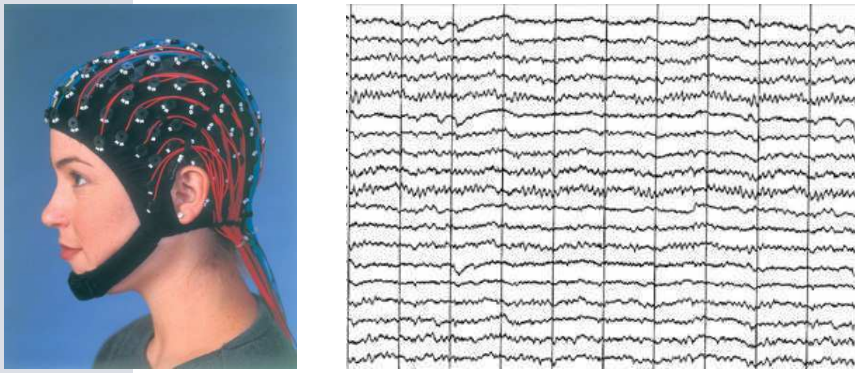

Figure 10: EEG electrodes on scalp and example of EEG signal (http://www.bioedge.org/index.php/bioethics/bioethics_article/9066/ and http://www.chp-neurotherapy.com/basic-qeeg.html).

Due to potential spreading, it is possible to detect the macro-column activity up to 10 cm from the source. This yields to registering the same source activity on the different electrodes. For the reason of the tissue barrier, which is between neurons and electrodes, it is practically impossible to register low-energy brain activity, as well as frequencies higher than 100 Hz. The lower limit of the EEG spectrum is 0.1 Hz. Generally the range from 0.3 Hz to 70 Hz is used in practice [17]. The amplitude of EEG signals ranges generally from 20 to 100 μV. Moreover, artifacts from eye blinks, movements and other muscle activity complicate analysis of the EEG data. The amplitude of the artifacts sometime significantly exceeds the amplitude of the signal of interest. Hence, artifact filtering must be applied to the signal before data will be used.

Spectrum of the EEG is divided on several bands (see figure 11), which have special names [17]: Delta (δ): <4 Hz, Theta (θ): 4-7 Hz, Alpha (α): 8-13 Hz, Beta (β): 14-35 Hz and Gamma (γ): ≥35 Hz.

The delta waves occur during deep sleep to rapid eye movement, and are sometimes correlates of brain damage.

The theta waves access to a state of deep relaxation. It is a state used in hypnosis. It reflects the state between sleep and completeness.

The alpha waves disappear when the eyes are open. Once eyes are closed during rest, the EEG shows a slowing of our brain waves. This stage close to the relaxation is a transition stage between wakefulness and sleep.

The beta brain waves pass during the short periods of sleep with dreaming. This is the cycle of awakening, one that rhythm brain when eyes are opened in the action.

The gamma waves (above 35Hz, up to 80Hz) are the only frequency group present in all part of the brain.

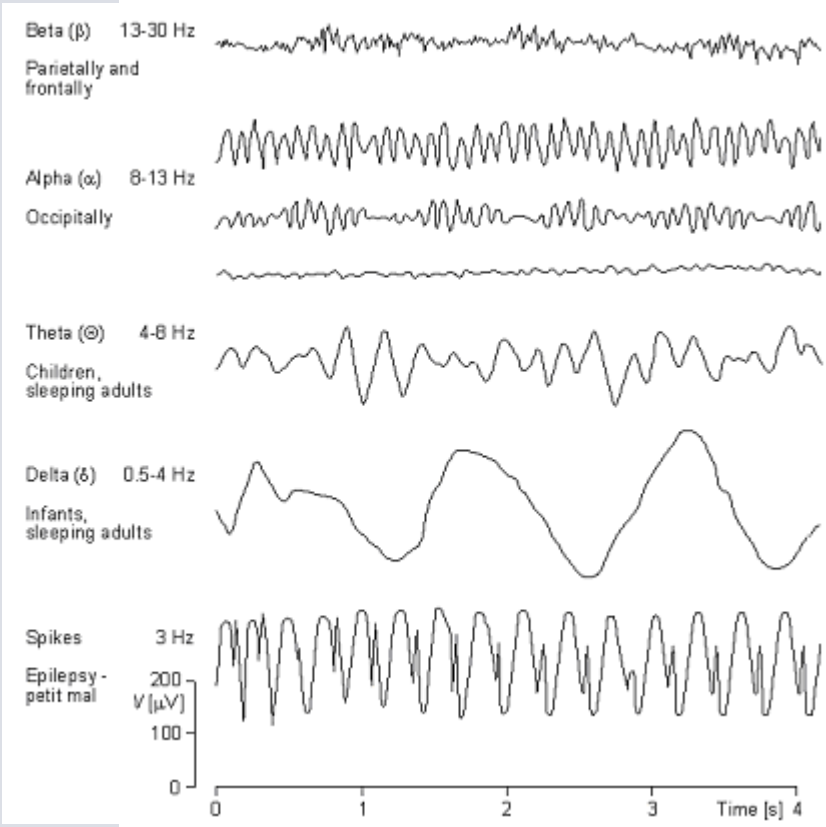

Figure 11: EEG spectrum (http://www.biogetic.com/research.html).

1_2_b2) The Microelectrode arrays

Microelectrode arrays (MEA) are a technique for registering activity of small groups of neurons (local field potentials) or even single neuron (single-unit APs). To record signals needle-like electrodes are placed into the brain cortex during surgery (see Picture 1).

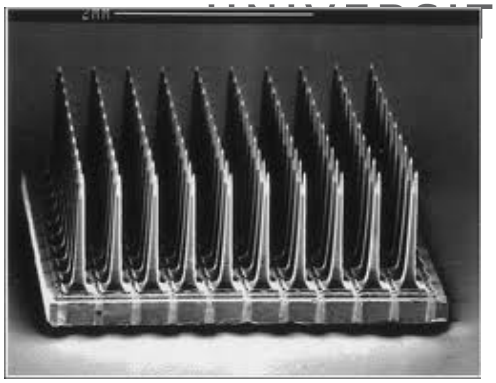

Picture 1: Example of a microelectrode array [18].

Firstly arrays were implanted by C. Thomas in 1972 [19]. Electrodes diameter ranges between 10 and 30 μm. The method allows register signals with frequency up to 5000 Hz.

The main advantage of MEA application in comparison with other approaches is its high spatial resolution, which gives opportunity to apply MEA for complex tasks, real-time 3D motion [13 and 20] and robotic arm control [21 and 22]. AP firing rate, containing motor information, allows estimation of subject's intention of movement [23 and 24]. In the work of Hochberg [2], 96 electrodes were implanted in a human subject suffering from tetraplegia.

1_2_b3) The ElectroCorticoGraphy (ECoG)

The Electrocorticography (ECoG) uses an electrode grid or strip to record the electrical activity of the brain's cortex (see picture 2).

Picture 2: Example of a ECoG electrode grid [25].

ECoG was pioneered by W. Penfield and H. Jasper in the 1950's [26 and 27] and now is considerably widespread in BCI [28, 29, 30 and 31], and used in routine presurgical explorations for epilepsy. Like the EEG, the ECoG is based on measuring the potential activity originating mostly in cortical pyramidal neurons (see picture 3). The difference is that

electrodes are placed immediately on the cortex surface. Thus, electrical signals bypass the skull, which significantly diminishes potentials due to the low conductivity of the bone. It leads to increasing of spatial resolution of the ECoG in comparison with the EEG (tens of millimeters versus centimeters), broader frequency bandwidth (exceeded 300 Hz), and higher signal's amplitude (50-100 μV). In addition, the ECoG recordings are less influenced by artifacts [29].

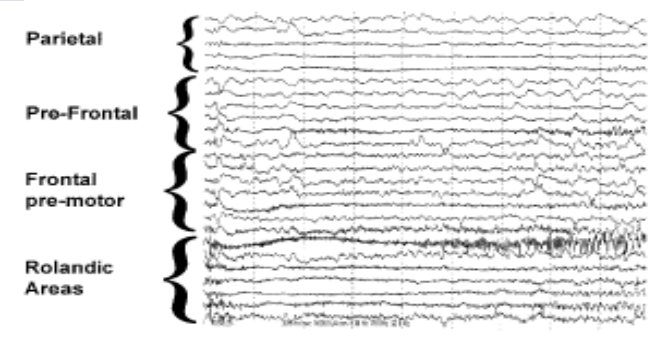

Picture 3: Example of ECoG recordings in different areas (http://www.scielo.br/scielo.php?pid=S0004-282X2001000500012&script=sci_arttext).

The electrodes arrays can be placed either on the surface of the dura mater (epidural) or under the dura mater (subdural). Mainly the ECoG electrodes are made from gold or platinum. They are attached to a flexible frame. Standard spacing between the electrodes in the frame is 1 cm; diameter of the electrodes is up to 5 mm. The electrodes are designed in the way to eliminate any injury of the brain during its movements.

The quality of the signal recorded with the ECoG is good enough to be used in the BCI project. Frequency band and spatial resolution as well as signal-to-noise ratio surpass correspondent parameters of non-invasive methods. The risk of implantation is not as high as for the microelectrode arrays. Furthermore, since recording does not depend on a single or several neurons, the system provides better long-term stability than invasive methods. Response time and size of the system allows its utilization in the real environment in the real-time mode. Hence, as a compromise between registered signal quality and safety, the ECoG was the selected method for brain activity recording for the experimental model for this study.

1_3) Rodents brain

The CNS of rodents is also composed of the brain and the spinal cord. The cerebellum is on the posterior part of the brain. The organisation of the brain of rodents is similar to the human brain but some differences in the size of specific areas are observable. For example, the olfactory bulb is bigger on rodents than in humans (see figure 12) related to a functional role more important in rodents. Each brain of each mammalian species presents high similarities with the general model of brain organisation, but with the evolution some areas of the brain have evolved in relation with their functional importance (size increased or decreased). In rodents, the olfactory function is most important for the behaviour and the life of the animal.

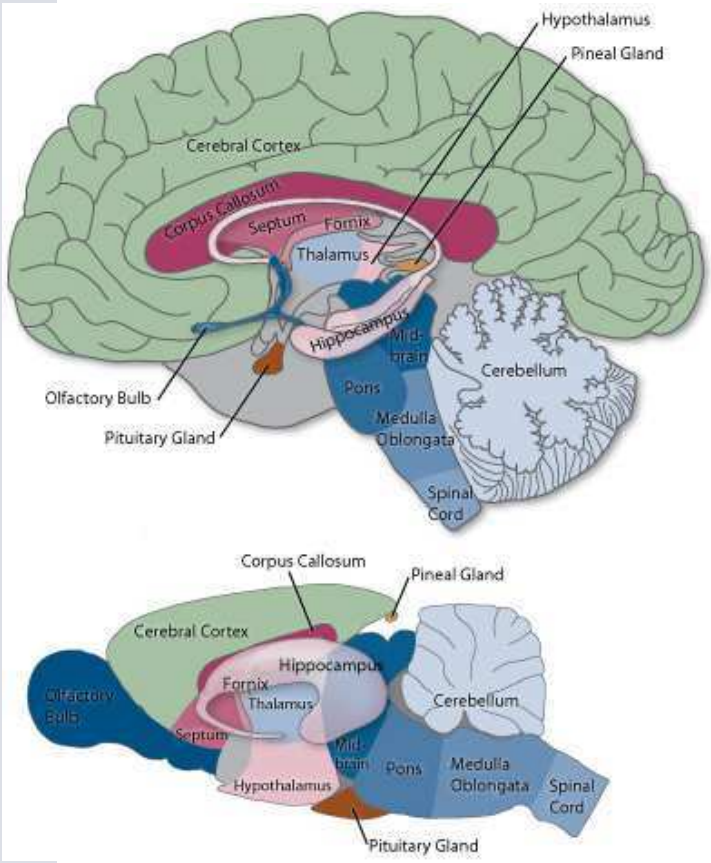

Figure 12: brains of human and of rodent (http://learn.genetics.utah.edu/content/addiction/genetics/neurobiol.html).

On rodents, the same functional areas of brain have been identified than in humans (see figure 5 for motor and sensory cortex in human). The figure 13 shows the position of the motor, the somatosensory, the auditory and the visual cortices on rodent brain.

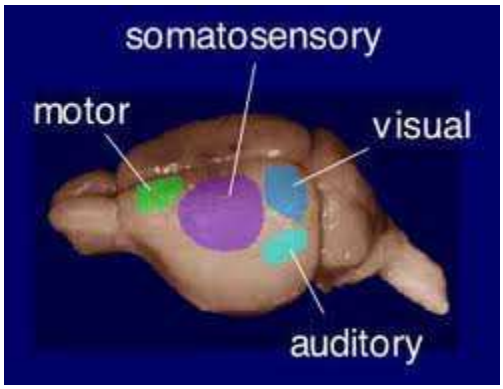

Figure 13: Rodent brain with functional areas (http://www.nibb.ac.jp/brish/Gallery/cortexE.html).

The human cerebral cortex is highly wrinkled. It increases the surface area of the brain and the amount of neurons within it. During the evolution, more species have become advanced and more cortex has become wrinkled, see figure 14.

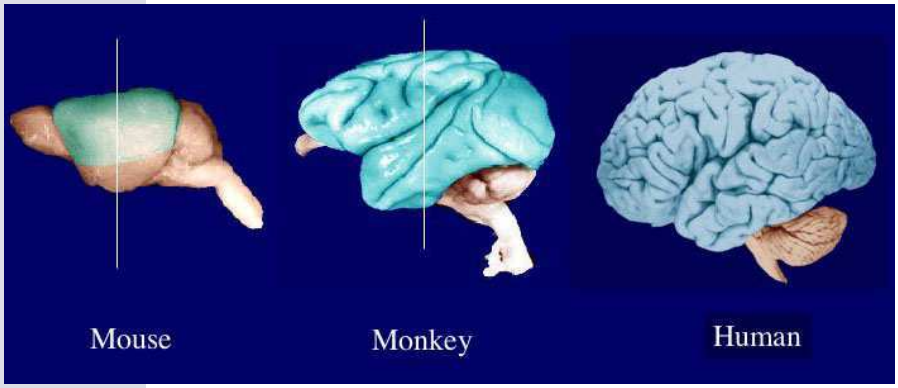

Figure 14: Comparison of brains of different species (http://www.nibb.ac.jp/brish/Gallery/cortexE.html)

2_ BCI state of the art

2_1) BCI definition and history

BCIs are being created to help the large number of people who have limited movement abilities owing to damage or disease of the motor system. A number of disorders disconnect

an otherwise healthy cerebral motor system from the muscles, leading to various degrees of paralysis, but with retention of the ability to plan and imagine making movements. These conditions include trauma, such as spinal cord injury, which renders ~250,000 Americans, ~200,000 in Europe and ~2 millions people in the world with spinal cord injury; strokes, which interrupt descending motor pathways, with the most devastating being a pontine stroke, which can disconnect all descending control to produce a locked-in state; and degenerative disorders such as amyotrophic lateral sclerosis (ALS, or Lou Gehrig's disease), in which alpha motor neurons (and likely cerebral neurons) progressively die. Most available information on prevalence and on incidence of SCI comes from Northern America, Europe and Australia. These three continents made up 20% of the world population in 1999. Data on prevalence and incidence of SCI from Asia, Africa and Latin America are necessary to permit a global estimate. Prevalence rates of Stockholm study (223/million) and of Helsinki study (280/million) are comparable. The same goes for the prevalence rates of Australia (681/million) and of the USA (700–755/million) [1 and 32]. Data on Asia, Africa, South-America, and the rest of Europe have not been found and therefore we cannot produce a complete worldwide SCI prevalence estimation.

In each case, muscle control by the brain is lost, while cerebral mechanisms to generate movement intentions could remain relatively intact [33 and 34]. Thus, a BCI may be a mean to directly deliver motor commands from the brain to assistive technologies, bypassing the biological lesion to restore control and independence to those with paralysis. Assistive technologies are aids to function; they can include any device from a simple switch, a computer cursor, a robot, or an artificial limb. A neural command with sufficiently rich and stable information could be used to operate any of these devices.

BCI also known as Brain Interface (BI), Direct Brain Interface (DBI), and Brain Machine Interface (BMI), is a system for translation of brain neural activity into commands for external devices [35]. In other words, BCI aims to provide an alternative non-muscular communication pathway for subjects to interact with their environment without using muscles. A common architecture of BCIs is illustrated in the figure 15.

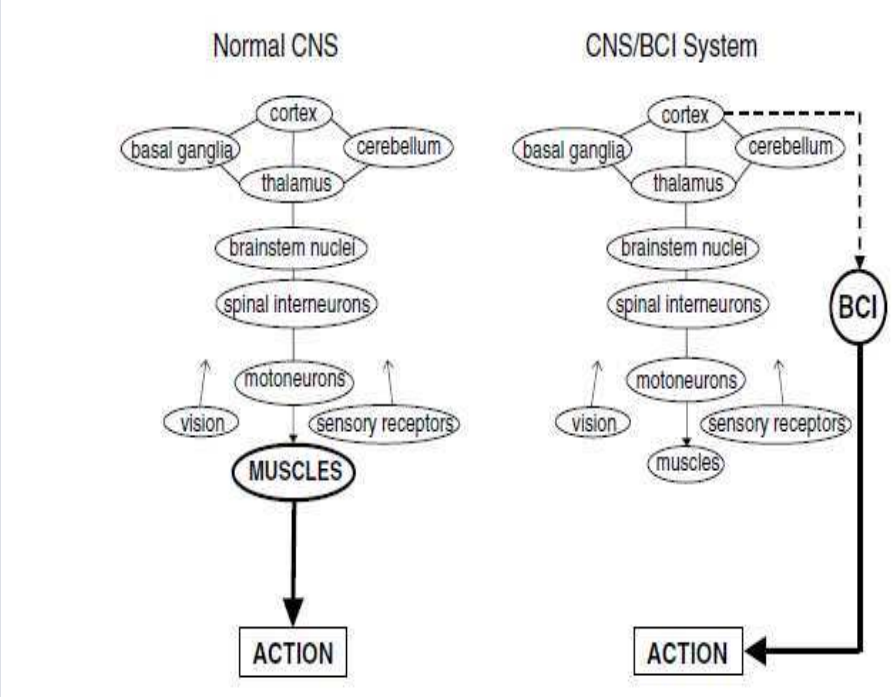

Figure 15: Comparison of CNS production of normal motor actions and CNS production of a BCI-mediated action [36].

The vastly oversimplified diagram on the left shows the production of normal action by the many CNS areas that collaborate to control spinal motoneurons and thereby activate muscles. The diagram on the right shows the production of a BCI-mediated action by the same CNS areas collaborating to control the cortical area that produces the brain signals used by the BCI to determine intents of action. Such a system could be developed for people suffering from severe motor disabilities to control wheelchairs, prostheses, etc.

The scientific origins of BCIs go back at least to the emergence of behavioural neurophysiology research in the 1960s when Evarts performed his electrophysiological experiments from primary motor cortex (MI) of awake, behaving primates [37]. Evarts found that the firing rates of individual MI neurons in monkeys were strongly correlated with the force or torque generated by the joints during arm movements. A paper published by Humphrey and colleagues [38] (1970) demonstrated that the kinematic and kinetic time course of a monkey's single-joint wrist movement could be predicted quite accurately using a small population of simultaneously recorded MI neurons, further elucidating the type of population or ensemble processing that occurs in the cortex to produce movement. Another

study, by Fetz (1969) [39], demonstrated that monkeys could control the activity of single MI neurons using visual biofeedback and reward. Monkeys were reinforced for moving an analog dial with a meter arm whose position was controlled by the firing rate of a neuron being recorded. This experiment provided initial evidence that primates could learn feedback control of neural activity without intervening movements.

However, this context has undergone radical change over the last two decades. BCI research, which was confined to only three groups 20 years ago and only six to eight groups 10 years ago, is now a flourishing field with more than 100 active research groups all over the World studying the topic [35]. The number of articles published regarding neural interface technology has increased exponentially over the past decade, see figure 16 [40]. Many researchers throughout the world are developing BCI systems that a few years ago were in the realm of science fiction. These systems use different brain signals, recording methods, and signal-processing algorithms. They can operate many different devices, from cursors on computer screens to wheelchairs to robotic arms.

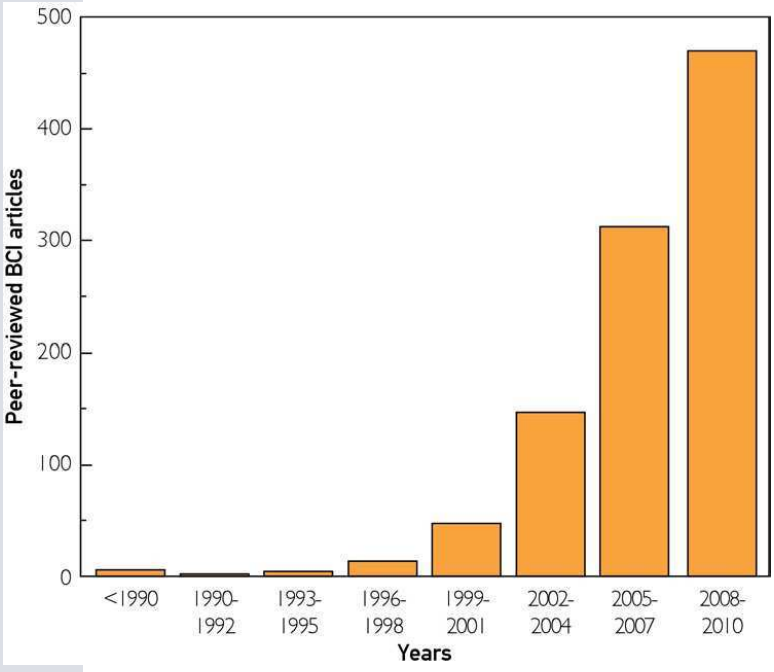

Figure 16: Brain-computer interface articles in the peer-reviewed scientific literature [40].

Successful studies on brain signal phenomena have lent further weight to these advances. The development of more and more inexpensive computer hardware and software has allowed

more sophisticated online analysis. The field of BCIs is actually quite broad and could include any form of connection between the brain and the outside world beyond the natural interfaces provided by the sensory and motor systems. The most successful neural interfaces today fall into the stimulation category because they are already available to humans. They include the cochlear implant [41 and 42] to restore audition in the hearing impaired and the deep brain stimulator (DBS) [43] to relieve the symptoms of Parkinson disease and dystonia. Output BCIs record electrical potentials from the brain to read out ongoing neural activity. Most commonly, this technic is used to predict cognitive intentions, motor plans, or actions of an organism to replace a lost connection to the outside world, but this information may also aid in diagnosis of disease or injury or to guide therapy.

Several approaches and methods have been developed yet using EEG. Commercial systems already exist, but EEG signal quality (in terms resolution and signal to noise ratio) implies to use evoked potentials, which is not very convenient to pilot efficiently an effector. Many research teams try to improve algorithms of EEG data treatment signalling, but they accord that signal quality is still insufficient to be used for asynchronous BCI. The most promising lead for human BCI seems the use of cortex surface electrical activity (ECoG), less invasive than implanted microelectrodes, and giving better signals than EEG [44, 45 and 46].

During the last decades several approaches were developed to face the problem of movement related signals decoding. Promising results were obtained both in animal [21, 22, 47, 48 and 49] and in human [29 and 35] studies.

To record neural activity systems with surface electrodes against the dura mater (epidural electrodes) [50 and 51] or with electrodes for EEG [52, 53 and 54] or MEA for deep brain recording of single units [47] or directly against the cortex (subdural electrodes) [29] have been used. Neural activity was analyzed using a variety of methods. The detection of event-related patterns allows triggering the action of an effector, e.g., a cursor on a screen [52], motorized device [21 and 47], etc. Experiments were carried out on rodents [47], primates [21 and 55], or in human patients [56 and 57]. Moreover, usually the duration of the experiments does not exceed several minutes (for instance, see [58]), the subject is being given a clue to start performing a task [35] and experiment conditions significantly differ from the natural environment of the subject (motion restriction, absence of significant external disturbances) [59].

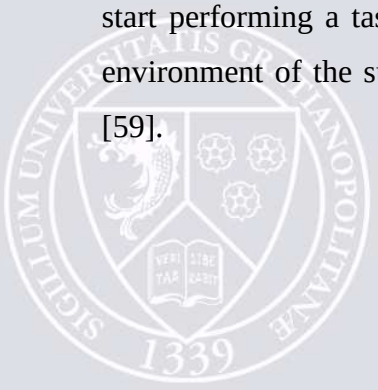

After initial developments in EEG-based BCIs by W. Gray Walter in the 1960s [60], neural interface research experienced a marked resurgence in the late 1990s with a number of demonstrations of closed-loop control using neuronal spikes. Chapin and colleagues [47] demonstrated a rat's ability to control a one-dimensional feeder using multielectrodes recordings from sensorimotor cortex. This was followed by a number of studies [13, 14, 61, 62, 63 and 64] showing that closed-loop control in primates is possible. That is, monkeys could replace actions of its hand with a command derived directly from neural populations in the cortex to perform actions. Importantly, the monkeys in these studies were observing the consequences of their control and could use that visual information to guide behaviour.

BCI research is a relatively young multidisciplinary field integrating researchers from neuroscience, physiology, psychology, engineering, computer science, rehabilitation, and other technical and health-care disciplines. As a result, in spite of some notable advances, a common language has yet to emerge, and existing BCI technologies vary, which makes their comparison difficult and, in consequence, slows down the research. The community of BCI researchers has therefore stressed the need to establish a general framework for BCI design [65]. Mason *et al.* [66], for example, proposed a new functional model for BCI systems and taxonomy design.

2_2) The BCI paradigms

Currently several control paradigms are used in the design of BCI systems. According to the work of Mason and Birch in 2005 [67], they can be classified as: self-paced (asynchronous) or synchronized (see figure 17).

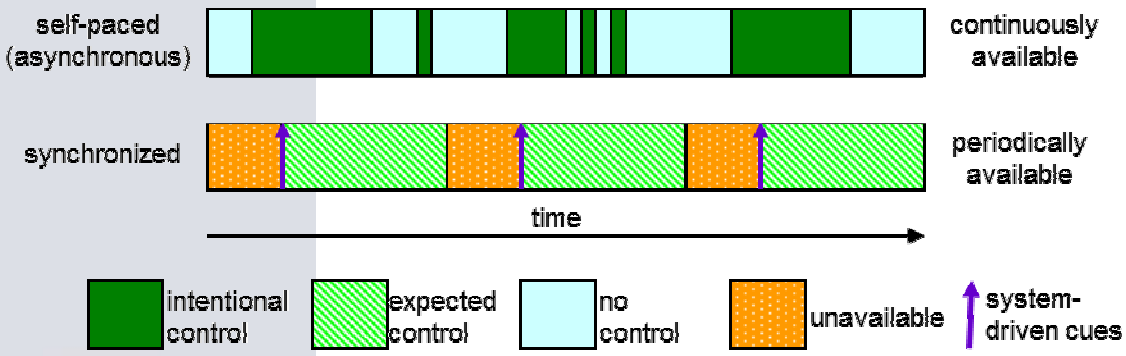

Figure 17: Schematic classification of different BCI paradigms [67].

Early studies also clarify an important distinction between two forms of this neural interface research: (*a*) open-loop prediction or decoding from multisite recordings, of which the Humphrey study is an example [35], and (*b*) closed-loop control, of which the Fetz [36] study is one of the first examples.

2_2_a) Synchronous and asynchronous paradigm

BCIs are limited by a low channel capacity. One of the main reasons for such a low bandwidth is that they are based on *synchronous* protocols where the brain signal recorded is time-locked to externally paced cues repeated every 4-10s and the response of the BCI is the average decision over this period [12, 53, 65, 68, 69, 70, and 71]. Such synchronous protocols facilitate signals analysis since the starting time of mental states are known and differences with respect to background activity can be amplified. Unfortunately, they are slow and BCI systems that use them normally recognize only 2 mental states, independently of the number of electrodes from which brain activities are measured. In a synchronous experimental protocol, the subject must follow a fixed repetitive scheme to switch from a mental task to the next. A trial consists of two parts. A first cue warns the subject to get ready and, after a fixed period of several seconds, a second cue tells the subject to undertake the desired mental task for a predefined time.

On the contrary, other BCIs utilize more flexible asynchronous protocols where the subject makes self-paced decisions on when to stop doing a mental task and start immediately the next one [70, 72, 73, 74, and 75]. In such asynchronous protocols the subject can voluntarily change the mental task being executed at any moment without waiting for external cues. The time of response of an asynchronous BCI can be below 1 second. For instance, in Millán's approach the system responds every 500 milliseconds (ms).

Most reported BCI are synchronous, for instance [35]. Nevertheless, recently more and more groups have conducted design of self-paced BCI model [76]. Our model of BCI is a binary self-paced BCI system. It allows us to concentrate on the essential question of the task. In asynchronous paradigm, the subject is not disturbed by a cue or by the fact that it's necessary to wait the cue to start the experiment. Contrary to synchronous experiments where the subject has to wait the signal "start" to change.

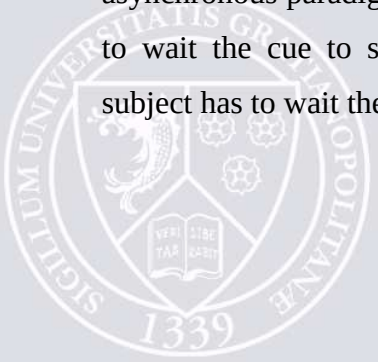

2_2_b) Open-loop and close-loop paradigms

In a more recent example of BCI research showing open-loop prediction, Wessberg and colleagues [21] demonstrated that it was possible to predict the 2D and 3D position of a monkey's hand in real time using neuronal ensembles from various cortical areas. This prediction signal was then used to move a robotic arm in a remote location, demonstrating that sufficient information was present in the sample of Hatsopoulos and Donoghue. This study is an example of open-loop prediction but not of closed-loop control because the animal did not receive any form of sensory feedback from the robot and thus was unaware that it was moving the robotic arm. In contrast, a recent study demonstrated that a monkey could control the 3D position of a robot's end effector as well as its 1D gripper to feed itself [77]. This finding is qualitatively different from the Wessberg study because the animal's goal was to control the robot, and not its own arm, to grab the food and bring it to its mouth. This study is an example of a closed-loop control BCI.

Thus, in case of close-loop studies the subjects receive a sensory feedback and in open-loop experiments they don't received it, but they can observe the consequence of the action realized (visual feedback per example).

2_3) Clinical applications

Like their preclinical counterparts, the clinical BCI must have a sensor for recording signals, a decoding algorithm, an effector, and some form of feedback. Here, we emphasize those recently tested systems that are based on intracortical signals to derive commands because they establish a new link between human and nonhuman primate behavioural neurophysiology experiments. They provide insights into human neural processes not available from surface field potentials, which is the other main control signal source being tested for BCIs [78]. Kennedy [79, 80 and 81] developed the first spike-based approach for BCIs using a sensor of individually implanted microwires encased in glass cones so that neurites would grow into the cone and establish long-lasting connections to the nervous system. Using few channels, humans with tetraplegia from stroke or degenerative disease showed that they could activate spiking or local field potentials (LFPs) from cortical neurons to move a cursor.

An ongoing pilot study of the first human chronically implanted MEA-based BCI has made several advances in recording, decoding, and demonstrating potential use of a pilot BCI system. This system, termed BrainGate (see picture 4), is based on spiking signals recorded

from a 4 × 4 mm array of 100 Si microelectrodes in a fixed 10-by-10 arrangement placed within the motor cortex arm area.

Picture 4: Brain Gate systems (http://www.braingate.com/videos.html).

Studies to date utilizing four patients with tetraplegia have demonstrated participants' ability to produce two-dimensional cursor control that can be used to operate a computer and control a robot arm to perform simple grip and transport actions [82 and 2]. These studies demonstrated that both spiking and LFPs remain in motor cortex and can be volitionally modulated in the absence of movement, years after spinal cord injury [2 and 82] or stroke [83]. Patterns of activity appear to be similar to those observed in intact monkeys when movement is actually performed. This demonstration, that MI displays similar activity when movement is imagined and performed, raises fundamental questions about the nature of neural activity in MI and provides a key finding necessary for any further development of spike-based BCIs.

Control achieved by human participants using continuous control commands derived from linear decoders was quite similar to that achieved with the same algorithms in preclinical studies using able-bodied monkeys, discussed above [13, 14, 61 and 77]. Improvements in the decoders showed not only the ability to make smooth point-to-point movements, but also the ability to stop cursor motion and select targets by clicking on the basis of decoding an intended hand squeeze [83]. Using this improvement, a participant in three test sessions was able to point and click to one of eight screen targets, never selecting the wrong target and rarely (<4%) failing to make correct target selections. However, to achieve this success, movements were slow, taking 6.4 s, on average, to move from the middle of the screen to a target at the screen's edge and click on it.

2_4) Requirements of clinical applications

BCI system for the real life clinical applications must meet a set of limitations, such as health safety, real-live conditions reliability, as well as long-term stability. The main requirements imposed on the system can be summarized as follows:

_Safety (risks of surgical implantation, infection, etc.): As the system is interacting with a brain, the safety question has paramount value. Using of deeper brain layers for data acquisition be means of invasive techniques increases risks for health such as brain damage or infection.

_System long-time stability: BCI system has to work during long periods of time (years). Over this period, the signal can change significantly due to numerous reasons, such as brain plasticity, electrodes degradation, etc. All these effects have to be properly treated by the system.

_Real environment/real-time conditions: Real life imposes strong restrictions on the system. As opposed to laboratory conditions when a subject is concentrated on the task, external noises are minimized, and computational resources could be rather considerable, it is almost impossible to provide these circumstances in the real environment. Thereby, the system must be robust enough to guaranty functionality of BCI in presence of noise and spurious signals. Moreover, its response time should be sufficiently small to provide operability in the real time.

_Equipment complexity and expensiveness: Mass production and practical application determine limitations imposed on the complexity and cost of the system. In addition, it must be easy for everyday use.

As neural interface technologies are extended to control the numerous degrees of freedom (DOF) of the hand as well as the arm, many independent control signals should be extracted from a neural ensemble. The arm has seven DOF, whereas the hand has more than 20 DOF. Several psychophysical studies have indicated that natural grasp postures reside in a much smaller subspace of physically possible movements [84, 85 and 86]. Using principal components analysis, these studies have shown that a large proportion (>75%) of grasping behaviours can be accounted for with two or three principal components. With restricted goals, neural interface technology that currently can recover four DOF (3 spatial dimensions plus 1 grasp DOF) is not that far from controlling the apparent complexities of certain natural motor behaviours.

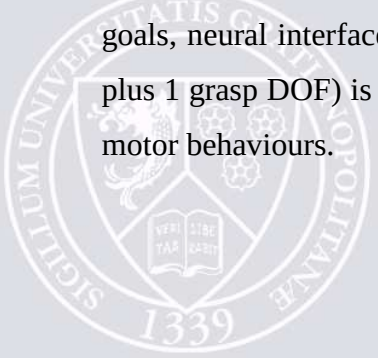

However, reach-to-grasp is only one category of neuroethological movement. Moreover, more encephalized vertebrates, particularly those with developed neocortex and rich cortico-spinal and corticomotoneuronal projections, can teach new arm and hand movements that include fractionated finger movements [87, 88 and 89]. The BCI paradigm may provide a unique opportunity to study the neuronal limits of independent control systematically.

In conclusion, every element of BCI system must be optimized. The use of a specific BCI model is a combination of technical choices (which type of brain signal is recorded and the quality of the signal, applicability in the real environment...) and criteria of safety for the patient.

Important technical issues must be addressed as BCIs become useful technologies for disabled patients. First, no multielectrode recording arrays have currently been fully verified to stably and reliably record action potentials from multiple single units for extended periods of time (over many years). Reliable chronic recording has been an area of considerable concern, although both cone electrodes [90] and MEA can record for many months in monkeys [91] and humans [83]. Ongoing testing of advanced and improved versions of these sensors will be required to achieve long-term viability of implants.

A second important technical challenge for a long-term human BCI is the creation of a fully implantable system that can provide high-bandwidth information. A fully implantable sensor is necessary to eliminate cabling, which limits mobility, as well as the need for percutaneous connectors, which can present an ongoing infection concern. In addition, implantable systems have the advantage that they are hidden from view, improving the cosmetic appeal of such systems. Creation of high-channel count, high-bandwidth implantable systems, which are required for spiking signals, is complex particularly because initial signal processing must now be completed inside the body. Active electronics of this complexity are difficult to seal fully, can induce excess heat, and require power and wireless communication.

3_Neuroplasticity

While in the past decade research on BCIs was primarily focused on providing alternative communication devices, recent years have witnessed a growing interest in extending the application range of BCI technology [92]. Among these new research directions, the use of BCIs for use or induce neural plasticity and restoring function has gained particular attention [93], as it substantially enlarges the size of the population that may benefit from BCI

technology. BCI technology could complement traditional rehabilitation efforts by providing patients with feedback on their brain states, which may be utilized to support the process of cortical reorganization required for functional recovery.

3_1) Physiologycal Neuroplasticity

The human brain is incredibly adaptive. The mental capacity is large and the ability to process widely varied information and complex new experiences with relative ease can often be surprising. The brain's ability to act and react in ever-changing ways is known, in the scientific community, as « neuroplasticity ». This special characteristic allows the brain's estimated 100 billion nerve cells to constantly lay down new pathways for neural communication and to rearrange existing ones throughout life, thereby aiding the processes of learning, memory, and adaptation through experience. Without the ability to make such functional changes, brains would not be able to memorize a new fact or master a new skill, form a new memory or adjust to a new environment.

Neuroplasticity is not a trait found in a single brain structure, nor does it consist of just one simple type of physical or chemical event. Rather, this ability, the plasticity, is the result of many different, complex processes that occur in our brains. A host of different structures and types of cells play some part in making neuroplasticity possible [94]. There are even different types of plasticity that, depending on one's age, are more or less involved in reshaping the brain as it handles new information. Plasticity works throughout the brain not just in the normal processes of learning and adaptation (most obvious in the early developmental years, though continuing throughout life), but also in response to injuries or diseases that cause loss of mental functioning [95, 96 and 97].

While genetics certainly play a role in establishing the brain's plasticity, the environment also exerts heavy influence in maintaining it. Environmental influence then plays the key role in forging a much denser, more complex network of interconnections. These smaller avenues and side roads, always under construction, can make the transfer of information between neurons more efficient and rich with situation-specific detail. This is clearly evidenced by the rapid increase in synaptic density that can be seen in a normally developing human. Genetics form a neural framework that, at birth, starts each neuron off with roughly 2,500 connections. By age two or three, however, sensory stimulation and environmental experience have taken full advantage of the brain's plasticity; each neuron now boasts around 15,000 synapses. This number will have declined somewhat by the time we enter adulthood, as many of the more

ineffective or rarely used connections formed during the early years, when neuroplasticity is at its peak.

Neuroplasticity can work in two directions; it is responsible for deleting old connections as frequently as it enables the creation of new ones. Through this process, called “synaptic pruning,” connections that are inefficient or infrequently used are allowed to fade away, while neurons that are highly routed with information will be preserved, strengthened, made even more synaptically dense. Closely tied in with the pruning process, then, is our ability to learn and to remember [98]. While each neuron acts independently, learning new skills may require large collections of neurons to be active simultaneously to process neural information; the more neurons activated, the better we learn.

While the precise mechanism that allows this process to occur is still unclear, some scientists theorize that long-term memories are formed successfully when something called “reverberation” occurs [99]. When we are first exposed to something new, that information enters our short-term memory, which depends mostly upon chemical and electrical processes known as synaptic transmission to retain information, rather than deeper and more lasting structural changes such as those mentioned above. The electrochemical impulses of short-term memory stimulate one neuron, which then stimulates another; the key to making information last, however, occurs only when the second neuron repeats the impulse back again to the first. This is most likely to happen when we perceive the new information as especially important or when a certain experience is repeated fairly often. In these cases, the neural “echo” is sustained long enough to kick plasticity into high gear, leading to lasting structural changes that hard-wire the new information into the neural pathways of our brains [100]. These changes result either in an alteration to an existing brain pathway, or in the formation of an all-new one. In this way, the new information or sensory experience is cemented into what seems, at its present moment, to be the most useful and efficient location within the massive neurocommunication network [101]. Further repetition of the same information or experience may lead to more modifications in the connections that house it, or an increase in the number of connections that can access it – again, as a result of the amazing plasticity of our brains.

3_2) Neuroplasticity associated with damages

Neuroplasticity is the saving grace of the damaged or disabled brain; without it, lost functions could never be regained, nor could disabled processes ever hope to be improved. Plasticity

allows the brain to rebuild the connections that, because of trauma, disease, or genetic misfortune, have resulted in decreased abilities. It also allows us to compensate for irreparably damaged or dysfunctional neural pathways by strengthening or rerouting our remaining ones. While these processes are likely to occur in any number of ways, scientists have identified four major patterns of plasticity that seem to work best in different situations. The case in which healthy cells surrounding an injured area of the brain change their function, even their shape, so as to perform the tasks and transfer the signals previously dealt with by the now-damaged neurons at the site of injury. This process, called "functional map expansion," results in changes to the amount of brain surface area dedicated to sending and receiving signals from some specific part of the body [102]. Brain cells can also reorganize existing synaptic pathways; this form of plasticity, known as a "compensatory masquerade," allows already-constructed pathways that neighbour a damaged area to respond to changes in the body's demands caused by lost function in some other area. Yet another neuroplastic process, "homologous region adoption," allows one entire brain area to take over functions from another distant brain area (one not immediately neighbouring the compensatory area, as in functional map expansion) that has been damaged [103]. And, finally, neuroplasticity can occur in the form of "cross model reassignment," which allows one type of sensory input to entirely replace another damaged one [104]. Cross-model reassignment allows the brain of a blind individual, in learning to read Braille, to rewire the sense of touch so that it replaces the responsibilities of vision in the brain areas linked with reading. One or several of these neuroplastic responses enable us to recover, sometimes with completeness, from head injury, brain disease, or cognitive disability.

Current research suggests that neuroplasticity may be key to the development of many new and more effective treatments for brain damage, whether resulting from traumatic injury, stroke, age-related cognitive decline, or any number of degenerative diseases (Alzheimer's, Parkinson's, and cerebral disease, among many others) [105]. Plasticity also offers hope to people suffering from cognitive disabilities such as dyslexia, and Down syndrome; it may possibly lead to breakthroughs in the treatment of depression, anorexia, and other behavioural and emotional disorders as well. Whether currently in use or only the product of futuristic hopes, the theory upon which harnessing the brain's plasticity is based is a relatively simple one. With "directed neuroplasticity," scientists and clinicians can deliver calculated sequences of input, and/or specific repetitive patterns of stimulation, to cause desirable and specific

changes in the brain. As further research reveals the best ways to create and direct these stimuli, the amazing potential of the brain's plasticity can begin to be taken advantage of in medicine, mental health, and a wealth of as-yet-uncharted territory in human behaviour and consciousness. Thus, increasing our understanding of neuroplasticity holds great promise through its complex workings skills lost can be relearned; the decline of abilities can be staved off, even reversed; and entirely new functions can even, perhaps, be gained.

At the present time, there remain many questions about how to best optimize an ECoG brain-computer interface. Specifically, it is still uncertain what frequency bands and power spectrum estimation algorithms are best suited for control. Choosing optimal control parameters is complicated by the cortical changes that occur once brain signals are directly used for a closed-loop BCI.

3_3) Importance of the feedback to induce efficient brain plasticity

When speaking of the induction of neural plasticity, it is important to be aware that neural plasticity may refer to a multitude of different processes of reorganization within the brain, each of which affects the way information is processed and may ultimately result in behavioural changes [106]. When investigating neural plasticity, it is thus crucial to precisely define what kind of metric is being used to measure experimental outcomes, e.g., whether changes are measured on a neuro-physiological or behavioural level. The induction of neural plasticity would correspond to the process by which lasting changes leading to desirable behavioural outcomes are caused by feedback of neural states. We consider any signal that is derived from recordings of the neural activity as a representation of a neural state. A BCI represents a system that provides a signal to its user that is a deterministic function of brain activity. According to this definition, any BCI constitutes a neuro-feedback system that may possess the capability of inducing neural plasticity. These considerations naturally lead to the question why neuro-feedback procedures may affect behaviour, the neural basis for inducing plasticity by means of BCI technology. This certainly constitutes a complex process, and may vary substantially across patient groups and experimental paradigms. One common concept crucial for the induction of neural plasticity may be that of Hebbian plasticity: coincident activation of pre-synaptic and post-synaptic neurons reinforces synaptic strength, resulting in increased and more reliable communication between the activated neurons. The potential relevance of this concept for changes in behaviour can be illustrated particularly well in the context of stroke rehabilitation [107]: assuming that the connection between peripheral

muscles and the sensorimotor cortex has been disrupted due to a sub-cortical stroke, a coincident activation of sensory feedback loops and primary motor cortex may reinforce previously dormant cortical connections by Hebbian plasticity and thus support functional recovery. Here, BCI technology may be used to detect primary motor cortex activation, movement intent, and provide matching sensory stimulation according to some haptic feedback procedures.

3_3_a) Feedback accuracy

It appears to be generally acknowledged that task learning requires accurate feedback. This also holds in the domain of BCIs, with recent evidence suggesting that subjects perform worse if they receive inaccurate feedback on their neural states [108]. While the relation of feedback accuracy and the induction of neural plasticity remain unexplored, it appears sensible to assume that a high degree of feedback accuracy, i.e. a low classification error, is crucial for inducing neural plasticity by means of BCI technology.

Accordingly, a BCI for communication as well as a BCI for rehabilitation aims for high classification accuracies. There is one potentially crucial difference, though, in which the latter may differ from the former. While only the objective classification accuracy is relevant for communication purposes, in a rehabilitation setting the subjectively perceived classification accuracy may have an impact on the induction of neural plasticity and thus on subsequent behavioural changes. While the objective and subjective feedback accuracy can be expected to be highly correlated, careful design of feedback procedures may have a beneficial impact on the perceived feedback accuracy for identical classification errors. Unfortunately, an investigation of the impact of the perceived feedback accuracy on the extent of behavioural changes in neurofeedback paradigms remains outstanding.

3_3_b) Feedback delay

If neural plasticity relies on Hebbian type learning rules, then the delay between the measurement of a neural state and the subsequent feedback of this state to the subject is of crucial importance. Any feedback that does not fulfill the requirement of coincident activation of the targeted brain regions is unlikely to result in long-term behavioural changes. This issue may be one cause of the so far only moderate success of utilizing BCI technology for stroke rehabilitation [109], as in these studies haptic feedback was not synchronized with movement intent. The maximum feedback delay that still induces coincident activation in the sense of Hebbian learning, however, remains unknown.

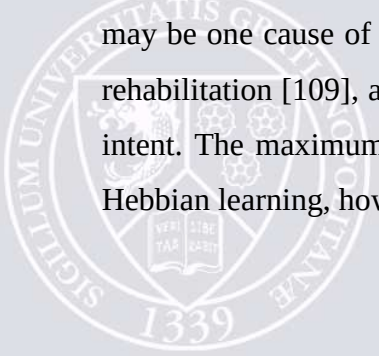

3_3_c) Choice of neural states for feedback

The choice of the signal modality (e.g., single cell recordings, fMRI, EEG, ECoG, or MEG), the brain areas from which signals are recorded, and the signal characteristics are utilized for providing feedback. In general, the choice of the neural states used for feedback may be driven by prior knowledge of desirable brain states, or it may be outcome driven. Certain target areas and signal characteristics may be identified in advance, and BCI technology may be designed to utilize these features only [110 and 111]. The drawback of this approach would be that the chosen brain areas and signal characteristics may not be optimal for providing accurate feedback. The outcome-driven determination of neural states, on the other hand, would aim to identify those brain states that are optimal for providing accurate feedback, at the probable expense of employing neural signals unsuitable for inducing beneficial changes in behaviour. For example, hemiparetic stroke patients who are being trained with a BCI based on motor imagery may learn to control the BCI by motor imagery involving ipsilesional cortical areas [112].

Furthermore, the type of feedback modality is likely to affect the perceived level of control over the BCI system as well as the feedback delay, both of which may influence the induction of neural plasticity [113]. It is at present unclear whether such factors can be optimized congruently. In general, the optimal design of BCI systems for inducing neural plasticity and restoring function is in its infancy, and many open questions remain to be answered by the BCI community.

III. MATERIALS & METHODS

1_Animals

All experiments are performed on female rats OFA (Oncins France strain A Charles River laboratories, Lyon France) weighting 250-300g. The rats are allowed to recover from surgery for a week. They have free access to food (SDS, Essex UK) and water; they are housed in GLP cages stored in an air conditioned closet (9ARMV2124LR, Techniplast France,) with temperature, light cycle and humidity control (12/12hours day night cycles; 25°C).

Ethical approval for all experimental procedures was obtained from ComEth (IRB of the University of Grenoble, France) following the FELASA (Federation of Laboratory Animal

Science Associations), in accordance with the European Communities Council Directive of 1986 (86/609/EEC) for care of laboratory animals.

2_Surgery protocol

Animals are anesthesied with chloral hydrate 4% (1ml/100g intraperitoneal) and placed on stereotaxic apparatus (David Kopf® Instruments, Tujunga, CA USA). An incision is realized on the top of the head, the muscles attached on the temporal face are separated to liberate the bone. 17 titanium self-tapering screw electrodes (3.6mm long, reference MXM: MP2997), including 3 references, were implanted into the bone through miniplates connected by a wire to a multipin SUBD connector (D micro pin 15Pts, Radiospare). Definite placements are referred to skull landmarks, (lambdatic and bregmatic sutures). The connector and all leads are included in a polymer (Methyl metacrylate polymer METHAX Generique International Laboratories). The screws allow ECoG recordings. To finish the skin is sutured around the connector.

The distribution of several electrodes permitted to record cerebral signals from different cortical regions of the brain (Figure 18).

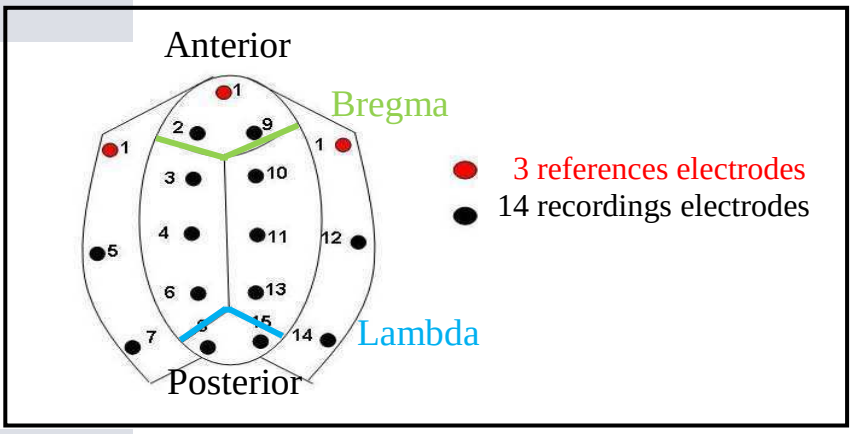

Figure 18: Localization of electrodes in rodents skull.

3_Experimental setup

Preliminary ECoG have been recorded on rodents placed in behavioural box (see picture 5). A Micromed® system (Micromed SD32, Micromed Italy, see picture 6) was used for ECoG recording.

The animal is trained to push on a lever to receive a reward (see picture 5). During training session, ECoG signals are recorded such as the indication of the push on the lever.

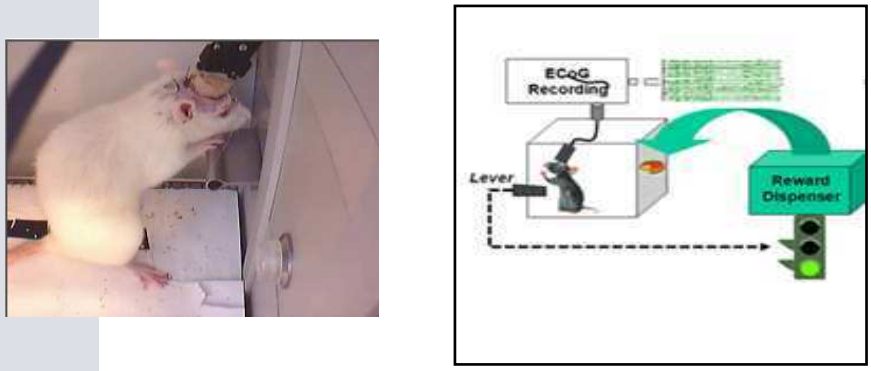

Picture 5: Rat pushing on the lever in a behavioural box and scheme of the behavioural task.

Picture 6: Acquisition systems (Micromed SD32, Micromed Italy).

4_Experimental set-up validation

Several tests are done before starting experiments, to check that no problems are present in the acquisition chain and system or on implanted electrodes.

The first test is to measure the noise of the electronic chain, at the end of the acquisition chain Where normally the head of the animal is connected, a mass is connected to all channels to estimate the noise generated only by the electronics elements (cables, amplifier, acquisition system etc. etc.). The noise is expressed in Root Mean Square (RMS), which is a standard and known unit in electronic studies. A second test done is to inject a current in all channels in order to check the current measured by the acquisition system and check that the current injected (1mV at 5 Hz by Tecktronic generator pulse) is measured correctly.

A last indicator permitted to check the state of the electrode just before starting experiments. The impedance is used to identify electrode disconnected or short circuited. The Micromed system is used to measure the impedance. The impedance is an indicator of the conductivity of the electrode and a value of 0 corresponds to short-circuit, and at the opposite a value too high indicate that the electrode is disconnected and record anything.

5_Visual Evoked Potential (VEP) and Sensitive Evoked Potential (SEP) experiments

Micromed system permits to done VEP (Micromed Flash 10S) and SEP (Energy light).

For VEP, luminous stimuli are applied in the behavioural box in front of the rodent with these parameters: 1Hz, 230mJ, 100 trials.

Concerning the SEP: Electrical stimulation is applied, bipolar electrodes planted in the hind paw to stimulate median nerve (1Hz, 5 volts and 200 microseconds pulse width, 300 trials). The brain activity in response of this electrical stimulus is known accurately (Micromed Energy light, Micromed, Italy).

6_Behavioural experiments

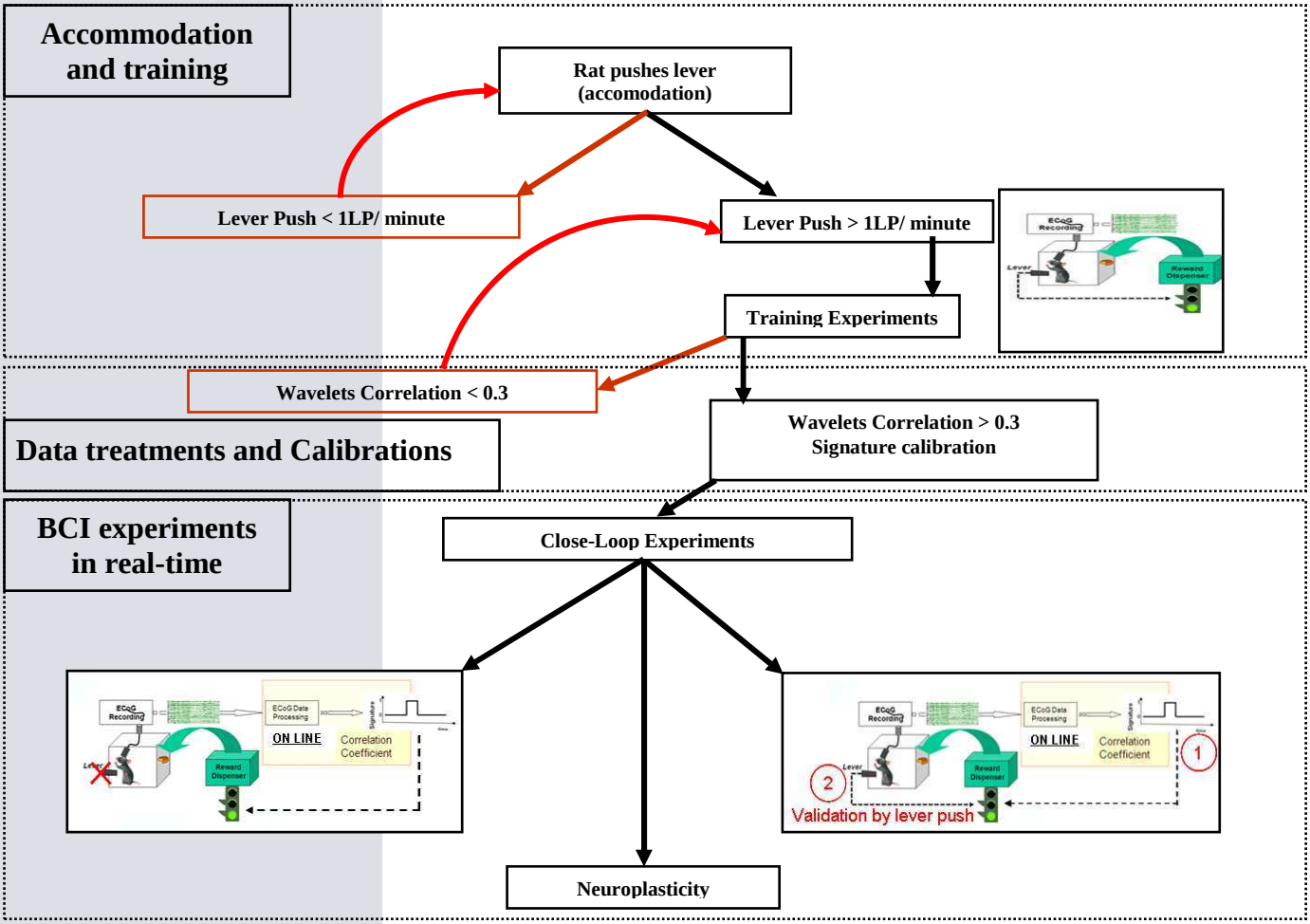

Figure 19: schematic representation of the experimental procedure.

The figure 19 illustrates the experimental protocol and represents schematically the different steps. Rats are previously acclimated to behavioural box (ABETT box, Lafayette Instruments, see picture 7) equipped with a lever triggering a food dispenser. The duration of this preliminary step is around 15 days (accommodation see figure 19). This can be initially a free running experiment to accustom the animal to this simple way to get a reward. ECoG brain activities are recorded during behavioural studies. Ten rats have been trained to realize this behavioural task. Experiments duration is around 40 minutes and they are done 3 times per week.

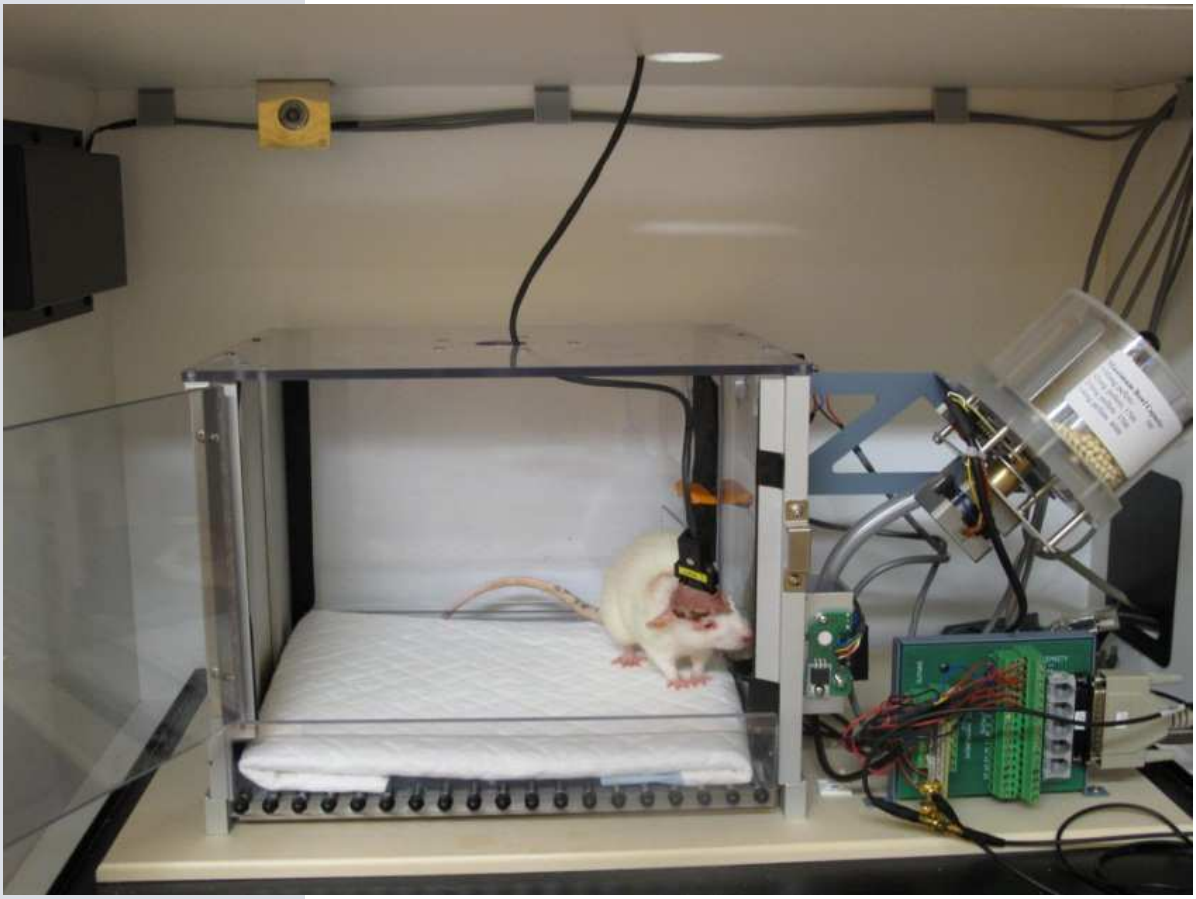

Picture 7: Behavioural box (ABETT).

The animals are ready to begin an experimental protocol when the number of pushes is around 1 per minute. The total time for one rat to be conditioned is around one month. These experiments are asynchronous (no cue).

A rodent, which presses the lever more than 1 time per minute, begin the training phase which consists on recordings brain activities during the behavioural experiments (push lever). These recordings are analyzed with mathematical treatment to identify specific brain signals correlated with the intention to press the lever. These specific brain signals are called signature.

Until Wavelets Correlation reaches about 0.3 (or more), the step for identify/calibrate the specific brain activity of the behavioural task can begin. If not (correlation less than 0.3), the animals stay longer in this step of training.

Once the calibration has been done, the close-loop experiments can be started. As described in the figure 19, several close-loop tasks have been designed.

The first correspond to the delivery of pellets directly by the detection of the signature calibrated just before. The food dispenser is triggered in real-time only by detection (left panel on figure 19).

A second behavioural task for close-loop experiment is the delivery of rewards by the combination of signature's detection followed by a lever push (right panel on figure 19). Both criteria must be presents.

These close-loop experiments will be analyzed with parameters defined in paragraph 9 below ("Evaluation of self-paced BCI performance") to know the quality of our BCI model.

A last step of close-loop experiments is indicated on the figure 19, it's the neuroplasticity study. The figure below (figure 20) represents the principle of this study.

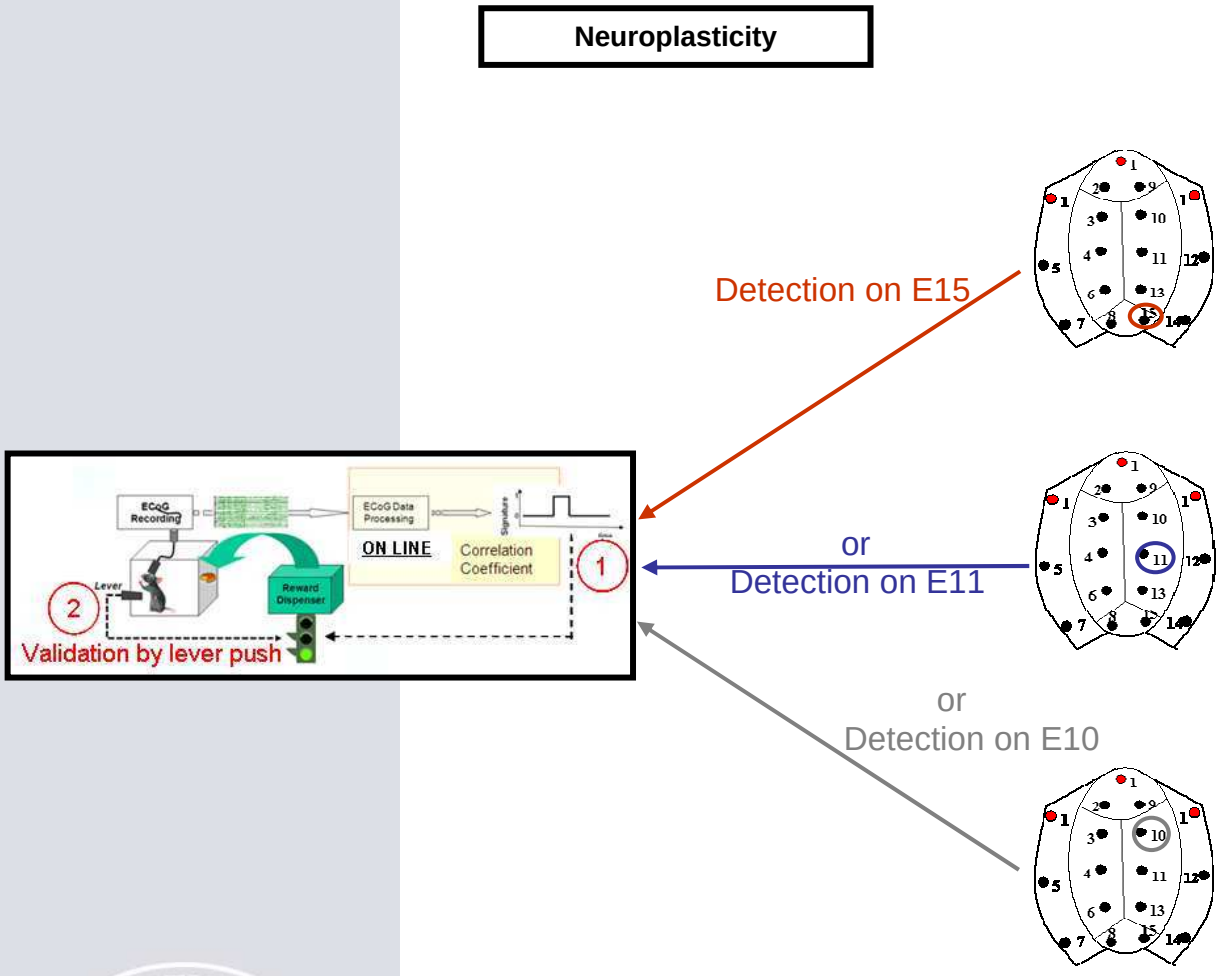

Figure 20: schematic representation of the protocol of neuroplasticity.

The behavioural task implicated here is the delivery of pellet by the combination of the detection of the signature and the validation by the rat in pressing the lever. The important modification is the use of different signatures. These signatures are identified in different areas of the brain corresponding to the signal recorded on different electrodes during training experiments (see figure 20).

Another aim of this study is to try to detect a signature in another area where this signature has been identified/calibrated. For example, the signature calibrated on the Electrode 15 (which serves to detect the signature in behavioural close-loop experiments done, see figure 19) is used in neuroplasticity close-loop experiments but this signature is detected in real time on another electrode (in a first time by electrode 11, then by the 10).

7_Data treatment

BCI signal processing consists in a) off-line data analyses and b) real-time signal processing during the self-paced BCI experiments. In both cases of online and offline analyses signals were down sampled to 1.3kHz and band-pass filtered in the range 10Hz - 300Hz. Common Average Reference (CAR) procedure (i.e., signal averaged among all the electrodes was subtracted) allows eliminating a “common source” and improve signal-to-noise ratio. Then Continuous Wavelet Transform (CWT) with 2Hz frequency bins is applied for time-frequency analysis.

ECoG activity and lever push are recorded all along the experimental sessions and are processed off-line:

-to calculate time shifted cross correlation of ECoG recordings followed CWT and lever pushes for each electrode. The best electrode is used as predictor provider.

-to identify specific predictor for each animal with training data set. The features corresponding to significant changes in ECoG signal are recognized by calibration algorithm as lever push related and automatically extracted.

-to validate the predictor with new recordings. Off-line simulation of BCI experiments, playing back the recordings with predictor detection, allows counting correct and false detections and estimating the performance of predictor.

During all experimental sessions, the ECoG activity on each 14 active electrodes is cross-correlated to the lever push to detect the electrode on which the best correlation is occurring. This allows recognizing the electrode on which the further step, predictor determination, is

performed by the calibration procedure.

BCI system calibration, i.e., an adjustment of the internal system parameters to an individual brain, is achieved using the training data set collected during behavioural experiments at the beginning of the series for a given animal. It consists in extracting from the ECoG recording the features related to BCI events, identification of predictive model for lever pushing depending on ECoG features and determining of the decision rule to produce control commands (reward delivery) during the real time BCI experiments.

The experiments provided recordings of brain activity in different cortical areas. To analyze the recordings, mathematical algorithms have been used. The principle of the algorithms is to research modifications in the electrical signals related to the action realized by the animal in pushing the lever to obtain a reward. The offline ECoG data processing provides the correlation coefficient between the two events (lever push and ECoG) for all electrodes. This analysis of brain recordings permitted to identify a cerebral signal in correlation with the push. This signal is called « signature ».

8_Evaluation of self-paced BCI performance

Binary BCIs classifies incoming data epochs on two types, based on presence or absence of some specific activity (for instance, behaviour activity). Every entering recording epoch is classified as “event” or “non-event”.

Another important characteristic of BCI performance, which should be taking into account, is decision rate, i.e., amount of decisions produced per a unit of time. It could be identical to the sampling rate of the input signal [28] or decimated to some extend [11]. It is clear that the more is decision rate the more absolute amount of errors could be made. Thus, it should be taken into account.

Following characteristics are used for evaluation of produced classification (see figure 21): Event corresponds to Lever Push, detection corresponds to signature detected.

	Event	Non-event
Event detection	TP (correct detection)	FP (false activation)
Event rejection	FN (event missing)	TN (correct rejection)

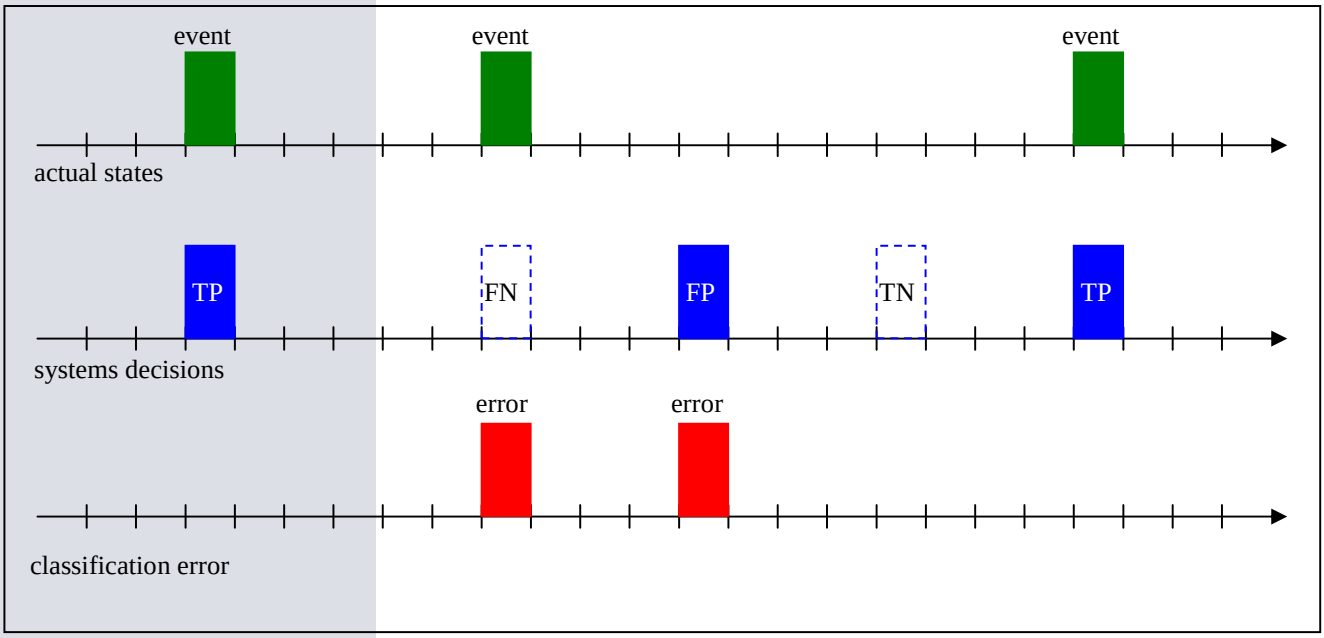

Figure 21: schematic representation of the parameters used to evaluate our BCI model.

_True Positive (TP), which is equal to amount of correctly detected “events”;

_True Negative (TN), which is equal to amount of correctly detected “non-events”;

_False Positive (FP), which corresponds to amount of non-event situations detected as “events”;

_False Negative (FN), which is missed “events” amount.

On the basis of these values, several more complicated characteristics for system evaluation could be involved. Among the most frequently used are [28, 114 and 115]:

_True Positive Rate (TPR): TPR = TP/(TP + FN)

_False Positive rate: FPR = FP/(TP + FP)

_Positive Predictive Value (Precision): PPV = TP/ (TP + FP) = 1 - FPR

_False Negative per minute: FP/min

In all studies realized, two parameters for evaluation of the BCI model are used, TPR and PPV. In addition, their average permitted the evaluation of the overall performance (OP) of BCI:

$$OP = (TPR + PPV) / 2$$

9_ Statistical significance and expected random detection

To analyze the statistical significance of the TP detection rate, the results were compared to random detection. The level of random TP detection was estimated for each recording. To this purpose Events and Detections were considered as random and independent (yes/no) with frequencies calculated for each recording.

Mean value of random TP is estimated taking into account that Detection is considered as TP if it occurs during ±1.5 sec time interval before/after Event. Corresponding confidence intervals are calculated from the binomial distribution (Binomial distribution describes series of Bernoulli trials). In this study the confidence level was set at 0.95.

10_Statistical analyses

Some statistical tests have been done to check the specificity of several results (correlation values for example). The Anova (ANalys Of VAriance) has been used.

11_Histological procedure

The behavioural experiments duration is around 8 months after implantation on animals aged of 8 months, the end of protocols is caused by old age.

Animals are euthanized by an overdose of chloral hydrate 4%, exsanguinated during 15 minutes with a flow of 16ml/minute and perfused with Paraformaldehyde (PFA) 4% during 15 minutes with the same flow. The head of the rats are placed in PFA 4% during 24h. The brain is dissected and placed in PBS with 30% sucrose during 24-48h and placed at -80°C.

The brain is cut in slices of 30µm thick for immuno-stainings: cresyl violet and hematoxylin.

The cresyl violet solution:

Acetate cresyl violet 0.5g (Sigma C5042), Acetate of sodium 0.1025g (Sigma S2889), Acetic acid 1.5ml (Sigma 242853) and complete with H_2O until 500ml. Shake during 5 hours and adjust pH to 3.5.

The cresyl violet staining:

The brains slices are put in cresyl violet during 5 minutes at room temperature and washed in 2 consecutives bath of H_2O. To finish the slices are immerged in a bath of ethanol 70% during 10 seconds and in a bath of ethanol 100% during 10 seconds at room temperature.

IV. RESULTS

1_Implantation and functional localization of electrodes

As described in Materials and Methods, seventeen screws are implanted thought the bone to record ECoG signals, including 3 reference electrodes (Figures 18, 22A and 22B). The functional localization of the electrodes (Figure 22B) was achieved by comparison with atlas (Figure 22C).

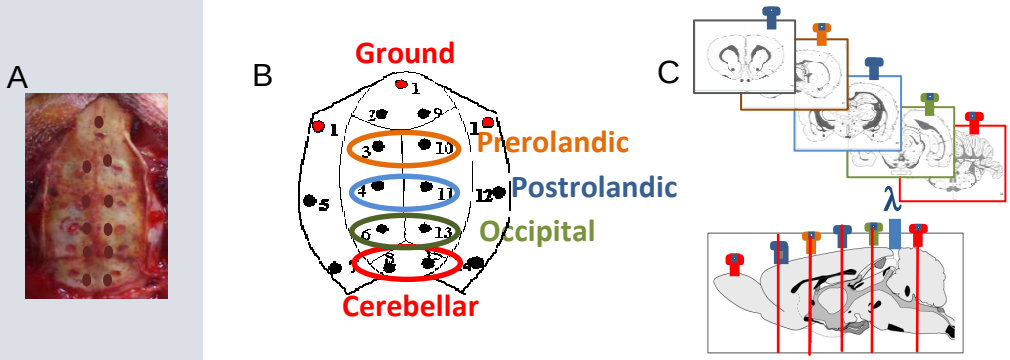

Figure 22: Implantation of electrodes.

A: Distribution of electrodes on the skull. B: from back to front, the electrodes are situated over the cerebellar cortex (behind Lamba, 8 and 15), the cerebral occipital cortex (visual area, 6 and 13), the postrolandic or postcentral cortex (4 and 12), then the prerolandic or precentral cortex (3 and 10), and the prefrontal cortex (2 and 9). 4 additional electrodes are temporal, left and right: 5 and 12 temporal anterior, 7 and 14 temporal posterior. C: Anatomical distribution of the electrodes as compared to atlas structures (L. Swanson plates) shown as coronal sections (above) and on a sagittal view of the brain (below), relative to the Lambda Suture.

VEP and SEP tests are done to check the functional localization of electrodes.

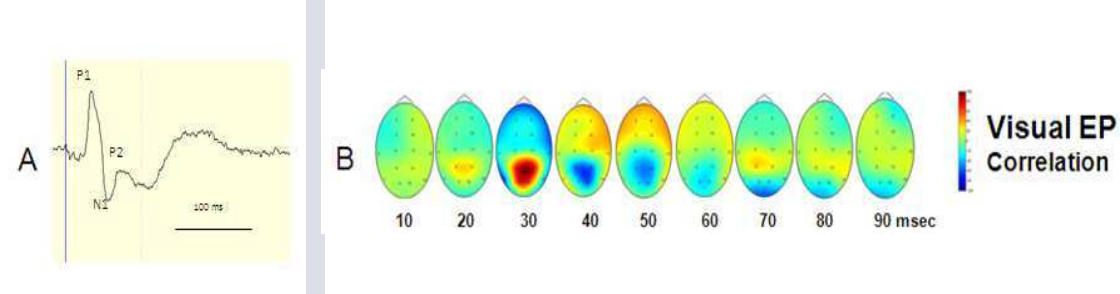

Figure 23: Visual Evoked Potential obtained by Flash light stimulation (1Hz, 100 flashes) A: average of 100 VEPs, B: Topoplot representation of the temporo-spatial distribution of VEP.

Visual occipital cortex electrodes (6 and 13) exhibit maximal amplitude potential evoked by flash light stimulation at 1Hz, obtained by ECoG signal averaging, with a first positive deflection P1 with a latency of 56.6 msec and and a negative potential N1 with a latency of 31.2 msec (see figure 23).

	P1 latency (ms)	N1 latency (ms)
Rat 1 (n=10)	36,67	60,67
Rat 2 (n=10)	37,33	56,67
Rat 3 (n=10)	34,00	56,33
Rat 4 (n=10)	30,00	52,67
Rat 5 (n=10)	32,00	54,33
Rat 6 (n=10)	28,67	52,33
Average	33,11±3,52	55,50±3,1

Table 1: Latencies of P1 and N1 of VEPs in the different animals.

The average values obtained in the different animals are shown in table 1 and the average P1 occurs at 33,11 ms and the N1 at 55,5 ms.

The largest SEP (about P1 at 19msec and N1 at 39msec) are also mostly visible on electrodes 6 and 13 (see figure 24).

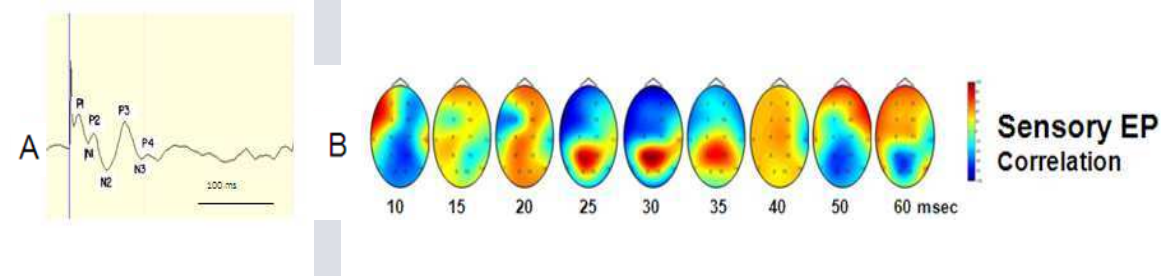

Figure 24: Somatosensory Evoked Potential obtained by electrical stimulation.
A: average of 300 SEPs. B: Topoplot representation of the temporo-spatial distribution of SEP.

The average values obtained in the different animals are shown in table 2.

	P1 latency (ms)	N1 latency (ms)
Average (6 animals, 30 experiments)	12,92±2,29	49,5±3,11

Table 2: latencies of P1 and N1 of SEPs.

Co-localization of the visual and sensory responses is observed (see topoplots Figure 23B and 24B) corresponding to electrodes 6 and 13.

2_Brain Computer Interface experiments

2_1) Validation acquisition chain

All the channels are connected to the mass and noise level is measured with the RMS indicator. The results show about 1,6µV RMS (corresponding to an amplitude around 10µV) and that each channel is well connected or no.

2_2) Training experiments

2_2_a) Protocol

Basically rodents stay in a behavioural box and are trained to push on a lever to deliver a reward (see figure 25).

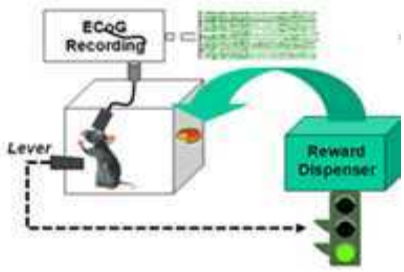

Figure 25: schematic representation of the phase of training. Within the experimental set-up, the rat presses a lever which delivers a square pulse activating the reward dispenser which delivers a food pellet.

2_2_b) Results

The number of pushes (NP) increases along time (see figure 26) and consistently starting about 1 push per minute which is a necessary parameter to start the training behavioural experiments (see figure 15).

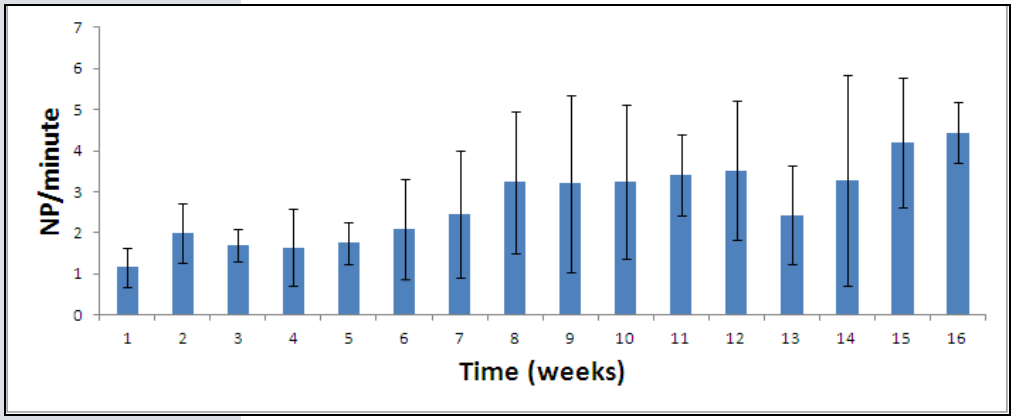

Figure 26: Evolution of pushes number along time (n=4 animals, 38 experiments for each).

The cross-correlation function between the lever push events and the ECoG activity preceding the event is maximal on the most posterior electrodes 8 and 15 (see figure 27).

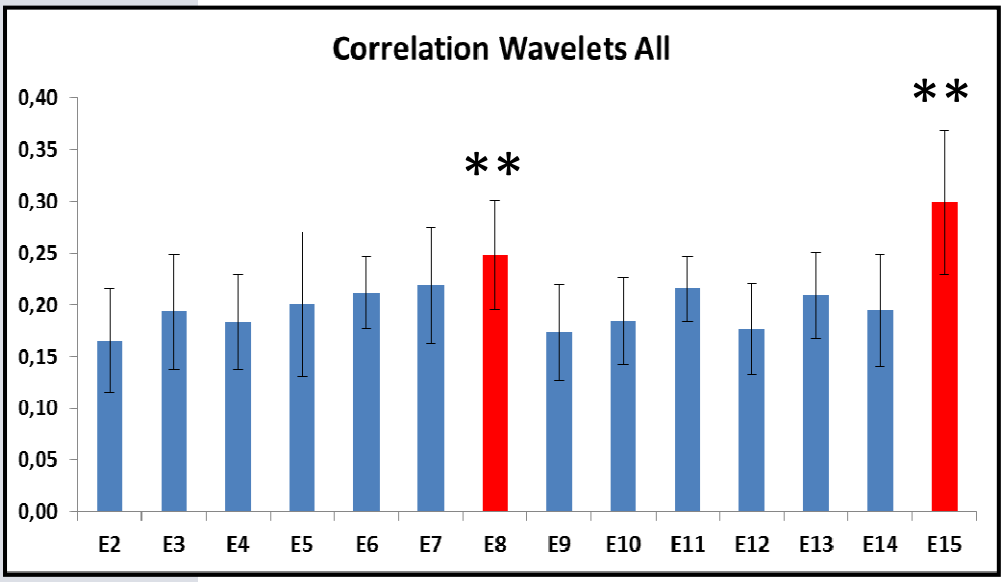

Figure 27: Histograms of the mean correlations values obtained by analysis of ECoG signals with algorithms on the 14 electrodes (n=10 rats).

The average of the maximal correlation is 0,3 ± 0,08 as shown in table 3 with the detailed results for each animal.

Correlation E15	
Rat 1 (n=41)	0.41±0.11
Rat 2 (n=63)	0.32±0.09
Rat 3 (n=32)	0.29±0.06
Rat 4 (n=32)	0.21±0.04
Rat 5 (n=32)	0.24±0.05
Rat 6 (n=32)	0.22±0.05
Rat 7 (n=25)	0.27±0.07
Rat 8 (n=38)	0.34±0.15
Rat 9 (n=56)	0.4±0.11
Rat 10 (n=25)	0.28±0.1
Average, SEM	**0.3±0.08**

Table 3: Values of best correlation (E15) for all animals in table 3.

The results in table 3 show differences between animals. The best correlations obtained are with the rat 1 and 9 with 0.41±0.11 and 0.4±0.11 respectively (41 and 56 experiments analyzed) and the smallest value is observed with rats 4 and 6 with 0.21±0.04 and 0.22±0.05 respectively (32 and 32 experiments analyzed). The correlation for the rats 2, 3, 5, 7, 8 and 10 are respectively 0.32±0.09, 0.29±0.06, 0.24±0.05, 0.27±0.07, 0.34±0.15 and 0.28±0.1.
The average value for the 10 rats (0,3 ± 0,08) corresponds to 376 experiments analyzed.

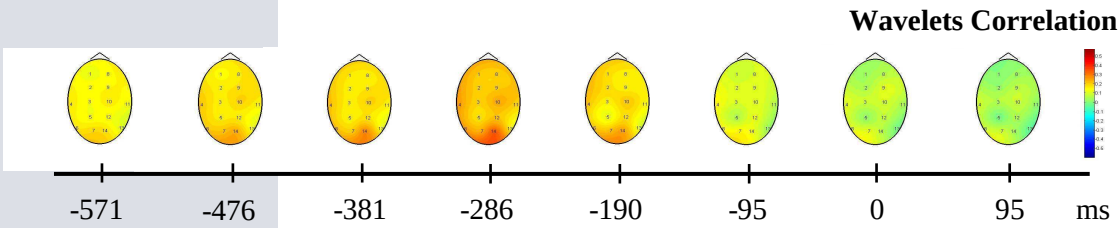

Figure 28: Example of spatial distribution of the correlation values along time in one experiment.

This topoplot (figure 28) shows the evolution of the correlation on all electrodes recording, the value of correlation is indicated by a color code (maximal values in red) and the time by a scale below (in ms). The time 0 correspond to a lever push. Electrodes 8 and 15 show the maximal correlation around 333ms before the lever push in this example.

	Time mean (ms before lever)	**Frequency mean (Hz)**
Rat 1 (n=16)	566±307	244±61
Rat 2 (n=16)	115±125	147±39
Rat 3 (n=16)	768±327	198±89
Rat 4 (n=16)	568±242	153±76
Rat 5 (n=12)	637±271	168±80
Rat 6 (n=28)	591±252	158±78
Rat 7 (n=28)	929±497	169±73
Rat 8 (n=28)	482±411	178±97
Rat 9 (n=28)	367±204	210±92
Rat 10 (n=28)	700±456	144±63
Average, SEM	**572±207**	**177±36**

Table 4: Values of frequency and time for the best correlation (E15) for all animals.

The results showed that wavelets correlation is maximal around 572 ± 207 ms before the lever push, in a frequency band of 177 ± 36 Hz (n=10 animals and 376 experiments in total, see table 4 for all results).

There are inter-animals variations, one animal (rat 2) shows shorter time between correlation and lever push : 115±125 ms and another animal (rat 7) presents longer time: 929±497 ms.
Concerning the frequency band of interest, there are less differences between animals. The high frequencies are concerned for the 10 rats (177 ± 36 Hz).

For each animal, the training experiments and the correlation analyses permit us to identify a brain activity correlated with the intention to press the lever to obtain pellets and maximal on E15.

2_3) Identification and calibration of a signature

2_3_a) Protocol

Wavelets analysis has been developed by the signal processing team to analyze the signals ECoG. The algorithm is based on a multimodal approach. It consists in simultaneous analysis of temporal, frequency and spatial dynamics of the signal represented by its continuous wavelet or spectrum decomposition. Then, signal data are mapped to a 4^{th} order tensor. To build a linear model for event classification, Iterative modification of the Multi Way Partial Least Squares Regression is applied to the obtained tensor.

2_3_b) Results

This treatment has been used to identify brain signals correlated with lever push intention, called **signature** which served in behavioural experiments. Only one electrode has been used to detect the signature. The electrode 15 has been chosen because the maximal correlation value in training experiments have been obtained on this electrode (se figure 27 and table 3).
Signature can be represented by several influence factors [116].
Some signatures have been identified for each rodent (n=10) and the mean factors with the standard deviation representing the signatures are shown in figure 29.

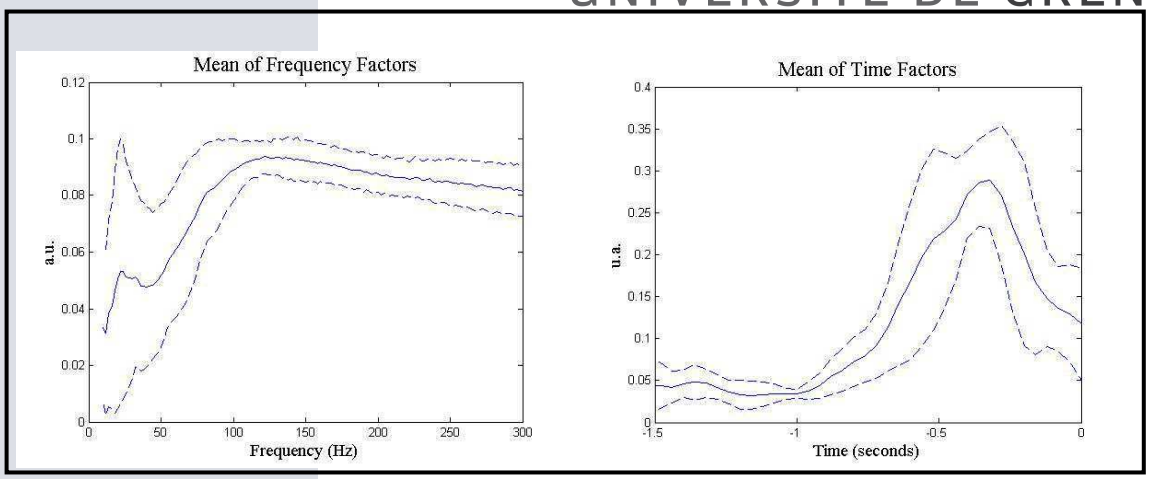

Figure 29: Means Factors of signatures identified in 10 animals and standard deviation (dotted).
A: Frequency factor; B: Temporal factor

The principal frequency band of interest of these signatures is between 50Hz to 300Hz and all signatures occur about 400ms preceding the lever push corresponding to point zero. For each animal an optimal signature has been identified and is stable along the time.
However the signatures are different between animals but have important similarities (bandwidth of interest, time delay), as we can see in figure 29.

2_4) Use of the signature calibrated in off-line analysis

2_4_a) Protocol

To estimate the quality and specificity of signatures, the previous ECoG recordings of training experiments are analyzed with several efficiency parameters as described in Materials & Methods.

2_4_b) results

In a first time, these off-line analyses permitted to choose the best signature for each animal and the results are presented in table 5 for one animal. The same experiments are treated in offline analysis but with signatures calibrated at different time (different experiments are used for the calibration of different signatures for the same animal).

	TPR (%)	FP/min	FPR(%)	PPV(%)	OP(%)	Push/minute
Signature 1	55,46±9,07	3,31±1,93	2,83±1,68	31,13±18,04	43,29±12,81	2,54±1,56
Signature 2	54,72±9,69	2,93±1,86	2,5±1,61	32,22±14,8	43,47±10,8	2,54±1,56
Signature 3	57,68±8,31	2,9±1,33	2,47±1,15	32,04±13,5	44,86±10,45	2,54±1,56
Signature 4	64,28±7,96	2,22±0,99	1,89±0,85	41,92±14,43	53,1±10,37	2,54±1,56

Table 5: Table represents datas for one animal (rat 9) for off-line analysis of experiments with different signatures. For each signature, the same 20 experiments have been analyzed.

For the rat 9, four different signatures have been calibrated and 20 experiments have been analyzed (off-line).The efficiencies of these different signatures, for the same animal, show important variations on the parameters observed. The number of push per minute is 2,54±1,56 and is the same for the four signatures because the same 20 experiments have been analyzed.

For this animal, the signature 1 shows 55,46±9,07 of TPR, 3,31±1,93 FP/min, a PPV of 31,13±18,04 and a OP of 43,29±12,81.

The signature 2 shows 54,72±9,69 of TPR, 2,93±1,86 FP/min, a PPV of 32,22±14,8 and a OP of 43,47±10,8.

The signature 3 shows 57,68±8,31of TPR, 2,9±1,33 FP/min, a PPV of 32,04±13,5 and a OP of 44,86±10,45.

The signature 4 is the better signature and shows a TPR of 64,28±7,96, which is higher than the previous results obtained with first three signatures. This TPR is associated with 2,22±0,99 FP/min, which is the lower obtained with the four signatures. The PPV is 41,92±14,43, which correspond also at the best PPV of the 4 analysis. The OP is 53,1±10,37.

The results for these four signatures show that 2 signatures give lower TPR associated with higher FP/min. These two signatures (called 1 and 2 in the table) are evaluated less efficient than the others. The quality of the signature is dependent of both criteria: high TPR and low FP/min. This combination is necessary for a good performance of our BCI. A high TPR associated with a high number of FP/min could be unsatisfactory for clinical applications (in our example the signature 3).

The signature 4 presents the best results in all parameters observed and it will be used in future BCI experiments.

In a second time, after having identified the optimal signature for each animal, this optimal signature is used to analyze all the experiments, 10 animals with 10 optimal signatures (each animal has its own signature). All the results are presented in table 6.

	TPR (%)	**FP/min**	**FPR(%)**	**PPV(%)**	**OP(%)**	**Push/minute**
Rat1 (n=16)	67,99±11,64	2,44±0,67	2,10±0,6	47,20±6,87	57,60±7,38	3,39±1,43
Rat2 (n=16)	68,95±4,64	2,36±0,65	2,03±0,57	48,98±5,81	58,96±4,27	3,31±1,01
Rat3 (n=16)	65,23±5,39	2,42±0,78	2,07±0,68	41,83±7,32	53,53±4,93	2,76±1,2
Rat4 (n=16)	64,19±4,8	2,23±0,79	1,90±0,7	40,77±8,35	52,48±5,42	2,56±1,35
Rat5 (n=12)	77,95±12,40	0,83±0,35	0,72±0,31	78,93±10,3	78,44±11,27	4,54±1,95
Rat6 (n=29)	64,44±19,86	1,79±0,78	1,53±0,68	47,37±17,5	55,90±17,73	2,92±1,73
Rat7 (n=27)	69,04±7,76	2,53±0,98	2,19±0,83	54,12±15,85	61,58±10,81	4,47±1,68
Rat8 (n=22)	63,79±5,77	2,39±0,79	2,08±0,79	51,16±17,51	57,47±10,38	4,53±2,62
Rat9 (n=35)	67,98±8,09	2,17±0,97	1,86±0,82	50,42±20,44	59,2±12,52	3,52±2,08
Rat10 (n=17)	68,66±9,87	2,5±1,24	2,16±1,04	51,94±23,63	60,3±15,15	4,11±2,17
Average (n=206)	**67,82±4,13**	**2,17±0,52**	**1,86±0,44**	**51,27±10,6**	**59,55±7,22**	**3,61±0,76**

Table 6: Table represents datas for each animal for off-line analysis of experiments.

The rat1 shows a TPR of 67,99±11,64 associated with a FP/min of 2,44±0,67 and a PPV of 47,20±6,87. The OP for this animal is 57,60±7,38 and the push per minute is 3,39±1,43.
The rat2 shows a TPR of 68,95±4,64 associated with a FP/min of 2,36±0,65 and a PPV of 48,98±5,81. The OP for this animal is 58,96±4,27 and the push per minute is 3,31±1,01.
The rat3 shows a TPR of 65,23±5,39 associated with a FP/min of 2,42±0,78 and a PPV of 41,83±7,32. The OP for this animal is 53,53±4,93 and the push per minute is 2,76±1,2.
The rat4 shows a TPR of 64,19±4,8 associated with a FP/min of 2,23±0,79 and a PPV of 40,77±8,35. The OP for this animal is 52,48±5,42 and the push per minute is 2,56±1,35.

The rat5 shows a TPR of 77,95±12,40 associated with a FP/min of 0,83±0,35 and a PPV of 78,93±10,3. The OP for this animal is 78,44±11,27 and the push per minute is 4,54±1,95. This animal presents the best results for all parameters.
The rat6 shows a TPR of 64,44±19,86 associated with a FP/min of 1,79±0,78 and a PPV of 47,37±17,5. The OP for this animal is 55,90±17,73 and the push per minute is 2,92±1,73.
The rat7 shows a TPR of 69,04±7,76 associated with a FP/min of 2,53±0,98 and a PPV of 54,12±15,85. The OP for this animal is 61,58±10,81 and the push per minute is 4,47±1,68.
The rat8 shows a TPR of 63,79±5,77 associated with a FP/min of 2,39±0,79 and a PPV of 51,16±17,51. The OP for this animal is 57,47±10,38 and the push per minute is 4,53±2,62.
The rat9 shows a TPR of 67,98±8,09 associated with a FP/min of 2,17±0,97 and a PPV of 50,42±20,44. The OP for this animal is 59,2±12,52 and the push per minute is 3,52±2,08.
The rat10 shows a TPR of 68,66±9,87 associated with a FP/min of 2,5±1,24 and a PPV of 51,94±23,63. The OP for this animal is 60,3±15,15 and the push per minute is 4,11±2,17.

The average percentage of TPR is **67,82±4,13** with **2,17±0,52** FP/min and a PPV of **51,27±10,6**. The OP average for all animals is **59,55±7,22** with an average push per minute of **3,61±0,76.**
The number of FP per minute is always low as described in the table 6, the average FP/minute is: **2,17±0,52**, knowing that the system makes one decision for each interval of 500 ms thus 2 decisions by second (with a maximum of 120 per minute).
The number of push per minute is consistent for all animals (3,61±0,76) and make the results more robust.

2_5) Study of the signature in off-line experiments

2_5_a) Protocol

Off-line analysis using signature calibrated in different frequency band have been done, the aim is to understand if a frequency band in particular is more important than the others. The major frequency band of interest is between 50Hz to 300Hz and all signatures are presents about 400ms preceding the lever push corresponding to the zero (figure 29).
The efficiencies of a same signature calibrated in different frequency bands are compared to confirm that the band used in our experiments (10-300Hz) is the optimal factor. In the figure 30, all the frequency bands tested in off-line analyses are presented.

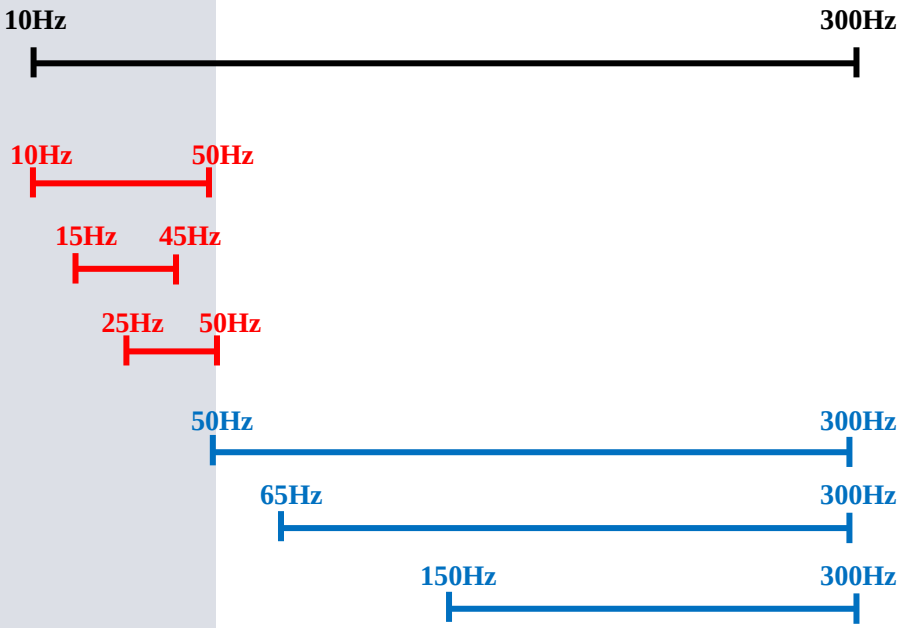

Figure 30: The different frequency bands used to calibrate signature (all values are in Hz). The black line represents the complete frequency band (10 to 300Hz). The red lines correspond to the low frequencies bands used during calibration. And the blue lines show the high frequencies bands.

2_5_b) Results

27 experiments (rat 7) have been treated in off-line analysis with the different signature calibrated. The comparison with the results obtained with the complete frequency band: 10-300Hz (see rat 7 on table 6) permits us to observe the importance of the frequency band used during calibration. In a first time, some signatures for the rat 7 have been calibrated in low frequencies bands, see table 7.

15Hz-45Hz			
TPR	**FP/min**	**PPV**	**OP**
58,15	3,67	41,51	49,83
5,15	1,27	14,84	8,56

10Hz-50Hz			
TPR	**FP/min**	**PPV**	**OP**
57,41	3,43	42,48	49,95
4,28	1,16	14,23	7,24

25Hz-50Hz			
TPR	**FP/min**	**PPV**	**OP**
55,70	4,98	33,06	44,38
3,57	1,12	12,08	6,12

Table 7: Table represents data for animal 7 for off-line analysis of 27 experiments with 3 different signatures calibrated in low frequencies bands: 10-50Hz, 15-45Hz and 25-50Hz.

The results of off-line analysis with the signature calibrated in 15-45Hz show a TPR of 58,15±5,15 associated with a FP/min of 3,67±1,27, a PPV of 41,51±14,84 and a OP of 49,83±8,56.

The results of off-line analysis with the signature calibrated in 10-50Hz show a TPR of 57,41±4,28 associated with a FP/min of 3,43±1,16, a PPV of 42,48±14,23 and a OP of 49,95±7,24.

The results of off-line analysis with the signature calibrated in 25-50Hz show a TPR of 55,7±3,57 associated with a FP/min of 4,98±1,12, a PPV of 33,06±12,08 and a OP of 44,38±6,12.

The off-line analysis of 27 experiments with signatures calibrated in low frequencies show poorer results than results obtained with complete signature (10-300 Hz, see results in table 6 rat 7).

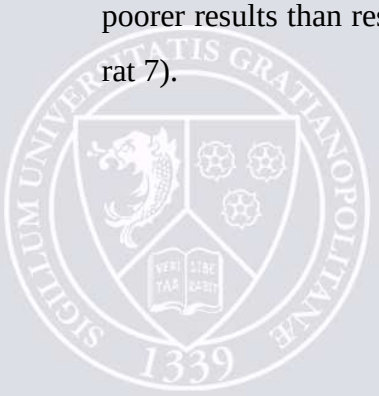

50Hz-300Hz			
TPR	FP/min	PPV	OP
61,60	3,71	46,85	54,22
6,66	2,62	15,81	9,85

65Hz-300Hz			
TPR	FP/min	PPV	OP
63,66	4,05	45,91	54,79
8,32	3,23	16,48	10,59

150Hz-300Hz			
TPR	FP/min	PPV	OP
60,82	4,36	43,34	52,08
8,36	3,05	17,12	10,20

Table 8: Table represents data for animal 7 for off-line analysis of 27 experiments with 3 different signatures calibrated in high frequencies bands: 50-300Hz, 65-300Hz and 150-300Hz.

The results of off-line analysis with the signature calibrated in 50-300Hz show a TPR of 61,6±6,66 associated with a FP/min of 3,71±2,62, a PPV of 46,85±15,81 and a OP of 54,22±9,85.

The results of off-line analysis with the signature calibrated in 10-50Hz show a TPR of 63,66±8,32 associated with a FP/min of 4,05±3,23, a PPV of 45,91±16,48 and a OP of 54,79±10,59.

The results of off-line analysis with the signature calibrated in 25-50Hz show a TPR of 60,82±8,36 associated with a FP/min of 4,36±3,05, a PPV of 43,34±17,12 and a OP of 52,08±10,2.

The off-line analysis of 27 experiments with signatures calibrated in high frequencies show poorer results than results obtained with complete signature (10-300 Hz, see results in table 6 rat 7), in particular concerning the parameters of FP/min..

These off-line results (see table 7 and 8) demonstrate that the signature used must be calibrated in the frequency band: 10 to 300 Hz. The others bands used, have shown less efficiency. The use of high frequency band (65-150 or 150-300 or 50-300 Hz) illustrates that the weight of the high frequencies are very important (the TPR is higher for high frequencies than for low frequencies), but the use of low frequencies is necessary to obtain high TPR and low FP/min.

The best parameters for the signature are the use of the frequency band 10 to 300 Hz for the calibration. In conclusion, all future experiments will be done with signatures calibrated in using the frequency band 10-300 Hz.

2_6) Use of the signature on-line to control an external effector

The aim of the next phases is to test the efficiency of the signature in real time close-loop experiments.

2_6_a) First protocol

The delivery of pellet is controlled by cerebral activity (the lever is disconnected, see figure 31).

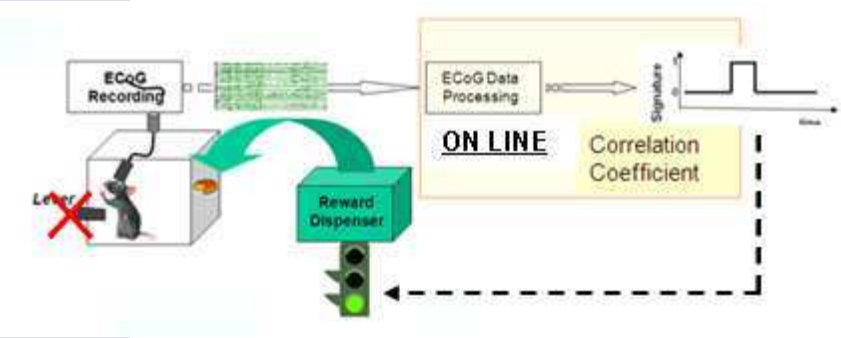

Figure 31: Schematic representation of this protocol. Within the experimental set-up, the lever is disconnected and the ECoG is recorded, the online ECoG data processing provides the correlation coefficient for all electrodes and thus the detection of the signature which activated the reward delivery.

2_6_b) Results of the first protocol

After several rewards obtained by detection of the signature (without pushing the lever) the rats stopped to push the lever and waited the reward in front of the “cup receiver”. The figure

below shows the results for one experiment (for a total of 69 experiments, on 10 rats, see table 9), and the evolution during this experiment of the number of TP, FP and events (figure 32).

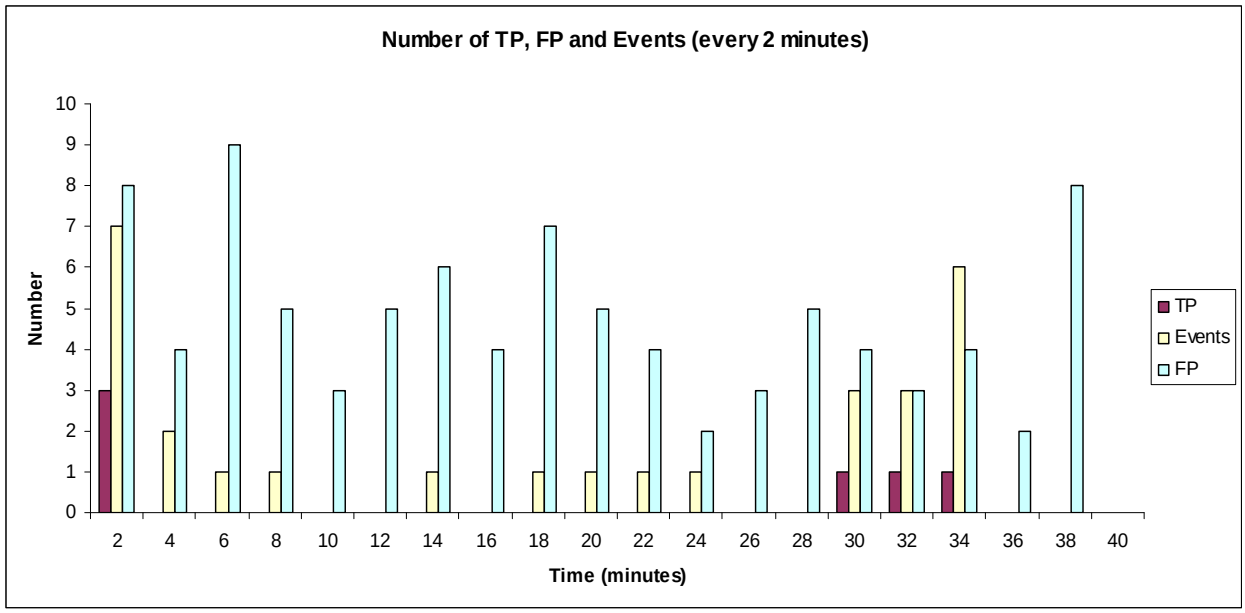

Figure 32: Histograms of the number of TP, FP and events every 2minutes during an experiment of 40 minutes.

The animal pushes the lever at the beginning of the experiments (11 pushes in 8 minutes), and stop to push in the following minutes (1 push in 8 minutes). Four news pushes are observed in the next 8 minutes and at the end of the experiments the rat had pressed 12 times in 14 minutes. The modification in behaviour of the animals is observed for all animals.
The table 9 represents all the results for this step for 10 animals and 69 experiments.

	TPR (%)	FP/min	FPR(%)	PPV(%)	OP(%)	Push/minute
Rat1 (n=2)	35,71±50,51	3,39±0,07	2,83±0,06	1,91±2,70	18,81±26,60	0,15±0,06
Rat2 (n=2)	46,67±18,86	3,78±0,38	3,16±0,32	2,63±0,10	24,65±9,48	0,23±0,06
Rat3 (n=2)	37,50±17,68	3,80±0,17	3,17±0,15	1,27±0,28	19,39±8,70	0,16±0,11
Rat4 (n=2)	50,79±8,98	3,04±0,21	2,54±0,18	4,37±0,80	27,58±4,89	0,27±0,02
Rat5 (n=4)	29,54±8,68	2,78±0,46	2,32±0,38	3,05±1,45	16,30±4,05	0,32±0,17
Rat6 (n=2)	25,60±10,94	2,78±0,21	2,32±0,17	3,38±2,50	14,49±4,22	0,47±0,46
Rat7 (n=15)	39,54±10,41	3,62±1,08	3,05±0,91	12,75±7,31	26,14±5,36	1,43±0,98
Rat8 (n=15)	25,50±7,71	3,37±1,81	2,84±1,52	13,01±11,53	19,26±7,36	1,35±0,78
Rat9 (n=15)	30,62±5,12	2,56±0,73	2,15±0,61	8,53±3,42	19,57±3,28	0,77±0,33
Rat10 (n=10)	40,25±14,65	3,00±1,47	2,51±1,23	7,52±6,06	23,89±8,79	0,50±0,28
Average 10 rats (n=69)	**36,17±8,53**	**3,21±0,44**	**2,69±0,37**	**5,84±4,37**	**21,01±4,33**	**0,57±0,47**
Average rats 7-8-9-10 (n=55)	**39,54±7,15**	**3,62±0,46**	**3,05±0,4**	**12,75±2,83**	**26,14±3,36**	**1,43±0,45**

Table 9: Results for all animals for the data of on-line analysis of behavioural experiments in which pellet are obtained by, only, the detection of the signature in real time (signature calibrated and detected on electrode E15).

The on-line experiments with rat1 show a TPR of 35,71±50,51 associated with a FP/min of 3,39±0,07 and a PPV of 1,91±2,7. The OP for this animal is 18,81±26,60 and the push per minute is 0,15±0,06.

The on-line experiments with rat2 show a TPR of 46,67±18,86 associated with a FP/min of 3,78±0,38 and a PPV of 2,63±0,1. The OP for this animal is 24,65±9,48 and the push per minute is 0,23±0,06.

The on-line experiments with rat3 show a TPR of 37,5±17,68 associated with a FP/min of 3,8±0,17 and a PPV of 1,27±0,28. The OP for this animal is 19,39±8,7 and the push per minute is 0,16±0,11.

The on-line experiments with rat4 show a TPR of 50,79±8,98 associated with a FP/min of 3,04±0,21 and a PPV of 4,37±0,80. The OP for this animal is 27,58±4,89 and the push per minute is 0,27±0,02.

The on-line experiments with rat5 show a TPR of 29,54±8,68 associated with a FP/min of 2,78±0,46 and a PPV of 3,05±1,45. The OP for this animal is 16,30±4,05 and the push per minute is 0,32±0,17.

The on-line experiments with rat6 show a TPR of 25,60±10,94 associated with a FP/min of 2,78±0,21 and a PPV of 3,38±2,50. The OP for this animal is 14,49±4,22 and the push per minute is 0,47±0,46.

The on-line experiments with rat7 show a TPR of 39,54±10,41 associated with a FP/min of 3,62±1,08 and a PPV of 12,75±7,31. The OP for this animal is 26,14±5,36 and the push per minute is 1,43±0,98.

The on-line experiments with rat8 show a TPR of 25,50±7,71 associated with a FP/min of 3,37±1,81 and a PPV of 13,01±11,53. The OP for this animal is 19,26±7,36 and the push per minute is 1,35±0,78.

The on-line experiments with rat9 show a TPR of 30,62±5,12 associated with a FP/min of 2,56±0,73 and a PPV of 8,53±3,42. The OP for this animal is 19,57±3,28 and the push per minute is 0,77±0,33.

The on-line experiments with rat10 show a TPR of 40,25±14,65 associated with a FP/min of 3,00±1,47 and a PPV of 7,52±6,06. The OP for this animal is 23,89±8,79 and the push per minute is 0,50±0,28.

The results for the 10 animals show an average percentage of TPR of **36,17±8,53** with **3,21±0,44** FP/min and a PPV of **5,84±4,37**. The OP average for all animals is **21,01±4,33** with an average push per minute of **0,57±0,47.**

All animals show a very low push per minute making it very difficult to interpret these results, in particular the six first rats with low push/min and only 2 experiments done per animals.

In the table 9, the average for the animals 7, 8, 9 and 10 is mentioned. The TPR is **39,54±7,15**, the FP/min **3,62±0,46**, the PPV **12,75±2,83**, the OP **26,14±3,36** and the push per minute **1,43±0,45.**

2_6_c) Second protocol

To check signature efficiency, on-line experiments in which rats obtain a reward if signature is detected and if detection is confirmed by a lever push within 1.5 seconds. In this configuration, the aim is to check that the signature detected is in relation with the action of

pushing the lever to have reward without behavioural changes observed previously (the lever permits to validate the on-line detection of the signature), see figure 33.

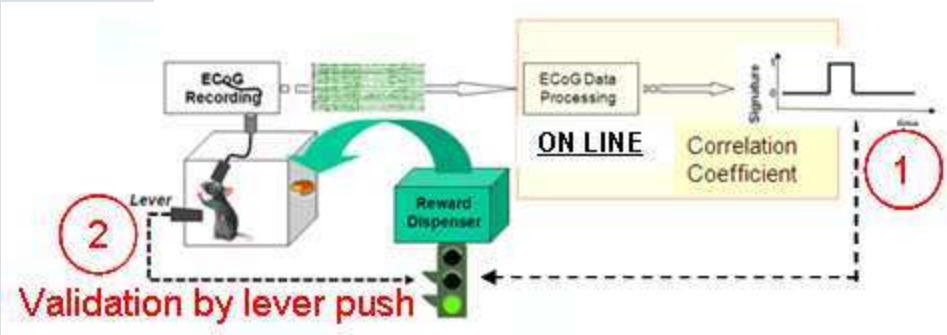

Figure 33: schematic representation of this phase of the protocol. A reward is obtained when the signature is detected on-line (1) and validated by lever push (2). The reward is delivered only when the detected feature is validated by a real lever push occurring within 1,5 second window following the feature detection.

2_6_d) Results

To analyze these different experiments, the same efficiency parameters have been evaluated, as described in Materials & Methods.

	TPR	FP/min	FPR	PPV	OP	Push/min
Rat1 (n=13)	36,65±13,8	1,48±0,27	1,27±0,23	43,89±13,31	40,27±12,43	3,50±1,18

Table 10: Average data for one animal (Rat1) in on-line analysis of experiments. The signature (calibrated on electrode E15) has been detected in real-time (detected on E15).

Results of table 10 indicate for one animal (rat1) a TPR of 36,65±13,8 in these asynchronous experiments associated with low percentage of FP per minute of 1,48±0,27, a PPV of 43,89±13,31 and the OP of 40,27±12,43. The push per minute is 3,5±1,18.

This protocol has been realized in 10 animals and all detailed results are presented in table 11.

	TPR	FP/min	FPR	PPV	OP	Push/min
Rat1 (n=13)	36,65±13,8	1,48±0,27	1,27±0,23	43,89±13,31	40,27±12,43	3,50±1,18
Rat2 (n=13)	19.25±15	1.94±0.47	1.67±0.4	22,69±14.5	20,97±14.5	3,45±1,13
Rat3 (n=13)	22.49±16.05	1.91±0.44	1.63±0.38	23.71±17.07	23.1±15.99	3,04±0,94
Rat4 (n=13)	35.64±17.18	1.55±0.42	1.33±0.36	40.56±17.73	38.1±16.44	3,38±1,27
Rat5 (n=14)	50.26±13.77	1.46±0.32	1.25±0.28	50,74±12.68	50,50±11.30	3,21±0,99
Rat6 (n=15)	39.87±19.04	1.31±0.74	1,11±0.63	34,42±16.43	37,14±16.03	1,73±0,93
Rat7 (n=13)	39,47±7,24	1,24±0,57	1,07±0,48	57,65±17,04	48,56±10,7	4,51±1,74
Rat8 (n=22)	39,51±5,77	1,76±0,88	1,51±0,74	47,21±20,72	43,36±11,40	3,65±1,48
Rat9 (n=24)	44,63±8,24	2,33±1,09	1,99±0,93	37,76±22,19	41,19±12,92	3,07±1,91
Rat10 (n=20)	38,92±6,32	2,70±0,87	2,30±0,74	29,83±18,91	34,38±11,69	2,85±1,45
Average 10 rats (n=172)	**36,67±9,34**	**1,77±0,47**	**1,51±0,4**	**38,85±11,48**	**37,76±9,64**	**3,24±0,7**

Table 11: Average data for each animal for on-line analysis of experiments. The signature (calibrated on electrode E15) has been detected in real-time (detected on E15).

Results for the rat1 are the same in table 10 and 11.

Results for the rat2 indicate a TPR of 19.25±15 in these asynchronous experiments associated with low percentage of FP per minute of 1.94±0.47, a PPV of 22,69±14.5 and the OP of 20,97±14.5. The push per minute is 3,45±1,13.

Results for the rat3 indicate a TPR of 22.49±16.05 in these asynchronous experiments associated with low percentage of FP per minute of 1.91±0.44, a PPV of 23.71±17.07 and the OP of 23.1±15.99. The push per minute is 3,04±0,94.

Results for the rat4 indicate a TPR of 35.64±17.18 in these asynchronous experiments associated with low percentage of FP per minute of 1.55±0.42, a PPV of 40.56±17.73 and the OP of 38.1±16.44. The push per minute is 3,38±1,27.

Results for the rat5 indicate a TPR of 50.26±13.77 in these asynchronous experiments associated with low percentage of FP per minute of 1.46±0.32, a PPV of 50,74±12.68 and the OP of 50,50±11.30. The push per minute is 3,21±0,99.

Results for the rat6 indicate a TPR of 39.87±19.04 in these asynchronous experiments associated with low percentage of FP per minute of 1.31±0.74, a PPV of 34,42±16.43 and the OP of 37,14±16.03. The push per minute is 1,73±0,93.

Results for the rat7 indicate a TPR of 39,47±7,24 in these asynchronous experiments associated with low percentage of FP per minute of 1,24±0,57, a PPV of 57,65±17,04 and the OP of 48,56±10,7. The push per minute is 4,51±1,74.

Results for the rat8 indicate a TPR of 39,51±5,77 in these asynchronous experiments associated with low percentage of FP per minute of 1.94±0.47, a PPV of 47,21±20,72 and the OP of 43,36±11,40. The push per minute is 3,65±1,48.

Results for the rat9 indicate a TPR of 44,63±8,24 in these asynchronous experiments associated with low percentage of FP per minute of 2,33±1,09, a PPV of 37,76±22,19 and the OP of 41,19±12,92. The push per minute is 3,07±1,91.

Results for the rat10 indicate a TPR of 38,92±6,32 in these asynchronous experiments associated with low percentage of FP per minute of 2,70±0,87, a PPV of 29,83±18,91 and the OP of 34,38±11,69. The push per minute is 2,85±1,45.

In these on-line experiments, the average percentage of TP for all rats is: **36,67±9,34**. The number of FP per minute is always low, the average FP/minute is: **1,77±0,47**. The average of PPV is **38,85±11,48** and the average OP **37,76±9,64**. The average push per minute is **3,24±0,7**.

2_7) Random detection analysis

2_7_a) Protocol

With a mathematical method, experiments are analyzed to estimate efficiency parameters with random detection. All the results are shown in the table 12.

Our random analyses generally correspond to the case when given numbers of events and of decisions are randomly distributed through the recordings.

The aim is to check if our results are totally random or in contrary statistically significant. These random detection analysis have been done for 6 rats for off-line analysis (105 experiments) and on-line analysis (81 experiments).

2_7_b) Results

	TPR random (%)	TPR (%)	Ratio TPR /TPR random
Off-line Rat 1 (n=16)	3,53	67,99	19,26
Off-line Rat 2 (n=16)	2,79	68,95	24,71
Off-line Rat 3 (n=16)	2,26	65,23	28,86
Off-line Rat 4 (n=16)	2,06	64,19	31,16
Off-line Rat 5 (n=12)	3,9	77,95	19,99
Off-line Rat 6 (n=29)	2,6	64,44	24,78
Average (n=105)	**2,86±0,72**	**68,06±5,05**	**24,66±4,31**
	TPR random (%)	**TPR (%)**	**Ratio TPR /TPR random**
On-line Rat 1 (n=13)	1,33	36,65	27,56
On-line Rat 2 (n=13)	1,2	19,25	16,04
On-line Rat 3 (n=13)	1,03	22,49	21,83
On-line Rat 4 (n=13)	1,41	35,64	25,28
On-line Rat 5 (n=14)	1,46	50,26	34,42
On-line Rat 6 (n=15)	0,73	39,87	54,62
Average (n=81)	**1,19±0,28**	**34,03±11,48**	**29,96±13,53**

Table 12: Table represents the data for off-line and on-line analysis of experiments. The values of percentage of True Positive are indicated. The signature has been detected in a randomly manner for the TPR random.

The results in table 12 indicated a very low percentage of TP in case of random detection. In comparison with our results with real detection concerning 6 animals (off-line or on-line), in average the random detection is 24.66 times lower for off-line experiments and 29.96 times lower for on-line.

This comparison with random detection demonstrates that our results of off-line and mainly on-line experiments are not randomly.

2_8) Neuroplasticity

2_8_a) Protocol

The rats obtained a pellet if there is a detection of signature followed by a lever push, see figure 34.

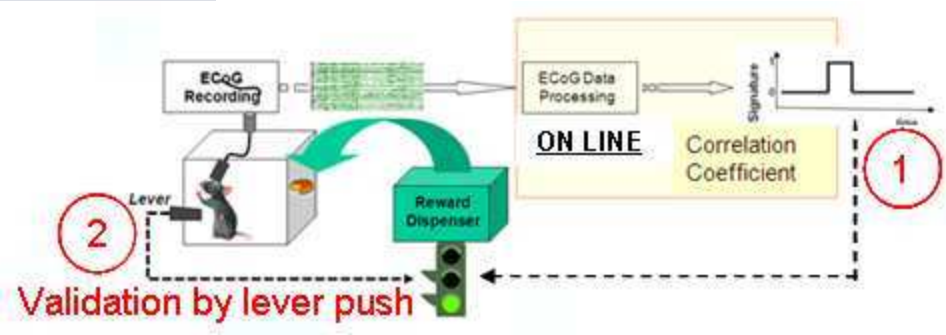

Figure 34: Schematic representation of the protocol of neuroplasticity. A reward is obtained when the signature is detected on-line (1) and validated by lever push (2). The reward is delivered only when the detected feature is validated by a real lever push occurring within 1,5 second window following the feature detection.

The experiments to test the possibilities of neuroplasticity in rodents can be divided in two groups, both are included in on-line experiments (see figure 35).

The first is to choose different electrodes to be used to detect the signature calibrated on the most optimal electrode (with the best score of wavelets correlation, as explain in the paragraph “2) Identification and calibration of a signature”).

The second group of neuroplasticity experiments is to try to change the area for identify/calibrate the signature, this is not the most optimal electrode which is used like before but others electrodes to calibrate.

The first aim is to observe if it's possible to detect the optimal signature in a different area than the area where the signature has been identified (see figure 35). A second aim is to see if it's possible to detect the signature not optimal and to observe the modification of this signature, maybe stronger along the time (see figure 35).

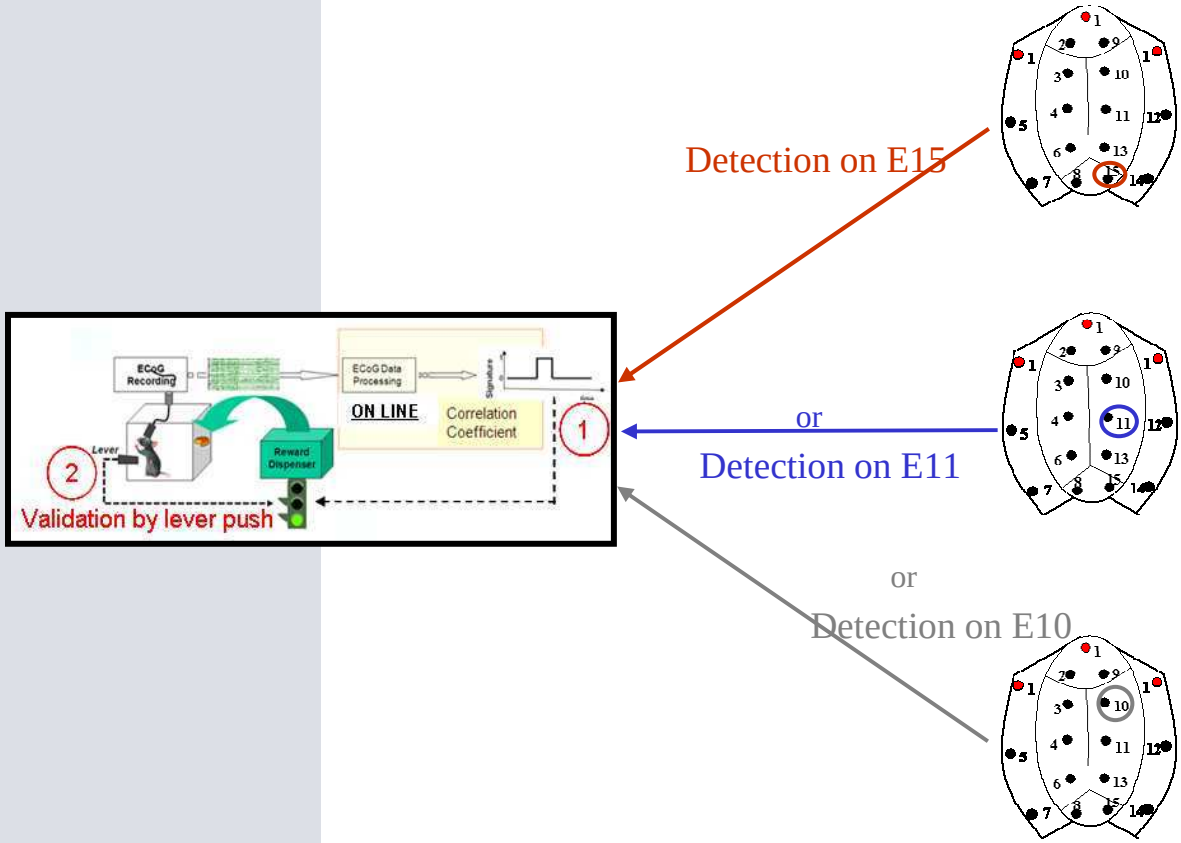

Figure 35: Schematic representation of the protocol of neuroplasticity. A reward is obtained when the signature is detected on-line on Electrode 15 in a first set of experiments, on E11 in a second set and on E10 in a last session of experiments. The reward is delivered only when the detected feature is validated by a real lever push occurring within 1,5 second window following the feature detection. The signature is calibrated on Electrode 15 for one set of experiments and on Electrode 10 or 11 for others sets.

2_8_b) Results

The table 13 shows all the results obtained for the study of the neuroplasticity in using Electrode 11 for the detection; The TPRs are lower than the previous studies. The use of a different electrode to detect the signature calibrated on the optimal electrode (the signature calibrated on electrode 15 is detected on-line by electrode 10 or 11, for E10 data are not shown) is less efficient that the detection by the electrode which has been used for calibration (electrode 15, see table 11).

	TPR	FP/min	FPR	PPV	OP	Push/min
Rat1 (n=10)	16,47±3,64	2,29±0,84	1,94±0,72	13,13±6,18	14,80±4,14	1,93±0,52
Rat2 (n=10)	11,69±2,66	2,30±0,88	1,96±0,76	11,06±4,33	11,37±2,54	2,44±1,08
Rat3 (n=10)	9,24±1,50	1,94±0,33	1,65±0,29	9,96±2,79	9,60±1,98	2,28±0,45
Rat4 (n=10)	14,74±1,62	2,25±0,61	1,92±0,52	16,62±6,57	15,68±3,57	2,90±0,84
Rat7 (n=15)	13,85±4,95	1,55±0,67	1,32±0,57	23,29±8,96	18,57±5,70	3,28±1,27
Rat8 (n=15)	14,15±3,72	3,09±1,37	2,64±1,17	12,31±7,65	13,23±4,58	2,75±1,47
Rat9 (n=15)	21,51±7,62	2,07±0,59	1,77±0,51	20,50±11,03	21,01±8,62	2,46±1,34
Rat10 (n=12)	19,20±7,29	3,32±1,24	2,83±1,06	14,86±11,98	17,03±9,24	2,83±1,91
Average 8 rats (n=97)	**15,11±3,93**	**2,35±0,59**	**2,00±0,5**	**15,22±4,67**	**15,16±3,75**	**2,61±0,42**

Table 13: Table represents the data for each animal (8rats) for on-line analysis of experiments of neuroplasticity (signature calibrated on E15 and detection on E11, see figure 35).

The results of table 13 indicate for rat1 a TPR of 16,47±3,64 in these asynchronous experiments associated with low percentage of FP per minute of 2,29±0,84, a PPV of 13,13±6,18 and the OP of 14,80±4,14. The push per minute is 1,93±0,52.

The results of table 13 indicate for rat2 a TPR of 11,69±2,66 in these asynchronous experiments associated with low percentage of FP per minute of 2,30±0,88, a PPV of 11,06±4,33 and the OP of 11,37±2,54. The push per minute is 2,44±1,08.

The results of table 13 indicate for rat3 a TPR of 9,24±1,50 in these asynchronous experiments associated with low percentage of FP per minute of 1,94±0,33, a PPV of 9,96±2,79 and the OP of 9,60±1,98. The push per minute is 2,28±0,45.

The results of table 13 indicate for rat4 a TPR of 14,74±1,62 in these asynchronous experiments associated with low percentage of FP per minute of 2,25±0,61, a PPV of 16,62±6,57 and the OP of 15,68±3,57. The push per minute is 2,90±0,84.

The results of table 13 indicate for rat7 a TPR of 13,85±4,95 in these asynchronous experiments associated with low percentage of FP per minute of 1,55±0,67, a PPV of 23,29±8,96 and the OP of 18,57±5,70. The push per minute is 3,28±1,27.

The results of table 13 indicate for rat8 a TPR of 14,15±3,72 in these asynchronous experiments associated with low percentage of FP per minute of 3,09±1,37, a PPV of 12,31±7,65 and the OP of 13,23±4,58. The push per minute is 2,75±1,47.

The results of table 13 indicate for rat9 a TPR of 21,51±7,62 in these asynchronous experiments associated with low percentage of FP per minute of 2,07±0,59, a PPV of 20,50±11,03 and the OP of 21,01±8,62. The push per minute is 2,46±1,34.
The results of table 13 indicate for rat10 a TPR of 19,20±7,29 in these asynchronous experiments associated with low percentage of FP per minute of 3,32±1,24, a PPV of 14,86±11,98 and the OP of 17,03±9,24. The push per minute is 2,83±1,91.
In these on-line experiments of neuroplasticity, the average percentage of TP for all rats is: **15,11±3,93**. The average FP/minute is: **2,35±0,59**. The average of PPV is **15,22±4,67** and the average OP **15,16±3,75**. The average push per minute is **2,61±0,42**.

This protocol shows us that a signature identified in an area of the brain can be detected in another area of the brain in real time to control an effector but with lower efficiency (**15,11±3,93** of TPR with electrode 11 versus **36,67±9,34** of TPR with electrode15, see table 11). Two different electrodes have been used to test this aspect of neuroplasticity (Electrode 11 and Electrode 10). The electrode 11 gives a better result than Electrode 10 (data not shown), but it's possible to detect in real-time the signature calibrated in electrode 15 implanted on the cerebellum.

Others aspects of the neuroplasticity are the evolution along time of the parameters, see the figure 36. During 2 months, 8 animals have realized on-line experiments in which the signature calibrated on electrode 15 has been detected in real-time by the electrode 11 (in a different area of the brain). The TPR, the FP/min, the PPV and the OP are described for 8 weeks for these 8 animals.

A

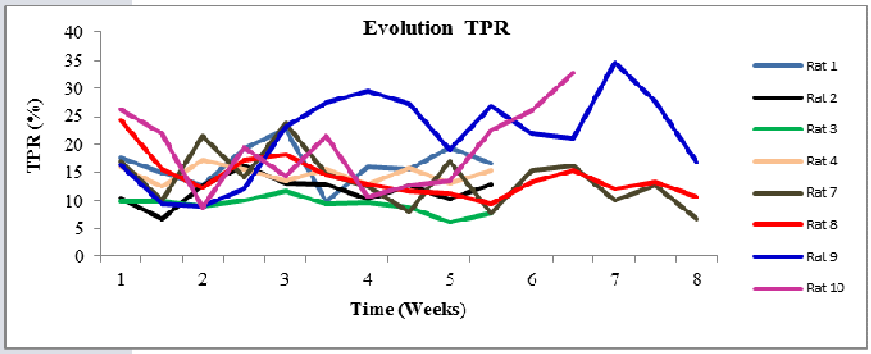

B

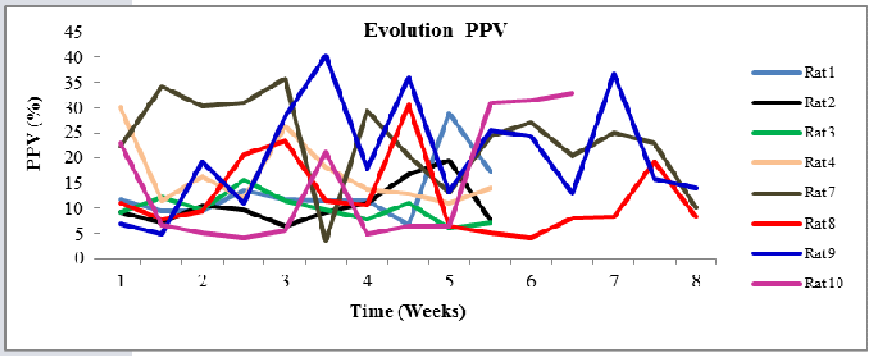

C

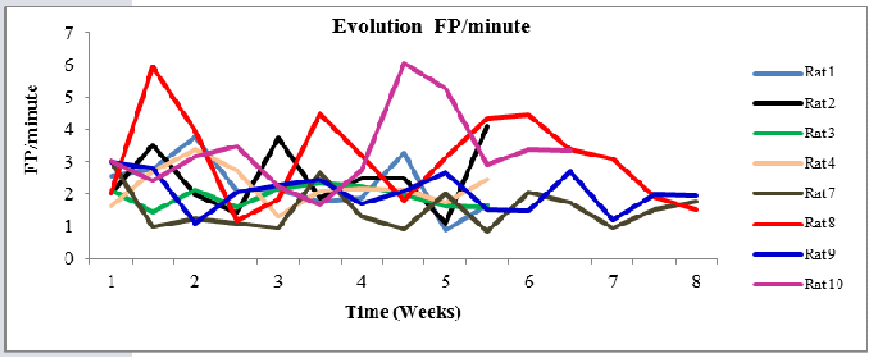

D

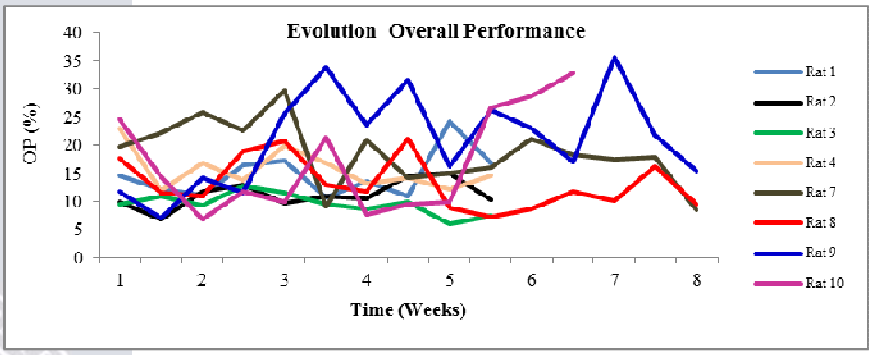

Figure 36: Represents the evolution along time of data for all animals for on-line analysis of experiments of neuroplasticity (signature calibrated on E15 and detection on E11, see figure 35). A: evolution of the TPR of 8 animals. B: evolution of PPV of 8 animals. C: evolution of FP/minute of 8 animals and D: evolution of the OP of 8 animals.

As we can see, there are variations along time for these four parameters. Concerning the TPR (figure 36A), a small increase is observed for the animal 9 and 10. For the 6 others animals, the TPR remained steady along time with daily variations. The PPV for all animals have presented more variation from one experiment to the other, see figure 36B. The evolution of FP/min is stable for 6 animals and shows bigger variations for the rat 8 and 10. The last parameter, the OP, is the average of TPR and PPV, which explains the variations observed due to changes in PPV.

3_Histological observations

All animals used in the experimental behavioural tasks, have been euthanazied at the end of the protocols and the brain have been observe to validate and confirm the locus of implanted electrodes. The principal cause or argument to finish a protocol is the old age of animals (around 1 year of implantation and around 2 years for the age, near the life expectancy of this animal model).

3_1) Histological procedure and preparation

In a first time, macroscopic analyses have been done. In the figure 37, brains are shown and the prints of the screws are observable on the cortex surface.

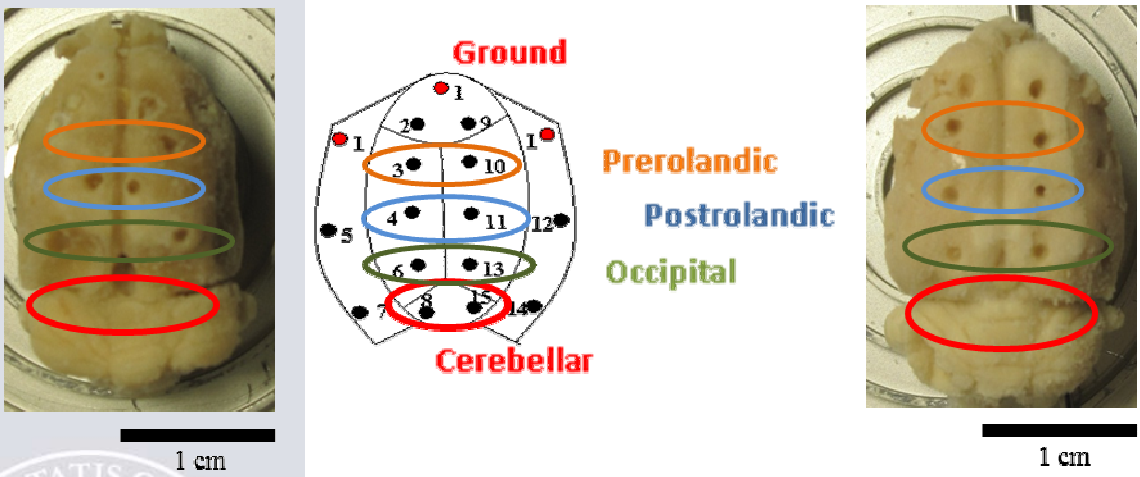

Figure 37: Pictures of two brains after 8 months of implantation and footprint corresponding with implanted electrodes.

These macroscopic observations permit us to check that electrodes used for our BCI are well-implanted as provided by the implantation map (the picture in the center of the figure 37). Two electrodes (2 and 9) are implanted in anterior of the Bregma, three pairs between Bregma and Lambda (3 and 10, 4and 11, 6 and 13), two electrodes on each temporal side (5 and 7 on left and 12 and 14 on right), and two electrodes on posterior, see electrodes 8 and 15 on cerebellum (figure 37). This verification is done for all animals (n=10).

In a second time, some histological stainings have been realized (crésyl or Rouge Neutre or hematoxyline) to validate that the brains at the end of the protocols (implantation and several months of behavioural experiments) have no important problem of degeneration due to the screws which could disturb or block the recordings of brain activities. The results are presented in figure 38 and 39.

3_2) Histological results

The brains were sliced (30µm) and the prints of the screws are easily observables on the sides of the brains. In the figure 38, we have compared the slices of a brain with the atlas of rat in order to check that electrodes have recorded the areas of the brain provided.

These observations on brains give us the confirmation (after macroscopic analysis, see figure 37) that the electrodes have been correctly implanted according to what was planned. In comparing the atlas slices and our slices of brain (with the footprints of screws), the electrodes 2 and 9 are in anterior position of the Bregma (in blue in figure 38). The electrode 3 and 10 are just in posterior position of the Bregma (in red in figure 38). The electrodes 4 and 11 are in the middle of the brain (in green in figure 38). The electrodes 6 and 13 are on posterior side of the brain, just anterior of Lambda (in black in figure 38). And to finish, the most posterior electrodes, 8 and 15, are implanted posteriorly of the lambda: on the cerebellum (in orange in figure 38).

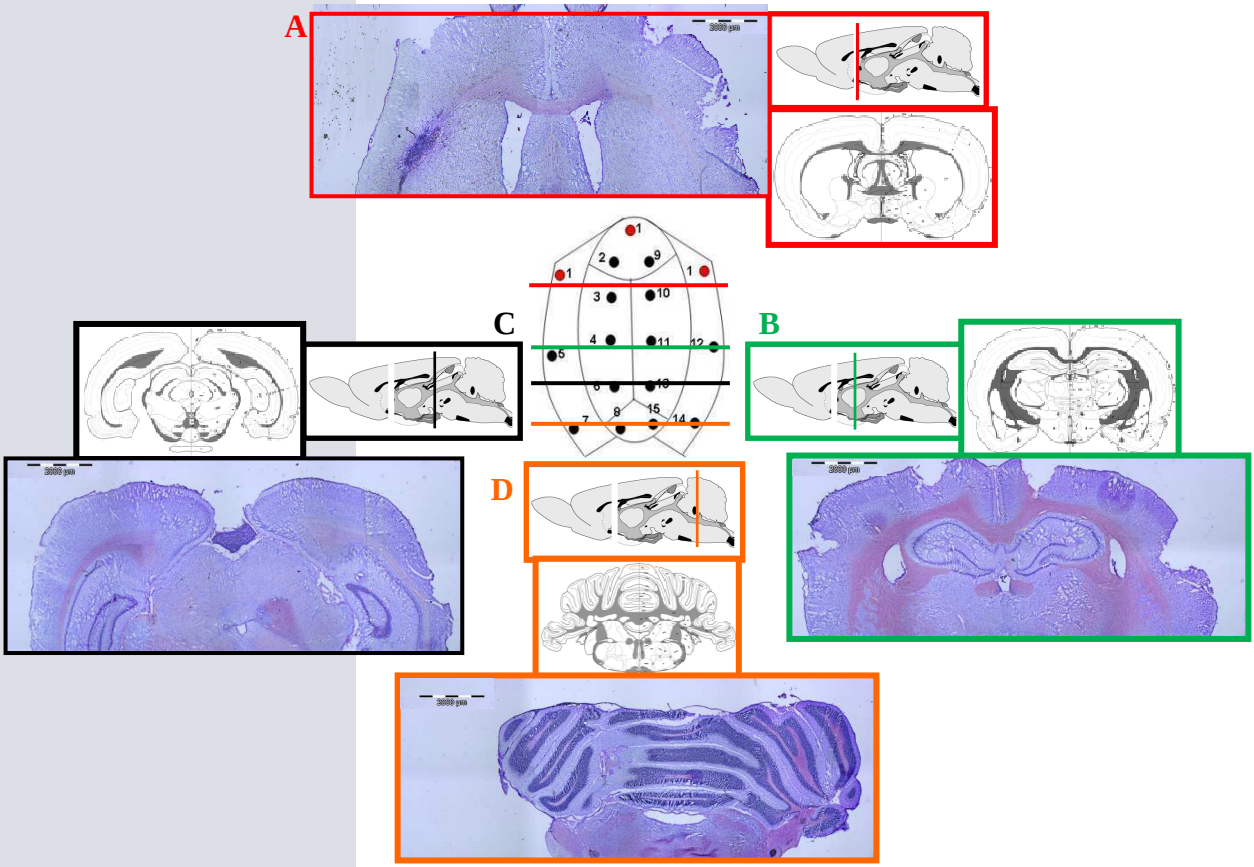

Figure 38: Comparison of the brain slices (stained with cresyl violet) with atlas (sagittal and coronal slices) and the implantation map provided. A: slice of the brain with footprints of electrodes 3 and 10 (in red). B: slice of the brain with electrodes 4 and 11 (in green). C: slice of the brain with footprints of electrodes 6 and 13 (in black). D: slice of the cerebellum with electrodes 8 and 15 (in orange).

The other aspect studied, by histological experiments, has been to check the neurons by staining the Nissl bodies (rough endoplasmic reticulum) and to confirm that the brain and the cellular components, more precisely, haven't problems of degeneration or phenomena of necrosis.

The results are shown in figure 39 with cresyl violet staining (for the Nissl bodies).

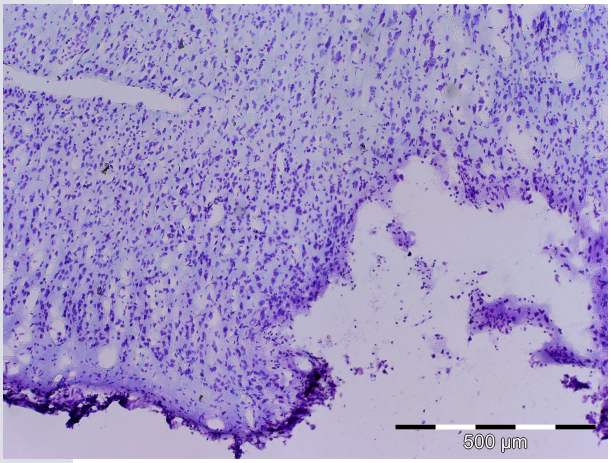

A

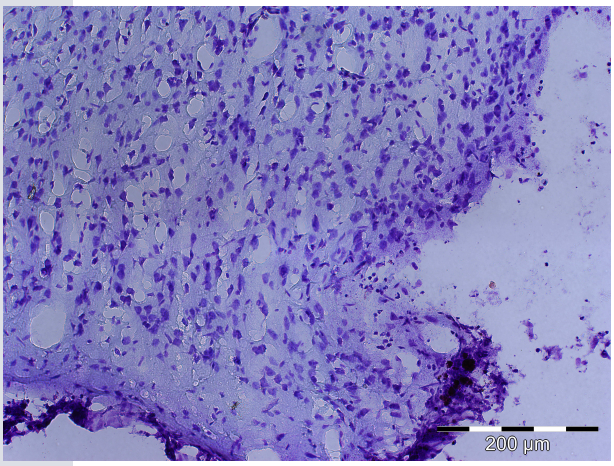

B

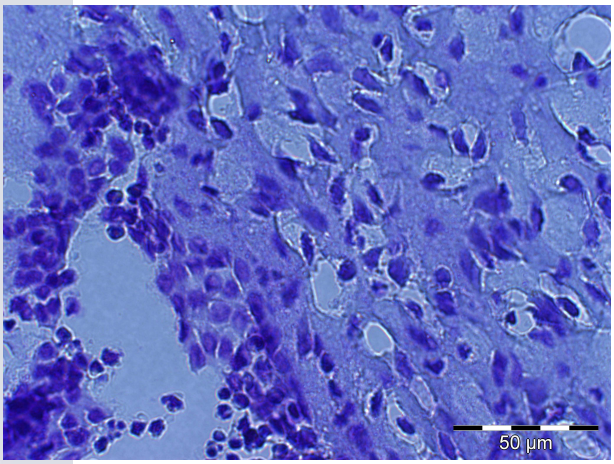

C

Figure 39: Crésyl violet coloration for identification of Nissl bodies inside neurons. A: with 10X, B: with 20X and C: with 40X.

As we can see in figure 39, the neurons are numerous and their general shapes show no problems. They are in front of a footprint of electrode indicating that the screw has well recorded some neural activities.

The observations of several slices after cresyl violet colorations (figure 39) permitted us to be sure that the brains of all animals at the end of these long protocols presented no important cellular problems, or problems of tumor and these conclusions are important for the validation of this ECoG model in rats and all the behavioural experiments and the BCI experiments, and especially for all the conclusions done for this BCI model.

V. CONCLUSIONS

In this model (rat OFA), several phases have been necessary to check that the brain activity identified is really a modification of the brain signals in correlation with the task and to evaluate the efficiency of our BCI model.

Rodents stayed in a behavioural box and have been trained to push on a lever to deliver a reward, experiments duration is around 40 minutes. The task is an asynchronous paradigm (which is not used in most experiments) and this is an important point for its proximity with the natural environment necessary for the future applications of BCI. ECoG brain activities are recorded during behavioural studies by seventeen screws implanted through the bone to record cortical signals, including 3 reference electrodes. Some tests have been done to verify the acquisition chain before each experiments, others tests to verify the functional localization of the electrodes (VEP and SEP). The largest SEP and VEP are mostly visible on electrodes 6 and 13 and this colocalization is known in bibliography [117].

Several experiments on several rats (n=10) have been realized during several months (around 1 year of implantation) and the brain signals recorded have been analyzed. The number of pushes increases along time until to obtain 1 push per minute which is a necessary parameter to start the analyses of the ECoG signals recorded. The results showed that electrodes 8 and 15 in the cerebellar area are mostly involved in the task performed by the rat and that correlation was maximal around 572±207 ms before the lever push and a frequency band of interest around 177 ± 36 Hz (n=10 animals and 376 experiments). The algorithms have

identified brain signals well correlated with the intention to push the lever (572±207 ms preceding the lever), this brain signals modification have been called signature. The signature can be represented by several factors, two are most influents: the frequency factor (band between 50Hz and 300Hz) and the temporal factor (around 400ms before to push the lever). For each animal several signatures have been identified. The off-line analysis permitted to choose the better signature for each animal. In off-line analysis, the Overall Performance (OP), which corresponds to the mean of True Positive Rate and Positive Predictive Value (PPV) is around 59,55%±7,22 (206 experiments). This parameter permits to represent the BCI performances more precisely than only the TPR (number of TP relative to the number of lever push, thus relative to the behavioural task, this parameter is the more used in BCI studies) because it integrates the PPV which corresponds to the number of TP relative to the total of signatures detected. The number of FP per minute is low, 2,17±0,52, and it's an important result in view of use of these signatures in real-time experiments, and especially in asynchronous experiments (fewer in BCI studies for the moment). The best parameters for the signature are the use of the frequency band 10 to 300 Hz for the calibration, several off-line experiments have been done to show that (best efficiency of the signature in our BCI compared at others frequency bands tested, see *"2_5) Study of the signature in off-line experiments"*).

Our self-paced BCI performs continuous monitoring of neuronal activity. In particular the decision is made two times per second (decision rate 2Hz), 120 per minute or 7200 decisions per hour. This is why self-paced BCI requires a high level of classification (events/non-events) accuracy. In our experiments the overall accuracy (AO = percentage of correct decision) reaches 97.3% in average through all the experiments, from 96.1% up to 99.3%. At the best experiment (AO=99.3%) the 42 errors (22 FP and 20 FN) were made among 6174 decisions. Let us note that AO cannot be efficiently used to characterize BCI performance in case of self-paced experiments because of non-equilibrated classes.

Two kinds of on-line studies have been done: the control of the dispenser directly by cortical activity or by the combination of motor task (push the lever) and detection of the signature. In studies of direct control by the detection the OP was 21,01%±4,33 (10 animals 69 experiments) but the number of push per minute fell to 1,43±0,45 making more difficult the interpretation of these results. Some FP in this case could be in real some TP but animals have modified their behaviours in decreasing the number of push in waiting directly pellets in front

of the cup receiver. In the lack of some lever push some detections are classified in FP but could correspond to a real intention to push the lever by the animals.

That's why the experiments, more complicated, requiring both lever activation and signature detection have been realized. The OP, in this case, is 37,76%±9,64 with a number of push which increased back to 3,24±0,7. The comparison with random detection permitted us to be sure that these results are not random (around 25-30 fold more than random analysis).

There are differences between the animals and the maximal percentage of TP obtained is 85%. The results obtained in these on-line asynchronous experiments indicated that these signatures are well implicated in this intention to push lever to obtain pellets.

In the BCI studies, results are often compared to the random classification. In the case of synchronized two class BCI, Bernoulli trials with equal probabilities of classes $p=0.5$ are applied as the bases for the comparison. The expected correct classification for random classifier is then 50%. This difference between synchronous and asynchronous experiments is very important for the future BCI because asynchronous situation is closer of natural environment necessary in human applications, but this kind of experiments is more difficult concerning the FP corresponding to false detection.

The main feature of this report is the demonstration that neural activity continuously recorded at the level of one single cortical electrode can be efficiently used to pilot an effector with one degree of freedom (DOF), during experiments up to 1 hour, in a freely moving individual making decisions in a random unsupervised manner. The specific signature detected in one animal is stable along time. This means that when the signature has been established by the self-learning algorithm during the calibration sequence, it is not necessary to recalibrate during subsequent experimental sessions, even if they are performed on different days, even over a period of up to 8 months in our model. This stability is partly due to the fixed situation of the implanted ECoG electrodes corresponding to the various functional cortical areas. In spite of the recent important advances in the BCI field, some issues still need to be solved. First, the relative advantages and disadvantages of the different signal acquisition methods are still unclear. Their clarification will require further animal studies. Our studies demonstrated that this ECoG model was stable along time and could be used for on-line detection during 8 months of implantation. Second, invasive methods need further investigation to deal with tissue damage, risk of infection, and long-term stability concerns. In our study, all the brains of all animals have been observe at the end of the experimental protocols in order to check that the electrodes used for the BCI are well-implanted on the cerebellum. No

neurodegenerative process is observed on these brains even after 1 year of implantation on rat. Our model of ECoG on rats showed a good quality of signal during a period of 8 months after implantation and can serve as a model for others behavioural tasks or others protocols requiring ECoG.

One of the most intriguing features of these experiments is that the area which seems prominently concerned by the execution of the motor task is the cerebellar area and not the central, motor and sensorimotor, areas which would be expected, as in human beings. Looking at the gross structure of the rodent brain, it in fact makes sense, as the folded cerebellar cortex is probably more able to handle the function of global control of movement as compared to the practically flat cerebral cortex. The cerebellar activity plays a major role in the motor activity of rodents, most of it being controlled by the coordination function of the cerebellum. In humans, the relative size of cerebellum, similarly folded, is much smaller, as compared to the predominant cerebral cortex, itself significantly folded. Motricity in rats is more globally postural as the outreaching movement of the forepaw is accompanied by an uprising of the body towards the lever area, every voluntary movement must be initiated upon a background of posture. It must be stressed that we deliberately concentrated on the time period preceding the lever push because we were interested in the ECoG activities related to the preparation and initiation of movement (maybe intention of action). Looking for prediction of movements our algorithm found mostly ECoG activity with negative delays in the cerebellum, preceding the activity in the central motor area.

These experiments demonstrate the feasibility of self-paced BCI command of effectors in freely moving rodents performing an asynchronous behavioural task, over long periods of time. They also shed light on the cortical mechanisms and structures involved to initiate and control motor activity. The performance of this detection algorithm now meets the criteria required for its extension into long term clinical application, such as compensation of motor deficits using BCI driven multiple axis exoskeletons. To reach this goal, complementary experimental steps have been undertaken in rodents and in primates and are currently in progress, to make the human implantation of the first prototype possible within a reasonable delay. In rodents, it is important to study the aptitude of the cortex for neuroplasticity, evaluated in terms of changes in the specificity of the signature along training time, as well as the possibility to train other cortical sites (corresponding to other electrodes) to achieve a task similar to the one using the original best electrode. This would suggest the possibility to enhance the functionality of the cortical area placed in front of the electrode matrices.

In our study, we have investigated the possibility to identify the signature (intention of action) in a different area of the brain where this signature is physiologically observed (data not shown).

A second aspect of our neuroplasticity study has been to demonstrate that the signature, once identified on cerebellum, can be detected in real-time in other areas of the brain.

Our results showed an OP of 15,16%±3,75 in 97 experiments done on 8 rats. These results showed that brain activities correlated with behavioural task identified firstly in cerebellum can be detected in a different area of the brain. Concerning these neuroplasticity studies, it should be noted that the evolution of the different parameters does not highlights some increases or ameliorations along time in these 8 animals. Some variations are observed but not tendency to increase. The different phases used in all these studies are very long and the study of neuroplasticity began after 6 months of implantation, which is the time necessary to train the animals, identify the signature and realize on-line asynchronous experiments to check this BCI model. Maybe the possibility to observe some evolutions of the parameters, translating neuroplasticity, is not optimal in old animals. But these results are a first step, showing that changing the area of detection is effective and further experiments will have to investigate the possibility of neuroplasticity more precisely.

These two important points are keys for futures BCI application with several degrees of freedom. The use of only one electrode for the detection of a signature is more difficult than using several electrodes but it will permit in the future to use several electrodes for the detection of several signatures. The demonstration that this is feasible is very important in the view of human BCI with several degrees of freedom (one degree of freedom per electrode). This was a first step, done on 8 rats which must be more investigated in primates for the applications of BCI which requires the possibility to change or modulate the electrode of interest (detection or identification).

The present study prepares the clinical application of BCI systems to compensate motor deficits. Success with one DOF suggests feasibility for applications using more DOFs.

Future experimentation will be aimed at exploring the neuroplasticity resulting from training and reward based feedback, in order to improve the selectivity of the detection (increasing TP, decreasing FP). The long term goal of the project is to drive more than one DOF using more than one electrode, or a combination of electrodes. Piloting a 3D robotized hand is in progress in our laboratory using primates.

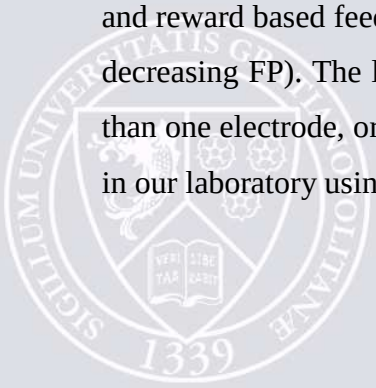

This work is a determining first step towards a larger program aiming at providing a certain level of mobility to young cervical spinal-cord injured patients with tetraplegia. The latest advances in BCI research suggest that innovative developments may be forthcoming in the near future. These achievements and the potential for new BCI applications have obviously given a significant boost to BCI research involving multidisciplinary scientists e.g., neuroscientists, engineers, mathematicians, and clinical rehabilitation specialists, among others. Interest in the BCI field is expected to increase and BCI design and development will in all probability continue to bring benefits to the daily lives of disabled people. Furthermore, recent commercial interest within certain companies suggests that BCI systems may find useful applications in the general population, and not just for people living with severe disabilities. In the near future, BCI systems may therefore become a new mode of human-machine interaction with levels of everyday use that are similar to other current interfaces

VI. BIBLIOGRAPHIE

[1] Wyndaele M, Wyndaele JJ. Incidence, prevalence and epidemiology of spinal cord injury: what learns a worldwide literature survey? *Spinal Cord*, 2006: 44(9):523-9.

[2] Hochberg LR, Serruya MD, Friehs GM, Mukand JA, Saleh M, Caplan AH, Branner A, Chen D, Penn RD, Donoghue JP. Neuronal ensemble control of prosthetic devices by a human with tetraplegia. *Nature*, 2006: 13;442(7099):164-71.

[3] Hochberg LR, Bacher D, Jarosiewicz B, Masse NY, Simeral JD, Vogel J, Haddadin S, Liu J, Cash SS, van der Smagt P, Donoghue JP. Reach and grasp by people with tetraplegia using a neurally controlled robotic arm. *Nature*, 2012: 16;485(7398):372-5.

[4] Schwartz AB, Cui XT, Weber DJ, Moran DW. Brain-controlled interfaces: movement restoration with neural prosthetics. *Neuron*, 2006: 5;52(1):205-20.

[5] Wilson JA, Felton EA, Garell PC, Schalk G, Williams JC. ECoG Factors Underlying Multimodal Control of a Brain–Computer Interface. *IEEE transactions on neural systems and rehabilitation engineering*, 2006: 14(2):246-50.

[6] Jackson A. Brain-controlled robot grabs attention. *Nature*, 2012: 16;485(7398):317-8.

[7] Aksenova T, Yelisyeyev A. A method calibrating and operating a direct neural interface system. 2011. *Patent* PCT/IB2011/054719.

[8] Aksenova T, Yelisyeyev A. Direct neural interface System and method of calibrating it. 2010. *Patent* PCT/IB2010/001528.

[9] Hitzig, E. Über die galvanischen Schwindelempfindungen und eine neue Methode galvanischer Reizung der Augenmuskeln. *Berl. Kiln. Wschr.*, 1870: 11:137–138.

[10] Hitzig, E. Hughlings Jackson and the cortical motor centres in the light of physiological research. *Brain*, 1900: 23:545–581.

[11] Kübler A, Nijboer F, Mellinger J, Vaughan TM, Pawelzik H, Schalk G, McFarland DJ, Birbaumer N, Wolpaw JR. Patients with ALS can use sensorimotor rhythms to operate a brain-computer interface. *Neurology*, 2005: 64(10):1775-1777.

[12] Wolpaw JR, McFarland DJ. Control of a two-dimensional movement signal by a noninvasive brain-computer interface in humans. *Proceedings of the National Academy of Sciences (PNAS)*, 2004: 101(51):17849–17854.

[13] Taylor DM, Tillery S, Schwartz A. Direct cortical control of 3D neuroprosthetic devices. *Science*, 2002: 296(5574):1829–1832.

[14] Serruya MD, Hatsopoulos NG, Paninski L, Fellows MR, Donoghue JP. Instant neural control of a movement signal. *Nature*, 2002: 416(6877):141-142.

[15] Levine SP, Huggins JE, BeMent SL, Kushwaha RK, Schuh LA, Passaro EA, Rohde MM, Ross DA. Identification of electrocorticogram patterns as the basis for a direct brain interface. *J. Clin. Neurophysiol*., 1999: 16:439-47.

[16] Fabes RA, Martin C L. Gender and age stereotypes of emotionality. *Personality & Social Psychology Bulletin*, 1991: 17:532-540.

[17] Nazarpour K. Brain Signal Analysis in Space-Time-Frequency Domain; An application to Brain Computer Interfacing. *PhD Thesis*, 2008, Cardiff University, UK.

[18] Normann RA, Maynard EM, Rousche PJ, Warren DJ. A neural interface for a cortical vision prosthesis. *Vision Res.*, 1999: 39:2577-2587.

[19] Pine J. A History of MEA Development. In: Baudry M, Taketani M, eds. Advances in Network Electrophysiology Using Multi-Electrode Arrays. *New York: Springer Press*, 2006: 3-23.

[20] Schwartz AB, Taylor DM, Tillery SI. Extraction algorithms for cortical control of arm prosthetics. *Curr. Opin. Neurobiol.*, 2001 : 11(6):701-7.

[21] Wessberg J, Stambaugh CR, Kralik JD, Beck PD, Laubach M, Chapin JK, Kim J, Biggs SJ, Srinivasan MA, Nicolelis MA. Real-time prediction of hand trajectory by ensembles of cortical neurons in primates. *Nature*, 2000: 408(6810), 361-365.

[22] Schwartz AB. Cortical neural prosthetics. *Annual Review of Neuroscience*, 2004: 27: 487–507.

[23] Mazzoni P, Bracewell RM, Barash S, Andersen RA. Motor intention activity in the macaque's lateral intraparietal area. I. Dissociation of motor plan from sensory memory. *J. Neurophysiol.*, 1996: 76(3):1439-56.

[24] Helms Tillery SI, Taylor DM, Schwartz AB. Training in cortical control of neuroprosthetic devices improves signal extraction from small neuronal ensembles. *Rev. Neurosci.*, 2003: 14(1-2):107-19.

[25] Miller K, Leuthardt E, Schalk G, Rao R, Anderson N, Moran D, Miller J, Ojemann J. Spectral Changes in Cortical Surface Potentials during Motor Movement. *Journal of Neuroscience*, 2007: 27:2424-2432.

[26] Penfield W, Flanigin H. Surgical therapy of temporal lobe seizures. *Arch. Neurol. Psychiat.*, 1950: 64:491-500.

[27] Penfield W, Jasper H. Epilepsy and the functional anatomy of the human brain (Vol 1). Boston, Mass : Little, Brown and al, 1954 ; (896 p).

[28] Huggins J, Levine SP, BeMent SL, Kushwaha RK, Schuh LA, Passaro EA, Rohde MM, Ross DA, Elisevich KV, Smith BJ. Detection of Event-Related Potentials for Development of a Direct Brain Interface. *Journal of Clinical Neurophysiology*, 1999: 16(5),448.

[29] Leuthardt EC, Schalk G, Wolpaw JR, Ojemann JG, Moran DW. A brain-computer interface using electrocorticographic signals in humans. *J. Neural Eng.*, 2004: 1(2):63-71.

[30] Felton EA, Wilson JA, Williams JC, Garell PC. Electrocorticographically controlled brain–computer interfaces using motor and sensory imagery in patients with temporary subdural electrode implants. Report of four cases. *J. Neurosurg.*, 2007: 106:495–500.

[31] Schalk G, Miller KJ, Anderson NR, Wilson JA, Smyth MD, Ojemann JG, Moran DW, Wolpaw JR, Leuthardt EC. Twodimensional movement control using electrocorticographic signals in humans. *Journal of Neural Engineering*, 2008: 5,75-84.

[32] Levi R. The Stockholm spinal cord injury study: medical, economical and psycho-social outcomes in a prevalence population. Doctoral Dissertation 1996, Karolinska Institutet: Stockholm.

[33] Enzinger C, Ropele S, Fazekas F, Loitfelder M, Gorani F, Seifert T, Reiter G, Neuper C, Pfurtscheller G, Müller-Putz G. Brain motor system function in a patient with complete spinal cord injury following extensive brain-computer interface training. *Exp. Brain Res.*, 2008: 190(2):215-23.

[34] Shoham S, Halgren E, Maynard EM, Normann RA. Motor-cortical activity in tetraplegics. *Nature*, 2001: 25;413(6858):793.

[35] Wolpaw JR, Birbaumer N, McFarland DJ, Pfurtscheller G, Vaughan TM. Brain–computer interfaces for communication and control. *Clin. Neurophysiol.*, 2002: 113,767-791.

[36] Wolpaw JR. Brain–computer interfaces as new brain output pathways. *J Physiol.*, 2007: 579.3:613–619.

[37] Evarts EV. Relation of pyramidal tract activity to force exerted during voluntary movement. *J. Neurophysiol.*, 1968:31:14–27.

[38] Humphrey DR, Schmidt EM, Thompson WD. Predicting measures of motor performance from multiple cortical spike trains. *Science*, 1970: 170:758–62.

[39] Fetz EE. Operant conditioning of cortical unit activity. *Science*, 1969: 163:955–58.

[40] Shih JJ, Krusienski DJ, Wolpaw JR. Brain-Computer Interfaces in Medicine. *Mayo. Clin. Proc.*, 2012: 87(3):268-79.

[41] Gifford RH, Shallop JK, Peterson AM. Speech recognition materials and ceiling effects: considerations for cochlear implant programs. *Audiol. Neurootol.*, 2008: 13(3):193-205

[42] Wilson BS, Dorman MF. Cochlear implants: current designs and future possibilities. *J. Rehabil. Res. Dev.*, 2008: 45(5):695-730.

[43] Arle JE, Alterman RL. Surgical options in Parkinson's disease. *Med. Clin. North Am.*, 1999: 83(2):483-98, vii.

[44] Anderson NR, Blakely T, Schalk G, Leuthardt EC, Moran DW. Electrocorticographic (ECoG) correlates of human arm movements. *Exp. Brain Res.*, 2012 Sep22: DOI 10.1007/s00221-012-3226-1.

[45] Schalk G, Leuthardt EC. Brain-computer interfaces using electrocorticographic signals. *IEEE Rev. Biomed. Eng.*, 2011: 4:140-54.

[46] Pistohl T, Ball T, Schulze-Bonhage A, Aertsen A, Mehring C. Prediction of arm movement trajectories from ECoG-recordings in humans. *J. Neurosci. Methods*, 2008: 15;167(1):105-14.

[47] Chapin JK, Moxon KA, Markowitz RS, Nicolelis MAL. Real-time control of a robot arm using simultaneously recorded neurons in the motor cortex. *Nat. Neurosci.*, 1999: 2(7):664-70.

[48] Nicolelis MAL, Dimitrov D, Carmena JM, Crist R, Lehew G, Kralik JD, Wise SP. Chronic, multisite, multielectrode recordings in macaque monkeys. *Proceedings of the National Academy of Sciences (PNAS)*, 2003: 100(19):11041–11046.

[49] Watanabe H, Sato MA, Suzuki T, Nambu A, Nishimura Y, Kawato M, Isa T. Reconstruction of movement-related intracortical activity from micro-electrocorticogram array signals in monkey primary motor cortex. *J. Neural. Eng.*, 2012: 9(3):036006.

[50] Rouse AG, Moran DW. Neural adaptation of epidural electrocorticographic (EECoG) signals during closed-loop brain computer interface (BCI) tasks. *Conf. Proc. IEEE Eng. Med. Biol. Soc.*, 2009:5514-5517.

[51] Torres Valderrama A, Oostenveld R, Vansteensel MJ, Huiskamp GM, Ramsey NF. Gain of the human dura in vivo and its effects on invasive brain signal feature detection. *J. Neurosci. Methods*, 2010: 187(2):270-279.

[52] Wolpaw JR, McFarland DJ, Neatb GW, Forneris CA. An EEG-based brain-computer interface for cursor control. Electroencephalogr. *Clin. Neurophysiol.*, 1991: 78(3):252-259.

[53] Birbaumer N, Ghanayim N, Hinterberger T, Iversen I, Kotchoubey B, Kübler A, Perelmouter J, Taub E, Flor H. A spelling device for the paralysed. *Nature*, 1999: 398(6725):297-298.

[54] Kübler A, Kotchoubey B, Hinterberger T, Ghanayim N, Perelmouter J, Schauer M, Fritsch C, Taub E, Birbaumer N. The thought translation device: a neurophysiological approach to communication in total motor paralysis. *Exp. Brain Res.*, 1999: 124(2):223-232.

[55] Donoghue JP, Sanes JN, Hatsopoulos NG, Gaál G. Neural discharge and local field potential oscillations in primate motor cortex during voluntary movements. *J. Neurophysiol.*, 1998: 79(1):159-73.

[56] Scherer R, Graimann B, Huggins JE, Levine SP, Pfurtscheller G. Frequency component selection for an ECoG-based brain-computer interface. *Biomed. Tech. (Berl)*, 2003: 48(1-2):31-36.

[57] Leuthardt EC, Miller KJ, Schalk G, Rao RP, Ojemann JG. Electrocorticography-based brain computer interface--the Seattle experience. *IEEE Trans Neural Syst. Rehabil. Eng.*, 2006: 14(2):194-198.

[58] Müller-Putz GR, Kaiser V, Solis-Escalante T, Pfurtscheller G, 2010. Fast set-up asynchronous brain-switch based on detection of foot motor imagery in 1-channel EEG. *International Federation for Medical and Biological Engineering*, 2010: 48:229-233.

[59] Zhao Q, Zhang L, Cichocki A. EEG-based asynchronous BCI control of a car in 3D virtual reality environments. *Chinese Science Bulletin*, 2008: 54(1):78-87.

[60] Bladin PF. W. Grey Walter, pioneer in the electroencephalogram, robotics, cybernetics, artificial intelligence. *J. Clin. Neurosci.*, 2006: 13(2):170-7.

[61] Carmena JM, Lebedev MA, Crist RE, O'Doherty JE, Santucci DM, Dimitrov DF, Patil PG, Henriquez CS, Nicolelis MAL. Learning to control a brain-machine interface for reaching and grasping by primates. *PLoS Biol.*, 2003: 1(2):E42.

[62] Musallam S, Corneil BD, Greger B, Scherberger H, Andersen RA. Cognitive control signals for neural prosthetics. *Science*, 2004: 9;305(5681):258-62.

[63] Santhanam G, Ryu SI, Yu BM, Afshar A, Shenoy KV. A high-performance brain-computer interface. *Nature*, 2006: 13;442(7099):195-8.

[64] Nicolelis MA, Chapin JK. Controlling robots with the mind. Sci. Am., 2002: 287(4):46-53.

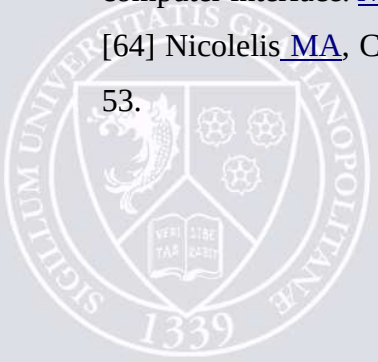

[65] Wolpaw JR, Birbaumer N, Heetderks WJ, McFarland DJ, Peckham PH, Schalk G, Donchin E, Quatrano LA, Robinson CJ, Vaughan TM. Brain- computer interface technology: A review of the first international meeting. *IEEE Trans. Rehabil. Eng.*, 2000: 8:164–173.

[66] Mason SG, Birch GE. A general framework for brain-computer interface design. *IEEE Trans. Neural Syst. Rehabil. Eng.*, 2003: 11:70–85.

[67] Mason SG, Jackson MM, Birch GE. A general framework for characterizing studies of brain interface technology. *Ann. Biomed. Eng.*, 2005: 33(11):1653-70.

[68] Obermaier B, Neuper C, Guger C, Pfurtscheller G. Information transfer rate in a five-classes brain-computer interface. *IEEE Trans Neural Syst. Rehabil. Eng.*, 2001: 9(3):283-8.

[69] Pfurtscheller G, Neuper C. Motor imagery and direct brain-computer communication. *Proceedings of the IEEE*, 2001: 89(7):1123–1134.

[70] Roberts SJ, Penny WD. Real-time brain-computer interfacing: a preliminary study using Bayesian learning. *Med. Biol. Eng. Comput.*, 2000: 38(1):56-61.

[71] Kronegg J, Chanel G, Voloshynovskiy S, Pun T. EEG-based synchronized brain-computer interfaces: a model for optimizing the number of mental tasks. *IEEE Trans Neural Syst. Rehabil. Eng.*, 2007: 15(1):50-8.

[72] Birch GE, Bozorgzadeh Z, Mason SG. Initial on-line evaluations of the LF-ASD brain-computer interface with able-bodied and spinal-cord subjects using imagined voluntary motor potentials. *IEEE Trans Neural Syst. Rehabil. Eng.*, 2002: 10(4):219-24.

[73] Millán Jdel R, Mouriño J. Asynchronous BCI and local neural classifiers: an overview of the Adaptive Brain Interface project. *IEEE Trans Neural Syst. Rehabil. Eng.*, 2003: 11(2):159-61.

[74] Millán Jdel R, Renkens F, Mouriño J, Gerstner W. Noninvasive brain-actuated control of a mobile robot by human EEG. *IEEE Trans Biomed. Eng.*, 2004: 51(6):1026-33.

[75] Scherer R, Müller GR, Neuper C, Graimann B, Pfurtscheller G. An asynchronously controlled EEG-based virtual keyboard: improvement of the spelling rate. *IEEE Trans Biomed. Eng.*, 2004: 51:979-984.

[76] Fatourechi M, Ward RK, Birch GE. A self-paced brain–computer interface system with a low false positive rate. *J. Neural. Eng.*, 2008: 5:9–23.

[77] Velliste M, Perel S, Spalding MC, Whitford AS, Schwartz AB. Cortical control of a prosthetic arm for self-feeding. *Nature*, 2008: 19;453(7198):1098-101.

[78] Birbaumer N, Weber C, Neuper C, Buch E, Haapen K, Cohen L. Physiological regulation of thinking: brain-computer interface (BCI) research. *Prog. Brain Res.*, 2006: 159:369-91.

[79] Kennedy PR, Bakay RA, Moore MM, Adams K, Goldwaithe J. Direct control of a computer from the human central nervous system. *IEEE Trans Rehabil. Eng.*, 2000: 8(2):198-202.

[80] Kennedy PR, Kirby MT, Moore MM, King B, Mallory A. Computer control using human intracortical local field potentials. *IEEE Trans Neural Syst. Rehabil. Eng.*, 2004: 12(3):339-44.

[81] Kennedy PR, Bakay RA. Restoration of neural output from a paralyzed patient by a direct brain connection. *Neuroreport*, 1998: 1;9(8):1707-11.

[82] Kim SP, Simeral JD, Hochberg LR, Donoghue JP, Black MJ. Neural control of computer cursor velocity by decoding motor cortical spiking activity in humans with tetraplegia. *J. Neural Eng.*, 2008: 5(4):455-76.

[83] Kim HI, Shin YI, Moon SK, Chung GH, Lee MC, Kim HG. Unipolar and continuous cortical stimulation to enhance motor and language deficit in patients with chronic stroke: report of 2 cases. *Surg. Neurol.*, 2008: 69(1):77-80; discussion 80.

[84] Ingram JN, Körding KP, Howard IS, Wolpert DM. The statistics of natural hand movements. *Exp. Brain Res.*, 2008: 188(2):223-36.

[85] Mason CR, Gomez JE, Ebner TJ. Primary motor cortex neuronal discharge during reach-to-grasp: controlling the hand as a unit. *Arch. Ital. Biol.*, 2002: 140(3):229-36.

[86] Santello M, Flanders M, Soechting JF. Patterns of hand motion during grasping and the influence of sensory guidance. *J. Neurosci.*, 2002: 15;22(4):1426-35.

[87] Nudo RJ, Sutherland DP, Masterton RB. Variation and evolution of mammalian corticospinal somata with special reference to primates. *J. Comp. Neurol.*, 1995: 24;358(2):181-205.

[88] Nudo RJ, Masterton RB. Descending pathways to the spinal cord, III: Sites of origin of the corticospinal tract. *J. Comp. Neurol.*, 1990: 22;296(4):559-83.

[89] Schieber MH. Individuated finger movements of rhesus monkeys: a means of quantifying the independence of the digits. *J. Neurophysiol.*, 1991: 65(6):1381-91.

[90] Kennedy PR, Mirra SS, Bakay RA. The cone electrode: ultrastructural studies following long-term recording in rat and monkey cortex. *Neurosci. Lett.*, 1992: 3;142(1):89-94.

[91] Suner S, Fellows MR, Vargas-Irwin C, Nakata GK, Donoghue JP. Reliability of signals from a chronically implanted, silicon-based electrode array in non-human primate primary motor cortex. *IEEE Trans Neural Syst. Rehabil. Eng.*, 2005: 13(4):524-41.

[92] Birbaumer N, Murguialday AR, Weber C, Montoya P. Neurofeedback and brain–computer interface: clinical applications. *Int. Rev. Neurobiol.*, 2009: 86:107–17.

[93] Fetz EE. Making the paper: computer-chip implants could help people with brain damage. *Nature*, 2006: 444(7115):xi.

[94] Pascual-Leone A, Amedi A, Fregni F, Merabet LB. The plastic human brain cortex. *Annu. Rev. Neurosci.*, 2005: 28:377-401.

[95] Rossini PM, Calautti C, Pauri F, Baron JC. Post-stroke plastic reorganisation in the adult brain. *Lancet Neurol.*, 2003: 2:493-502.

[96] Flor H, Birbaumer N. Phantom limb pain: cortical plasticity and novel therapeutic approaches. *Curr. Opin. Anaesthesiol.*, 2000: 13(5):561-4.

[97] Tecchio F, Zappasodi F, Tombini M, Oliviero A, Pasqualetti P, Vernieri F, Ercolani M, Pizzella V, Rossini PM. Brain plasticity in recovery from stroke: an MEG assessment. *Neuroimage*, 2006: 32(3):1326-34.

[98] Edelman G M. Neural Darwinism: selection and reentrant signaling in higher brain function. *Neuron*, 1993: 10:115–25.

[99] Yao H, Shi L, Han F, Gao H, Dan Y. Rapid learning in cortical coding of visual scenes. *Nat. Neurosci.*, 2007: 10(6):772-8.

[100] Han F, Caporale N, Dan Y. Reverberation of recent visual experience in spontaneous cortical waves. *Neuron*, 2008: 23;60(2):321-7.

[101] Wu JY, Huang X, Zhang C. Propagating Waves of Activity in the Neocortex: What They Are, What They Do. *Neuroscientist.*, 2008: 14(5):487–502.

[102] Donoghue JP. Plasticity of adult sensorimotor representations. *Curr. Opin. Neurobiol.*, 1995: 5(6):749-54.

[103] Chugani HT, Müller RA, Chugani DC. Functional brain reorganization in children. *Brain & Development*, 1996: 18:347-356.

[104] Cohen LG, Celnik P, Pascual-Leone A, Corwell B, Falz L, Dambrosia J, Honda M, Sadato N, Gerloff C, Catalá MD, Hallett M. Functional relevance of cross-modal plasticity in blind humans. *Nature*, 1997: 11;389(6647):180-3.

[105] Ashford JW, Jarvik L. Alzheimer's disease: does neuron plasticity predispose to axonal neurofibrillary degeneration? *N. Engl. J. Med.*, 1985: 8;313(6):388-9.

[106] Wieloch T, Nikolich K. Mechanisms of neural plasticity following brain injury. *Curr. Opin. Neurobiol.*, 2006: 16:258–64.

[107] Murphy TH, Corbett D. Plasticity during stroke recovery: from synapse to behaviour *Nature Rev. Neurosci.*, 2009: 10:861–72.

[108] Barbero A, Grosse-Wentrup M. Biased feedback in brain–computer interfaces. *J. Neuroeng. Rehabil.*, 2010: 27;7:34.

[109] Buch E, Weber C, Cohen LG, Braun C, Dimyan MA, Ard T, Mellinger J, Caria A, Soekadar S, Fourkas A, Birbaumer N. Think to move: a neuromagnetic brain–computer interface (BCI) system for chronic stroke. *Stroke*, 2008: 39:910–7.

[110] Mintzopoulos D, Khanicheh A, Konstas AA, Astrakas LG, Singhal AB, Moskowitz MA, Rosen BR, Tzika AA. Functional MRI of Rehabilitation in Chronic Stroke Patients Using Novel MR-Compatible Hand Robots. *Open Neuroimag. J.*, 2008: 27;2:94-101.

[111] Astrakas LG, Naqvi SH, Kateb B, Tzika AA. Functional MRI using robotic MRI compatible devices for monitoring rehabilitation from chronic stroke in the molecular medicine era. *Int. J. Mol. Med.*, 2012: 29(6):963-73.

[112] Fisher S, Lucas L, Thrasher T A. Robot-Assisted Gait Training for Patients with Hemiparesis Due to Stroke. *Top Stroke Rehabil.*, 2011: 18(3):269–276.

[113] Dobkin BH. Brain-computer interface technology as a tool to augment plasticity and outcomes for neurological rehabilitation. *The Journal of Physiology*, 2007: 579:637-642.

[114] Rijsbergen CJ. Information retrieval. 1979: Available at http://www.dcs.gla.ac.uk/˜iain/keith/.

[115] Schlögl A, Kronegg J, Huggins J, Mason SG. Evaluation criteria in BCI research. In Towards Brain-Computer Interfacing 2007 (G. Dornhege, J. R. Millan, T. Hinterberger, D. McFarland and K. R. Muller, Eds.), MIT Press, 2007.

[116] Eliseyev A, Moro C, Costecalde T, Torres N, Gharbi S, Mestais C, Benabid AL, Aksenova T. Iterative N-way partial least squares for a binary self-paced brain-computer interface in freely moving animals. *J. Neural Eng.*, 2011 : 8(4):046012.

[117] Vasconcelosa N, Pantojaf J, Belchiora H, Caixetaa FV, Faber J, Freirea MA, Cota VR, Anibal de Macedo E, Laplagne DA, Gomes HM, Ribeiro S. Cross-modal responses in the primary visual cortex encode complex objects and correlate with tactile discrimination. *Proceedings of the National Academy of Sciences (PNAS)*. 2011: 13;108(37):15408-13.

VII. ABBREVIATIONS

BCI: Brain-Computer Interface

SCI: Spinal Cord Injury

EEG: ElectroEncephaloGraphy

ECoG: ElectroCorticoGraphie

CNS: Central Nervous System

PNS: Peripheral Nerve System

CSF: CerebroSpinal Fluid

AP: Action Potential

MEA: MicroElectrode Arrays

ms: Milliseconds

ALS: Amyotrophic Lateral Sclerosis

BI: Brain Interface

DBI: Direct Brain Interface

BMI: Brain Machine Interface

MI: primary motor cortex

LFP: Local Field Potential

DOF: Degrees Of Freedom

OFA: Oncins France strain A

RMS: Root Mean Square

VEP: Visual Evoked Potential

SEP: Sensitive Evoked Potential

CAR: Common Average Reference

CWT: Continuous Wavelet Transform

TP: True Positive

TN: True Negative

FP: False Positive

FN: False Negative

TPR: True Positive Rate

FPR: False Positive rate

PPV: Positive Predictive Value

OP: Overall Performance

PFA: ParaFormAldehyde

PBS: Phosphate Buffered Saline

LP: Lever Push

OA: Overall Accuracy

VIII. ANNEXES

1_List of Figures

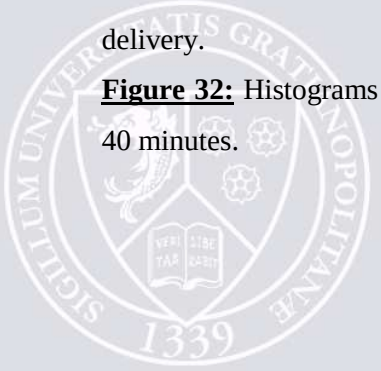

Figure 33: schematic representation of this phase of the protocol. A reward is obtained when the signature is detected on-line (1) and validated by lever push (2). The reward is delivered only when the detected feature is validated by a real lever push occurring within 1,5 second window following the feature detection.

Figure 34: Schematic representation of the protocol of neuroplasticity. A reward is obtained when the signature is detected on-line (1) and validated by lever push (2). The reward is delivered only when the detected feature is validated by a real lever push occurring within 1,5 second window following the feature detection.

Figure 35: Schematic representation of the protocol of neuroplasticity. A reward is obtained when the signature is detected on-line on Electrode 15 in a first set of experiments, on E11 in a second set and on E10 in a last session of experiments. The reward is delivered only when the detected feature is validated by a real lever push occurring within 1,5 second window following the feature detection. The signature is calibrated on Electrode 15 for one set of experiments and on Electrode 10 or 11 for others sets.

Figure 36: Represents the evolution along time of data for all animals for on-line analysis of experiments of neuroplasticity (signature calibrated on E15 and detection on E11, see figure 35). A: evolution of the TPR of 8 animals. B: evolution of FP/minute of 8 animals. C: evolution of PPV of 8 animals and D: evolution of the OP of 8 animals.

Figure 37: Picture of a brain after 8 months of implantation and footprint corresponding with implanted electrodes.

Figure 38: Comparison of the brain slices (stained with cresyl violet) with atlas and the implantation map provided. A: slice of the brain with footprints of electrodes 2 and 9 (in blue). B: slice of the brain with footprints of electrodes 3 and 10 (in red). C: slice of the brain with footprints of electrodes 4 and 11 (in green). D: slice of the brain with footprints of electrodes 6 and 13 (in black). E: slice of the brain with footprints of electrodes 8 and 15 (in orange).

Figure 39: Crésyl violet coloration for identification of Nissl bodies inside neurons. A: with 10X, B: with 20X and C: with 40X.

2_List of Pictures

3_List of Tables

Table 13: Table represents the data for each animal for on-line analysis of experiments of neuroplasticity (signature calibrated on E15 and detection on E11, see figure 35).